Geology and petrology of Sierra Grande, a volcano in the Raton-Clayton volcanic field of northeastern New Mexico

by

Matthew Gerard Trainum

A Thesis Submitted to the

Graduate Faculty in Partial Fullfillment of the

Requirements for a Degree of

MASTER OF SCIENCE

Department: Geological and Atmospheric Sciences
Major: Geology

Iowa State University
Ames, Iowa

1992

TABLE OF CONTENTS

INTRODUCTION

The Raton-Clayton volcanic field in northeastern New Mexico represents the eastern most region of Cenozoic volcanism within the United States. It has been active over a period of 8 m.y. and has been associated with the tectonic and volcanic activity of the Rio Grande Rift. Sierra Grande, the largest volcano in the Raton-Clayton field, has been described previously as the only andesitic feature within a volcanic field of primarily alkali olivine basalts and mafic feldspathoidal lavas. The volcano is approximately 1.9 Ma and is located near the center of the Raton-Clayton field.

A representative portion of the volcano has been mapped and described in detail. Mapping was based on the textural characteristics of eleven identifiable units (seven major units and four subunits). Field observation has revealed that Sierra Grande is composed of a sequence of basaltic andesites followed by andesites and a remnant andesitic and pyroclastic summit that may obscure a central crater. The volcano has also been intruded by andesitic dikes. Two cinder vents were found on the volcano and three cinder cones were identified along the perimeter. Two of the cones have been intruded by basaltic dikes. The peripheral volcanics are unrelated, spatially and temporally, with the formation of Sierra Grande.

A comparison of phenocryst compositions between the lavas of Sierra Grande and the surrounding volcanics of the Raton-Clayton field indicate that: the volcano contains basaltic andesites with olivine phenocrysts that are more Mg-rich, an andesite with both augite and enstatite phenocrysts, and basaltic andesites and andesites with plagioclase phenocrysts and groundmass microlites that are relatively more Ca-rich. Petrographic and microprobe analyses indicate that Sierra Grande's lavas are calc-alkaline and are transitional; modally the andesitic lavas are equivalent to anorogenic volcanics while the composition of the minerals suggest an orogenic origin.

The mineral compositions of the lavas of Sierra Grande indicate that the magma experienced some differentiation to produce the successive lithologic/flow units. Stratigraphic trends of Mg depletion and Ca depletion is evident in the olivine and pyroxene phenocrysts, and plagioclase

phenocrysts respectively. Therefore, Sierra Grande was produced by differentiation of a magma derived by the partial melting of the upper mantle during a late extensional faulting episode of the Rio Grande rift. The peripheral volcanics may have originated from either a separate source, the original parent magma or the mafic residual after differentiation.

The presence of a two pyroxene andesite typical of volcanic regimes associated with the compressional tectonics at continental margins poses an interesting problem to the tensional tectonics of rifting. Further investigation will require additional sampling, microprobe analyses, and bulk chemical analyses.

REGIONAL GEOLOGIC SETTING

Raton-Clayton volcanic field

The Raton-Clayton volcanic field is located in the northeast corner of New Mexico, east of the Sangre de Cristo Mountains and the Rio Grande Rift. The field is the eastern most location of Cenozoic volcanism within the United States (Stormer, 1972b) and occupies an area of approximately 4000 sq km, extending from east-south central Colorado southeastward to near the New Mexico-Texas border (Figure 1). Situated on the east margin of the Raton basin, the field overlies a sedimentary stratigraphic section composed of a sequence of limestones, sandstones, conglomerates, shales and siltstones of Triassic to Tertiary age (Appendix A).

The Raton-Clayton field is late Tertiary to Holocene in age and is dominated by alkali olivine basalts. Extrusives have erupted over the last 8 million years (Stormer, 1972a), the most recent activity occurring between 10,000 and 4,500 years ago (Baldwin and Muehlberger, 1959). Intrusives within the field have been identified as being Oligocene in age, 37 to 26 Ma (Staatz, 1985).

The volcanics of the field have been described and interpreted primarily by: Mertie in Lee (1922), Collins (1949), Stobbe (1949), Baldwin and Muehlberger (1959), Jones et al. (1972), Stormer (1972a & b, 1987) and Phelps et al. (1983). Intrusions of the field have been studied most recently by; Staatz (1985), Scott (1986), Potter (1988) and Taylor (1989). A nomenclature, based on stratigraphic succession, was established by Collins (1949); this was revised by Stormer (1972b) and Taylor (1989). Collins divided the stratigraphy into three series: the Raton Basalts, the Clayton Basalts, and the Capulin Basalts, each composed of numerous lava flows or sequences. The classification was based on previous mapping in Lee (1922), Collins' field and lithologic study, and the petrographic/petrologic study by Stobbe (1949). Individual flow units include the Raton basalts, the Red Mountain dacite, the Turkey Mountain andesite, the Slagle trachyte, the Chico phonolites (interpreted as flows), the Clayton basalts, and the Capulin basalt. Stormer (1972b) proposed

Figure 1. Index map of the Raton-Clayton volcanic field, northeastern New Mexico. Distribution of petrographic groups is approximated and shown by the patterns in the key (modified after Stormer 1972b).

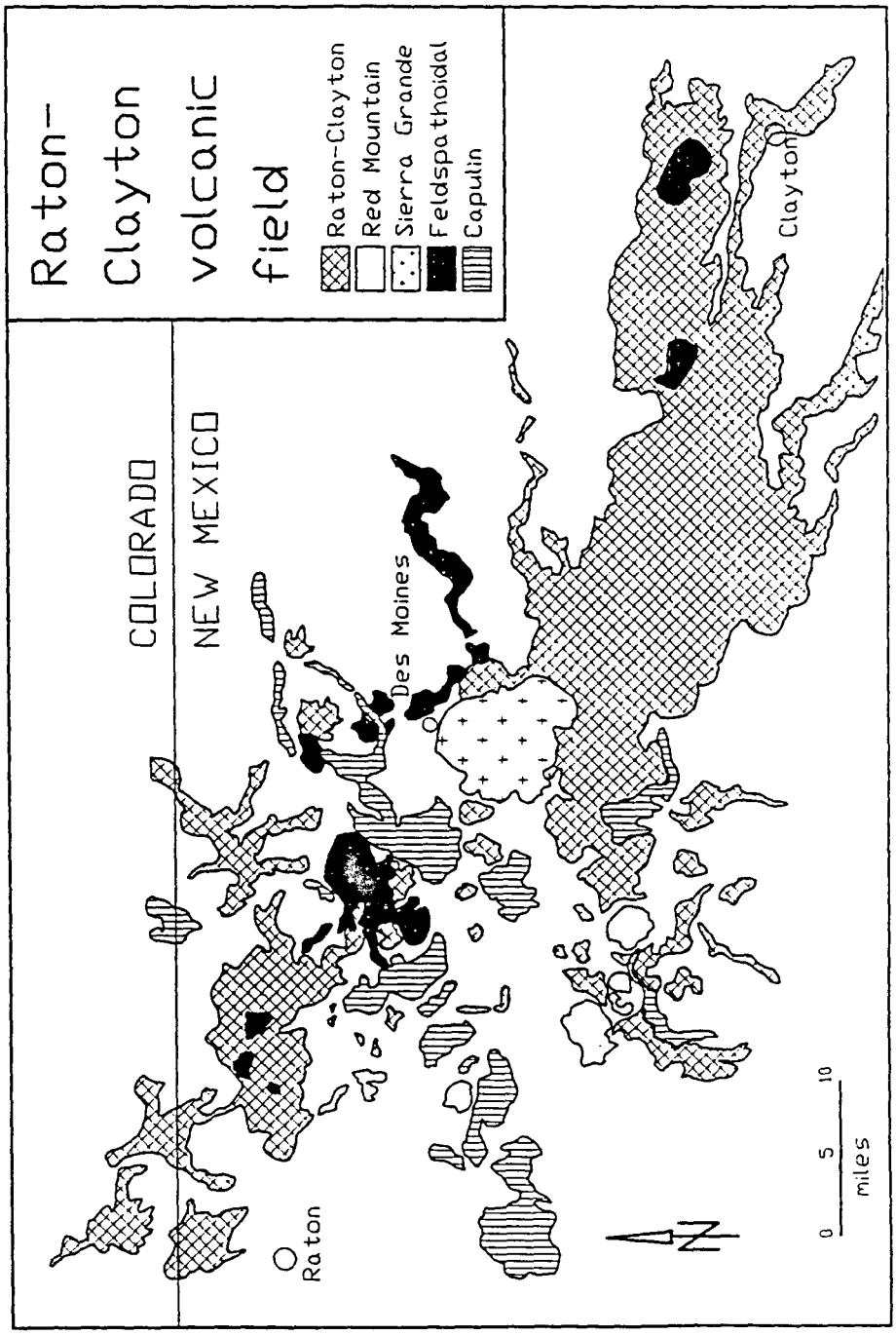
Raton-
Clayton
volcanic
field
Raton-Clayton
Red Mountain
Sierra Grande
Feldspathoidal
Capulin
COLORADO
NEW MEXICO
Raton
Des Moines
Clayton
0 5 10
miles
N

Figure 1

another petrographic grouping to designate differences and/or similarities between rock and flow units, based on chemical-petrological distinctions. This includes the Raton-Clayton Basalt, the Red Mountain Lavas, the Feldspathoidal Lavas, the Sierra Grande Andesitic Lavas and the Capulin Basaltic Lavas. Taylor (1989) suggested an alternative classification (Appendix B) based on chemical delineations which rearranged the previous stratigraphic units into five groups reducing the confusion caused by retaining stratigraphic distinctions that are not chemically valid.

Rio Grande Rift

The Raton-Clayton field has been associated with the tectonic and volcanic activity of the Rio Grande Rift (Lipman, 1969; Stormer, 1972a; Gornitz, 1982). The majority of the rift extends from Colorado to Mexico (Figure 2) and merges with the southeastern area of the Basin and Range Province.

It has been suggested and is generally accepted that the western edge of the North American craton had experienced two major orogenic events involving the subduction of oceanic material to the west, prior to the rift's formation. One was the Sevier Orogeny (155 - 85 Ma), characterized by large thrust belts that moved eastward along the length of the cratonic apron and by magmatic activity along its edge. The other was the Laramide Orogeny (80 - 40 Ma) which involved asymmetrical basement uplift and a northeastward migration of magmatism into the craton's interior (Coney, 1978; Suppe, 1985; Cross, 1986). Then around 40 to 20 Ma ago the western edge of the North American plate experienced a second migration of magmatism eastward into the interior (Coney, 1978; Cross, 1986) and subsequent extensional faulting (Elston and Bornhorst, 1979), which has been attributed to a rapid rate of convergence between the Farallon and North American plates (Atwater, 1970; Eaton, 1979; Coney, 1987) and a subsequent low angle of subduction (Coney, 1978; Cross, 1986). At about 20 Ma the convergence rate apparently slowed and either a sinking or breakup of the subducted plate occurred (Coney and Reynolds, 1977; Coney, 1987), resulting in a return to a steeper angle of subduction and a reverse migration in magmatism (Cross, 1986). The

Figure 2. Index map of the Rio Grande Rift in New Mexico and southern Colorado. Location of major tectonic features and associated volcanic provinces within the region (modified after Potter 1988).

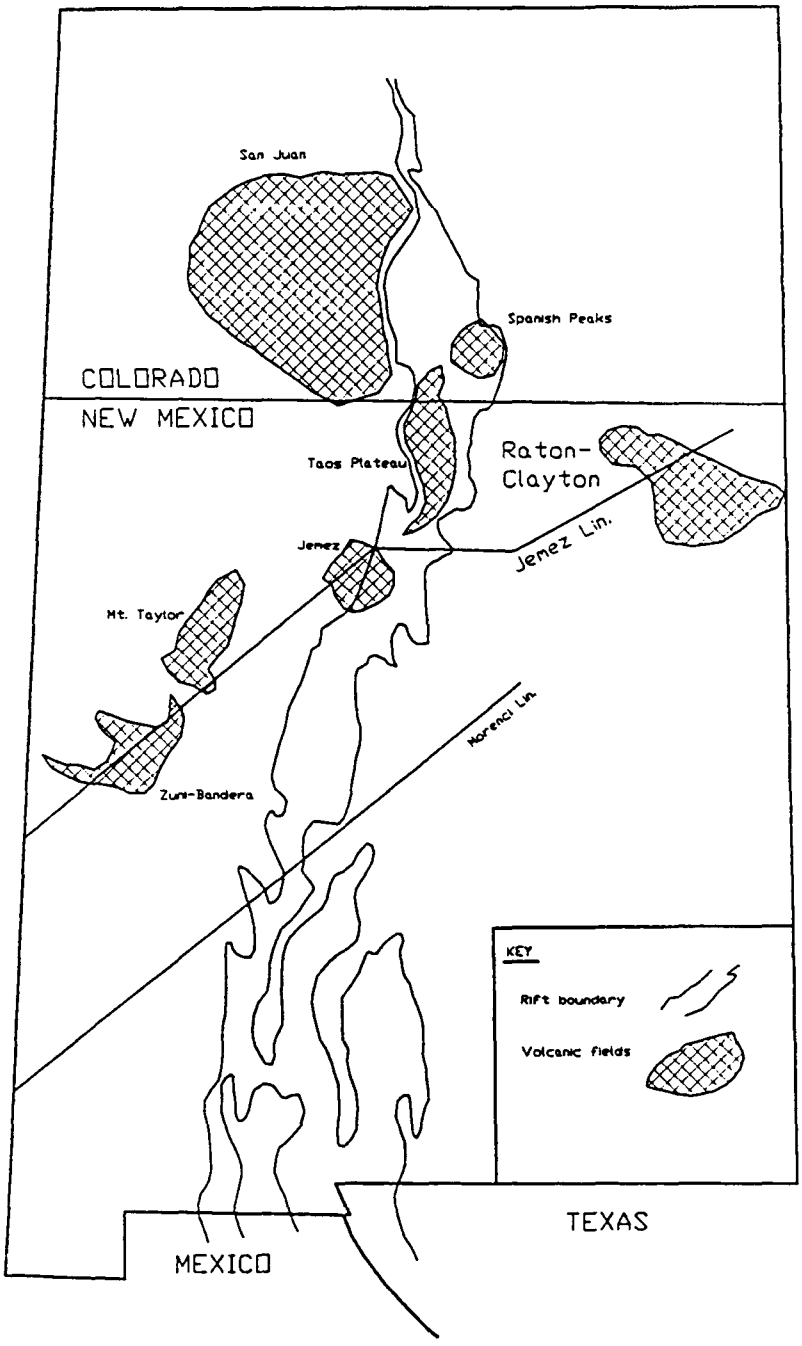
San Juan
Spanish Peaks
COLORADO
NEW MEXICO
Taos Plateau
Raton-
Clayton
Jemez
Jemez Lin.
Mt. Taylor
Zuni-Bandera
Morenci Lin.
KEY
Rift boundary
Volcanic fields
TEXAS
MEXICO

Figure 2

formation of the Rio Grande Rift has been attributed to this decrease in convergence rate which is suggested to also have caused a reverse flow in the asthenosphere (Lipman, 1980; BVSP, 1981; Coney, 1987). Movement of the asthenosphere and its interaction with the overlying lithosphere resulted in uplift, extensional faulting and volcanism (BVSP, 1981; Eaton, 1986).

Four major geologic events have been identified in the northern region of the Rio Grande Rift by Morgan and Golombek (1984). They are: 1) Laramide compressional deformation (70 - 40 Ma), 2) Oligocene to early Miocene volcanism (36 - 20 Ma); 3) an early phase of extension (30 Ma to ?); and 4) a late phase of extension (13 Ma to recent) and associated volcanism. This last event followed an apparent lull in volcanic activity during the middle Miocene.

Elston and Bornhorst (1979) proposed that the rift occurred in three overlapping events: beginning with a modified Andean arc stage (40-29 Ma) with calc-alkaline volcanism and early extension, followed by a modified back arc stage (peaking at 27 Ma) with major extension and rhyolite and basaltic andesite volcanics, and finally an intraplate block faulting stage (21 Ma to present) with dominant basaltic volcanism. Intrusive igneous activity associated with the formation of the rift are the Spanish Peaks (21.7 - 25.6 Ma)(Stormer, 1972a), the Questa district (22.3 - 23.5 Ma)(Laughlin et al., 1969), the Chico Hills sill complex and the Laughlin peak area (36.7 - 24.2 Ma)(Staatz, 1985; Scott, 1986). It is further suggested that the rift experienced two primary episodes of extension: the first began about 30 Ma and lasted until about 12 Ma, the second began around 10 Ma and continued to around 3 Ma(Eaton, 1979; Baldridge et al., 1984). During the first episode it has been proposed that there was a decrease in volcanic activity around 20 to 15 million years ago (Eaton, 1979; Elston and Bornhorst, 1979) while a maximum in volcanic activity occurred during this last episode (BVSP, 1981; Gornitz, 1982).

Jemez Lineament

The Raton-Clayton field has also been spatially associated with the volcanic events of the Jemez Lineament; the later a northeast trending alignment of volcanic fields (Lipman and Mehnert,

1975; Lipman, 1980). The lineament begins at the southeast margin of the Colorado plateau, intersects the Rio Grande Rift at its west margin and traverses the rift in a west-east direction. At the east margin of the rift, the lineament continues on a northeast trend into northeast New Mexico and southeast Colorado (Figure 2). The Jemez Lineament has been inferred as a major zone of weakness in the lower lithosphere (Baldridge, 1979; Gornitz, 1982; Baldridge et al, 1984), one of many such structural features that exist throughout the western United States as a result of early Proterozoic tectonic events (Warner, 1978; Kerr, 1985; Tanaka, 1986).

The Raton-Clayton field is situated on the eastern end of the lineament (Figure 2). Volcanism along the lineament began during mid-Miocene, for example in the Jemez Mountains approximately 13 Ma (Gardner and Goff, 1984), and continued uniformally along its length over the last 5 million years (Lipman and Mehnert, 1975). A slight asymmetrical age relationship exists with the volcanics on the west side of the rift being relatively older than those on the east. For example, the volcanics of the Raton-Clayton field began approximately 8 Ma and continued until late Holocene time (Stormer, 1972a). The volcanics along the lineament, but outside the rift, are generally alkali basalts while those within the rift are predominately tholeiitic basalts (Lipman, 1969).

SIERRA GRANDE VOLCANO

Sierra Grande, the largest volcano in the Raton-Clayton volcanic field, is approximately 15 km in diameter, 2658 m in maximum elevation and rises approximately 600 m above the plain on which it is situated. The volcano has a shield profile and the topography appears smooth from a distance. However, a more rugged terrain is created by numerous, often deep, ravines that form a radial pattern on the slopes of Sierra Grande. Many flows, flow fronts or portions of flows are well exposed as ridges, small bluffs or cliffs perpendicular to the slopes. Much of the surface area is covered with a thin soil and is often quite grassy. The slopes of the volcano are very rocky with both large and small float. The lower half of the north side of the volcano is thickly forested in areas. The summit of the volcano consists of two peaks, one east and one west, which are connected by a saddle. Two, almost cirque-like, depressions are on either side of the saddle, one facing northeast and the other facing south-southwest. The slopes of the summit are very steep and very grassy with few outcrops exposed. However, those outcrops that are present are a few small flows that appear to have been extruded from the summit sides, near the top of the peaks and along the saddle area.

The volcano has been referred to as an anomaly and described as a shield volcano (Stormer, 1987) of andesitic composition (Collins, 1949; Baldwin and Muehlberger, 1959; Stormer, 1972b) within a volcanic field of predominately alkali olivine basalt (Collins, 1949; Stobbe, 1949; Baldwin and Muehlberger, 1959; Stormer, 1987). Sierra Grande has been described as petrographically and petrologically unique for the area (Collins, 1949; Stormer, 1972b) in that it contains a two-pyroxene andesite (augite and orthopyroxene) (Stormer, 1972b); lavas such as these are typically found in volcanic regimes associated with compressional styles of plate tectonics at continental margins rather than the tensional tectonics typical of the Rio Grande Rift.

Studies of the Raton-Clayton volcanic field have concentrated on the basaltic and feldspathoidal volcanics or earlier intrusives (Collins, 1949; Stobbe, 1949; Baldwin and Muehlberger,

1959; Stormer, 1972 a & b; Phelps et al., 1983; Potter, 1988; Taylor, 1989) while Sierra Grande has remained relatively untouched. The dozen or so reported samples attributed to Sierra Grande have come from either; near the base of the volcano, more than several miles from the volcano, or are of unknown location. No geologic mapping or comprehensive collecting has been done prior the present work.

Clarke (1915) reported a chemical analysis by W. F. Hillebrand on a sample from Sierra Grande. The report included a petrographic description by Whitman Cross, who identified the sample as pyroxene andesite (Tonalose) containing augite, a minor amount of hypersthene, microliths of plagioclase, apatite, magnetite and smokey brown glass. Washington (1917) reported the very same chemical analysis but identified the rock only as andesite. A reference by Mertie in Lee (1922) cited the lava of Sierra Grande as pyroxene andesite, however, no further description, reference or location was given.

Collins (1949) described the volcano as "relatively inaccessible and unexplored" and stated that although there is no crater visible, Lee (1912) had inferred one. In fact, Lee (1912) reported a crater, briefly described its morphology and outlined its evolution. In further describing the volcano, Collins proposed that it was a source for extrusion of every flow composition found in the field, with the exception of the Raton basalt and stated that there is feldspathoidal basalt on the volcano's west flank, olivine basalt on the west and south-to-east flanks, olivine-free basalt on the southwest to west flanks, Capulin basalt on the northeast flank from a vent with an associated narrow 8 km flow, and Red Mountain dacite as float on the north slopes. The east flank sample of olivine basalt was identified as being the typical Clayton basalt, which is also located between Sierra Grande and the town of Clayton; however, Collins suggested that it is only a fraction of the volcano. A sample from the northeast region was identified as being either olivine-free basalt or pyroxene andesite. A chemical analysis of an andesite in Collins' paper was the same as the one from Clarke's 1915 report.

There are not enough chemical analyses support or refute Collins' assumption that Sierra Grande may have been a source of every flow composition and without more precise sample locations (e.g., flank or base) the association of the samples to the volcano proper is questionable. Subsequent workers (Baldwin and Muehlberger, 1959; Stormer, 1972a & b) have not suggested that Sierra Grande is composed of such flows. In fact, the age of some of the flow units of the Raton-Clayton field described by Collins have been found to be either older or younger than the apparent age of Sierra Grande extrusives (Stormer, 1972a).

Stobbe (1949) suggested that the olivine-free basalt might be the pyroxene andesite referred to by Mertie in Lee (1922). Stobbe described the volcano as being composed of numerous lava types and identified three samples. Two samples came from an area located four to seven miles from the town of Clayton (i.e., a lava flow between Sierra Grande and Clayton). The other sample came from the west base of the volcano. All three were classified by Stobbe as Clayton basalt. The first two were described as olivine basalt and the third as olivine-free basalt. Stobbe stated that the latter resembled olivine basalt but had quartz inclusions, was olivine free and had a higher concentration of glass thus making it difficult to identify as a basalt. The glass was reported as having a lower index of refraction than that for andesitic glass and therefore Stobbe suggested that all the samples could be grouped with the olivine basalts of the Raton-Clayton volcanic field, based on the presence of pyroxene, type of feldspar and color index.

Baldwin and Muehlberger (1959) described Sierra Grande as being composed of pyroxene andesite or olivine-free basalt and suggested that the volcano preceded the late Clayton basalt extrusions. They stated that, although Collins (1949) noted olivine basalt and feldspathoidal basalt around the perimeter, the main bulk of the volcano was pyroxene andesite. Baldwin and Muehlberger suggested that the andesite was chemically and petrographically similar to the Red Mountain dacite of Collins (1949) and that Sierra Grande preceded the late stages of the Clayton basalt, possibly as an earlier silicic differentiation, and was stratigraphically in place prior to the

Capulin basalt. Baldwin and Muehlberger made a single traverse across the volcano from the northeast to the peak and down the south side and stated that a remnant rim may exist at the peak and that, although no actual crater exists now, volcanic breccia is present at the summit. They also suggested that the region of the summit may be part of a crater rim and that the most eastern ridge could be a late and smaller crater within the larger crater. Baldwin and Muehlberger also identified some peripheral cones and flows on the east and north slopes, the basalt of which was more siliceous than other basalts in the volcanic field, based on a low index of refraction, and contained small amounts of olivine. In their report, a chemical analysis of a sample from Sierra Grande was grouped with the Red Mountain dacite of Collins (1949) and was also the same as the one in Clarke's 1915 report.

Stormer (1972b) has given the most recent information on Sierra Grande as part of his survey of the Raton-Clayton volcanic field and presents the only other two chemical analyses of samples from Sierra Grande. He stated that the volcano overlies the typical Clayton basalt and may be contemporaneous with the mafic feldspathoidal volcanics of the field. Stormer identified two samples as pyroxene andesite from the northwest base of Sierra Grande and stated that the volcano is the only one in the Raton-Clayton field containing a two-pyroxene andesite). Stormer noted that the andesite was olivine free (except as rare microphenocrysts), had some quartz inclusions, and contains feldspars that were more sodic than similar volcanics found in orogenic suites. He also noted phenocrysts of clinopyroxene coexisting with phenocrysts of orthopyroxene which have a reversed zoning (hypersthene cores surrounded by more magnesium-rich margins). Stormer interprets this mineralogy as evidence that the initial growth of the orthopyroxenes was not in equilibrium with the growth of the clinopyroxenes and states that the presence of these hypersthene cores and quartz inclusions might represent remnants of metamorphic rock assimilated by an olivine basaltic magma. However, according to Stormer, a typical Clayton basalt would have to assimilate an unreasonable amount of quartz and alkali feldspar to be chemically equivalent to the andesite.

Stormer (1990 personal communi.) suggests that the lavas of Sierra Grande have a wide variation in textures across the volcano but are chemically the same.

Sierra Grande lavas

The Sierra Grande andesitic lavas have been described as being different in chemistry and mineralogy from the andesites of the Red Mountain lavas and yet possibly having a common origin (Stormer, 1972b). The phenocrysts identified are orthopyroxene, some with hypersthene cores, and augite, which are often glomeroporphyritic. The microphenocrysts are clinopyroxene, orthopyroxene and rare olivine within a groundmass composed of feldspar, oxides, pyroxene and rare quartz in a microcrystalline and/or glassy texture (Stormer, 1972b).

The Sierra Grande lavas and the Feldspathoidal lavas are contemporaneous, 1.9$\pm$ 0.05 and 1.8$\pm$ 0.1 Ma respectively (Stormer 1972a), and Stormer suggests that there might have been an equivalent origin for the two or, at least, the possibility that two magma sources existed with separate systems but with a common requirement (e.g., water enrichment). Stormer (1972b) proposes that the origin of Sierra Grande lavas is the result of partial melting in the upper mantle, similar to that for the Red Mountain lavas and suggests that there has not been any fractional crystallization. Also, that a mechanism under relatively high partial pressures of water, approximately 3.8 kb derived from an Fe-Ti oxide geothermometer, would be a possible magmatic origin. However, Stormer also stated that if the quartz grains in his samples from Sierra Grande were not xenolithic, then a minimum on the estimated depth of melting would be about 13.8 kb or 40-45 km.

In summary, previous work provides no detailed mapping, minor sampling and only three chemical analyses to serve as a basis for understanding the structure and petrology of Sierra Grande. The purposes of this study are to provide a more detailed field description of Sierra Grande, to describe more accurately its lithology and how it relates to the volcanic field in which it resides. This has been accomplished by completing a stratigraphic survey and geologic map of the northern half of the volcano, petrographic analyses of 84 thin sections, and microprobe analyses of 23 samples.

VOLCANIC STRATIGRAPHY AND LITHOLOGY

The geological field study was conducted in June and July 1990, during which the northern half of Sierra Grande was mapped (Appendix H, Geologic Map). The strategy, based entirely on lithologic characteristics and topographic relationships, was regularly revised and updated using the collected samples and accumulated field-site descriptions to arrive at a relatively uniform division of mappable units.

The observations recorded included the color of samples and outcrops (usually of both weathered and fresh surface), textural features and mineral identification of samples, the locality, and stratigraphy and structure of outcrops. Sample descriptions were initially organized into lithologic units; each included samples with similar color, texture, and apparent mineralogy. This synthesis resulted in identifying 9 major lithologic/flow units (0, 1, 2, 3, 4, 5, 6, 7 and 8), most with several subdivisions, and was then used to establish 12 mapping units. This was accomplished by designating units 1, 2, 3, 4, and 5 as lithologically and stratigraphically distinct flow units of the volcano proper. Lithologic/flow unit 6 was subdivided into 4 separate lithologic units (6a, 6b, 6c, 6d) based on stratigraphic position and isolated occurrence at the summit of the volcano. Samples of lithologic/flow unit 7 belong to the peripheral cinder cones that flank Sierra Grande. Dike rocks, which are found on Sierra Grande and the peripheral cones, occur in stratigraphic positions that indicate emplacement late in the volcano's history and were grouped together as lithologic/flow unit 8. Of the 12 mapping units, 11 were used for the completion of the geologic map (Map 1). Unit 0 was omitted from the map as it was determined to be of the surrounding plain on which the volcano is situated. The field descriptions of the lithologic/flow units are arranged in relative stratigraphic position from the oldest to youngest. An exception to the order is the dikes; their descriptions follow the units in which they are found to occur. Sample locations are listed in Appendix F and the Topographic Map in Appendix H.

Unit 0 - olivine basalt

The extrusive flow forming the surrounding plain on which the volcano is situated is an olivine basalt. This basalt crops out in the ditches and outwash areas away from the base. The rock is jagged and has the typical malpais appearance. Larger outcrops have the typical pahoehoe features of basaltic lavas. These rocks are of the Clayton basalt which forms a large flow that extends from the vicinity of Sierra Grande southeastward to near the town of Clayton (Figure 1).

The basalt is black to greenish black, moderately vesicular (relatively small vesicles) and moderately porphyritic. Phenocrysts are green to dark green (olivine and pyroxene). Much of the rock is in the form of float blocks that have weathered to a dull brown to dark brown and some of the rock has been weathered to a greenish friable state. A sample was collected at a ditch next to Highway 64/87 [NE1/4, NE1/4, Sec 23, T29N, R29E].

Unit 1 - first basaltic andesite

The first basaltic andesite flows form the lower slopes and base of the volcano of the west half of the volcano. The andesite crops out along the north-northeast side between 2050 - 2090 m and around to the west side between 2130 - 2180 m. The flows extend a short distance onto the surrounding plain as hummocky and malpais hills, particularly on the northeast side (Geologic Map).

Samples are black to very dark gray, moderately vesicular (small to medium) and slightly porphyritic. Phenocrysts are olive green to green (olivine and pyroxene). The rock weathers to a dark gray to gray and then a dull brown and exfoliates a weathered skin of about 5 mm in thickness. There is secondary mineralization (calcite) filling some vugs, which have been enlarged by weathering. Flow identification is inferred from the shape of the hills and slopes, and from a few larger continuous outcrops. A fresh sample was taken from a recent excavation [SE1/4, NE1/4, SE1/4, Sec 18, T29N, R29E].

Unit 2 - second basaltic andesite

The second basaltic andesite is exposed in a small but rather broad ravine on the lower west-southwest slope of the volcano between 2155 - 2215 m. This basaltic andesite is younger than the first basaltic andesite and older than the flows of the first andesite, but its relationship to the third basaltic andesite is unclear in the field (Geologic Map). The flow or flows form a gentle sloping rise within the ravine and are blocky, but the blocks are relatively small in comparison to subsequent andesite flows.

The rock is gray to dark gray, moderately to very vesicular and moderately to very porphyritic. The phenocrysts are dark green to green (pyroxene and olivine) and many have weathered to a reddish copper or copper brown color. The rock weathers to a gray to dull brown to dull reddish brown. Secondary mineralization (calcite) occurs primarily along fractures and in some surface to near surface vugs. This is the most porphyritic rock of the volcano. Two fresh samples were obtained about halfway up the ravine at a flow front [N1/2, NW1/4, Sec 1, T29N, R29E].

Unit 3 - third basaltic andesite

Cropping out at mid to lower slope is a third basaltic andesite. Exposures can be found on the north side between 2090 - 2185 m and on the east side between 2005 - 2095 m. This basaltic andesite is younger than the first basaltic andesite since it is exposed above it on the north-northeastern side (Geologic Map). This andesite extends from the north to east sides, forming the lower slopes and the base of the volcano, where it resides directly on the surrounding plain. The flows are blocky and platy, and the blocks are larger than those of the first basaltic andesite.

This andesite is dark gray to steel blue gray (with an almost grainy appearance), very vesicular, and slightly porphyritic. Phenocrysts are green to olive green (pyroxene and olivine). There are also some xenoliths (4 to 5 cm in diameter) composed of white and rounded grains of quartz. An origin for these might be a quartz sandstone in the underlying country rock, possibly the

Dakota sandstone. The rock weathers to shades of dull brown and reddish brown and the outer layers exfoliate exposing inner layers which are gray and only slightly altered. Fresh samples were obtained from a quarry located on the east-southeast side of the volcano [SW1/4, NE1/4, Sec 26, T29N, R29E].

Unit 4 - first andesite

The first andesite appears to have originally covered most if not nearly all of the previous flows of the volcano and occurs in the form of float and platy flow structures exposed above the lower slopes. Outcroppings, from east to west, are composed of 6 subunits which have a common stratigraphic position and similar texture, and therefore have been combined into one mapping unit. The andesite flows overlie the first basaltic andesite along the north to west sides, the third basaltic andesite along the northeast to east sides, and appear to underlie the flows of the second andesite almost everywhere (Geologic Map). Most of this andesite has apparently been removed from above the second basaltic andesite. The flows form the gentle to almost flat areas on the east side of the volcano at mid slope between 2060 - 2155 m. Flow and float plates have a rather flinty appearance and the float is somewhat altered. At some outcrops the platy flows are horizontal and sparsely exposed while at other places the platy flow blocks are nearly vertical with a dike-like aspect and most are only a meter or two thick. This andesite appears to have been the most eroded flow sequence, leaving platy blocks as float.

The rock is generally very dense, breaks in a flinty manner and has a tuffaceous appearance; it is bluish gray to light gray to pinkish gray to red, very slightly vesicular to vesicular, and very slightly porphyritic. Phenocrysts are dark to light green (pyroxene). The rock weathers to a light brown or very light brown. Some weathered samples have banding with various colors (e.g. purple, violet, red, orange, yellow, blue and green) and a very few have lenses of varying colors. The banding appears to extend into the outcrops and the styles of banding either vary or are not present at all, making it difficult to correlate between outcrops. Samples were collected at numerous locations (Appendix F).

Unit 5 - second andesite

The thickest and most voluminous flow sequence, covering nearly the upper 2/3 of the volcano, is the second andesite (Geologic Map). It is exposed above 2185 m on the west side, above 2150 m on the north side and above 2090 m on the east side. Flows have cooled to form very massive and blocky structures, with blocks ranging from .5 meter to over 6 meters. At some outcrops, particularly on the east side, the flows are underlain by a thin platy flow which belongs to the first andesite. The ends of some flows on the west slopes form ramping structures with typical curved fronts. This feature is believed to have been created by drag due to the vertical difference in viscosity within the flow as exhibited by a blocky flow above a platy flow. Erosion of this andesite, at some flow edges, has formed the deep ravines found on the volcano. Individual flow distinctions were not made except for a series of later extrusions that occur at or near the summit, which are smaller in length and composed of angular blocks.

Samples are gray to bluish gray to dark gray or mottled in appearance (gray to light gray or purplish gray to very light gray), are moderately to very vesicular and moderately porphyritic. Phenocrysts are olive green to green to dark green (pyroxene). In a few samples, minor amounts of quartz are present as secondary mineralization or inclusions. The rock weathers either to a dull light brown or dark brown, often with a reddish to very dark red tint. There are 3 distinct petrographical subunits of this andesite, however in the field these samples are found at various locations (Appendix F) and elevations, and were therefore mapped as a single unit.

Unit 8a andesitic dikes

Approximately 25 percent of the float rock that occurs on the slopes, from the high elevations to the base, has been inferred as being dike material. Andesitic dikes crop out on the lower slopes, upper slopes and just below the summit in contact with either the first or second andesite (Geologic Map). The rock is black to greenish black, dense, usually jointed, vesicular to moderately vesicular, and porphyritic to slightly porphyritic. The phenocrysts are green to olive green

(pyroxene). The vesicles are a few millimeters in diameter, often ovate and are very uniformally distributed. The rock weathers to a light brown to brown. A sample used for microprobe analysis was taken from a dike above mid-slope (2,285 m) [SE1/4, SE1/4, Sec 20, T29N, R29E].

Unit 6a - summit andesite

The summit andesite appears to comprise the outer surface of the summit area (Geologic Map) and underlie the weathered slopes above 2550 m. It crops out at and just below the top of the eastern peak and occurs as a minor amount of float along the slopes of the summit. There is no contact between this lithologic unit and any other present at the summit, and the slopes are very weathered making it difficult to be confident of outcrops or to obtain fresh samples. The andesite has a cinder and/or tuffaceous appearance and is stratigraphically younger than all previous flows (first basaltic andesite through the second andesite) with the exception of the flows of the second andesite that occur at the summit.

The rock is either reddish gray to bluish-red gray often with a purplish banding, dense, with a grainy to crystalline texture, and aphanitic to slightly porphyritic with dark green to green phenocrysts (pyroxene) or orange red to red, dense, with a sandy texture, slightly vesicular, and very slightly porphyritic with dark green phenocrysts (pyroxene). Weathered cavities and/or vugs are filled with a brown to yellow mineralization. This rock weathers to a very dull orange, orange red or red. The above rock descriptions were grouped together as a mapping unit because of the lack of outcrops and generally poor quality of samples, which were collected near the top of the east peak [SW1/4, SE1/4, Sec 32, T29N, R29E].

Unit 6b - andesitic breccias

Andesitc breccias occur at the summit of Sierra Grande (Geologic Map). The breccias occupy the saddle area, from just below the east peak at about 2615 m to 2675 m near top of the west peak. There are three breccias, which have been grouped together on the basis of their generally common lithology and stratigraphic position. Fresh samples were only collected for the first

breccia; the others appear somewhat weathered and occur mostly as float. Samples were collected at several locations along the saddle [NW1/4, SE1/4, to SE1/4, NW1/4, Sec 32, T29N, R29E].

The first breccia (clasts 2 - 3 cm), is bluish gray and greenish gray, very slightly mottled, very dense and aphanitic to slightly porphyritic. The phenocrysts are dark green to green (pyroxene). The rock weathers to a dull brown or dark brown and with a bumpy appearance and crops out all along the saddle as a prominent ridge.

The second breccia (clasts .5 - 2 cm), is red, bluish gray, purple, light purple and very light brown, slightly dense, grainy, slightly porphyritic and slightly vesicular. Phenocrysts are dark green or black (pyroxene) and are small but have definite distinguishable euhedral and/or subhedral shapes. This breccia occurs near the west peak as small blocks but mostly as float. The rock weathers to a light brown to brown.

The third breccia (blocks .5 - 3 cm), is red, purple, blue, gray, light brown and orange, dense, slightly porphyritic and very slightly vesicular. Phenocrysts are very fine and dark green (pyroxene). The rock weathers to a light brown to brown and occurs only as float at the very top of the western peak.

Unit 6c - andesitic plug

Appearing as a cairn-looking structure, a possible andesitic plug crops out on the east edge of the saddle area just below the eastern peak (Geologic Map), at approximately 2620 m. This structure is approximately 4 to 5 meters in height, about 3 to 4 meters in diameter at the base and about 1 to 2 meters in diameter at the top. The rock forms platy and/or lenticular slabs that are very angular.

The rock is dark gray to gray, mottled, slightly vesicular (few vesicles, however they are rather large and flattened) and slightly porphyritic, at the base of the plug. The few phenocrysts are dark green to green (pyroxene), very crystalline and some have a bluish brown tint (most likely from weathering). Above the base, the rock is dark gray to dark bluish gray, very dense and aphanitic to

porphyritic. Phenocrysts are brown to dark green to olive green (pyroxene), very dark bluish gray or clear crystals (most likely quartz) and some brown specks that have a metallic luster. This andesite does not appear to be very weathered and where it is weathered, the surfaces are brown to light brown, and very thin and flaky. Samples were obtained from the base and halfway up the structure [NW1/4, SE1/4, Sec 32, T29N, R29E].

Unit 6d - saddle andesite

Exposed as a blocky flow situated in and perpendicular to the saddle area between the peaks (Geologic Map) is another andesite. It crops out between 2630 -2660 m, is small in area near the center of the saddle and extends down both sides of the saddle for a short distance. This andesite crops out within the first andesitic breccia.

Samples are dark gray to bluish gray and aphanitic to porphyritic. The phenocrysts are dark green to olive green (pyroxene) and there are some inclusions that are pinkish brown to pinkish gray which appear to be a secondary mineralization. Some of the olive green phenocrysts are rather powdery, probably due to weathering. Weathered surfaces are light brown to brown with a pink tint. Samples were taken from the north side of the flow [NE1/4, SW1/4, Sec 32, T29N, R29E].

Unit 7 - basaltic scoria and basalt

Basaltic scoria occurs at the three peripheral cinder cones around the base of the volcano and at two cinder vents on the lower slopes (Geologic Map). A basalt crops out at the base of a cone on the east side. The smallest cone, located in an isolated and broad ravine on the west side of the volcano [NE1/4, NE1/4, Sec 35, T29N, R28E], is the most circular. It rises approximately 32 m and the scoria overlies the first basaltic andesite and the first andesite. The next largest cone is located on the east side [SW1/4, NW1/4, Sec 36, T29N, R29E]. It is slightly elongated in a northeast to southwest direction, has one dike associated with it, rises nearly 93 m and overlies the second basaltic andesite. The largest peripheral cone occurs on the west-northwest side of Sierra Grande[Sec 26, T29N, R28E]. This cone is elongated in an east-northeast to west-southwest direction

and widens out at its west-southwest end. It rises approximately 123 m and is connected to the main volcano by a small saddle area. The basaltic scoria of this cone overlies the first basaltic andesite, the first andesite and second andesite. The two vents found on Sierra Grande have roughly circular outlines. One is situated on the lower east slopes at about 2142 m [SW1/4, S 1/4, Sec 26, T29N, R29E]. The other is on the north side, mid slope at about 2302 m [NW1/4, SW1/4, Sec 21, T29N, R29E]. The vents have extruded through the second andesite.

Fresh exposures of the scoria are red and black and the basalt is greenish black. Both are vesicular to very vesicular and slightly to moderately porphyritic with dark green to green phenocrysts. The rocks vary in density and in some cases the scoria appears almost welded. The rock weathers to a dull red to reddish orange for the red scoria, a dull brown to light brown to yellow ocher for the black scoria and green for the basalt. Vugs are filled with secondary mineralization (calcite). In addition, one sample of scoria found on the east cinder cone is black to brown and very glassy. Also, several volcanic bombs were found near the base of the west-northwest cinder cone. Samples were obtained from all locations (Appendix F).

Unit 8b - basaltic dikes

A basaltic dike grouping occurs on a saddle area between the main volcano and the peripheral cinder cone on the west-northwest side (Geologic Map). It is composed of three separate dikes radiating away from a circular outcropping. One dike, which trends west, is actually a set of parallel dikes that traverse the saddle, intrude into the cinder cone and then split near the cone's center with one trending southwest and the other trending west-southwest. The second dike trends northwest and the third dike trends south-southwest. This rock is greenish black to black, dense, slightly to moderately porphyritic, and slightly to moderately vesicular. Phenocrysts are dark green to green (olivine and pyroxene) and vesicles are small to medium in size (less than a centimeter). Weathering gives the rock an almost phaneritic texture; it weathers to a greenish brown to dark brown. A sample was collected from the parallel dikes about midway along the saddle [SE1/4,

NE1/4, Sec 26, T29N, R28E].

The other basaltic dikes, which occur at the peripheral cones, include an additional dike found on the west-northwest cinder cone and a dike that parallels the slightly elongated shape of the east cone (Map 1). The first dike is composed of rock that is steel gray to gray, very dense and aphanitic to slightly porphyritic. Phenocrysts are black to dark green (pyroxene and olivine). The rock weathers to a bluish gray to brown to bluish black and it breaks in a flinty manner. The other dike is composed of rock that is very dark gray with a purplish tint, slightly vesicular and slightly porphyritic. The phenocrysts are dark green to green (pyroxene and olivine). This rock weathers to a dull brown to dark brown and breaks into very angular blocky shapes. Samples were obtained from both dikes (Appendix F).

VOLCANIC HISTORY

Field interpretation of the lithologic/flow units previously described suggests a sequence of events for the formation of Sierra Grande. These events have been separated into five stages.

Stage 1 pre-Sierra Grande

The largest flow of Clayton basalt occupies the eastward dipping plain on which Sierra Grande is situated (Figure 1). Within the volcanic field, the basalt emanated from vents and cones above fissures in the underlying sedimentary rocks and Precambrian basement (Baldwin and Muehlberger, 1959; Stormer, 1987). Judging from the location and orientation of the flow, it is possible that the source vent may have coincided with or was adjacent to the conduit for the lava flows of Sierra Grande. This could add some support for Collins' (1949) statement that the volcano was a vent for many of the rock types in the volcanic field.

Baldwin and Muehlberger (1959) identified a vent on the east side of the volcano, which corresponds to the second largest cinder cone, and stated that this vent was most likely the source for the Clayton basalt flow that extends from the vicinity of Sierra Grande to near the town of Clayton. However, this would require that the cinder cone was emplaced prior to Sierra Grande. The problem with this scenario is that the cinder cone partially overlies the second basaltic andesite of Sierra Grande (Geologic Map) which in turn overlies the Clayton basalt.

Stage 2 the early flows

The first flows of Sierra Grande were three successive, but distinctly separate, basaltic andesites (unit 1 followed by unit 2 and then unit 3). These lithologic/flow units, based on field interpretation of their overall flow direction, erupted from a central vent, the location of which coincides with the position of the present day summit.

The first basaltic andesite is the most mafic appearing rock of the volcano, based on color index. The flows that comprise this unit extruded to the northeast, north, northwest, west and

southwest. These flows appear to exhibit a typical basalt viscosity, at least at the distal margins as represented by present day exposures and lateral extent. The next lavas to extrude were the second and third basaltic andesites. Judging from the flow fronts at an isolated outcrop, the second basaltic andesite extruded to the southwest overlapping the first basaltic andesite. It is conceivable that flows of this unit also extruded west and south, however, there were no other outcrops exposed in the mapped area. The third basaltic andesite extruded to the north-northeast overlapping in part the first basaltic andesite, and to the east and southeast onto the Clayton basalt. Interpretation of the flow extent for and general thickness of the first and third basaltic andesites suggests that at the end of this stage the volcano was; an asymmetrical feature, had reached its maximum lateral extent, and may have reached about 1/3 its present height. Erosion of these units has been only moderate with most of the flow fronts retaining much of their original shapes.

Stage 3 the later flows

The extrusions of this stage include the extensive flows of the first andesite and the dominating flows of the second andesite. The source vent for these flows, based on the their symmetrical arrangement and radial pattern, was a crater that formed above the central vent, during the extrusions of the earlier basaltic andesites.

The first andesite, which had a greater lateral extent toward the east, covered much if not nearly all of the volcano's previous lateral extent and has been extensively eroded with much of it occurring as float on the lower slopes of the volcano. This andesite was apparently less viscous, resulting in broad and rather thin outcrop units as compared to previous and subsequent flows. This andesite covered earlier flows in a somewhat blanket manner by apparently filling in depressions between previous flows and thinly covering the tops of the flows, thereby smoothing out the general topography. A few upright structures of this andesite are interpreted as being the remnants of flows that had filled areas between earlier flows and which, upon erosion of the higher portions that covering the earlier flow tops, have been left remaining with dike-like appearances. At the end of

this eruptive sequence the volcano was probably a nearly symmetrical topographic feature, based on field interpretation of the uniform coverage and thickness of the first andesite.

The second andesite followed as numerous, very large and voluminous flows that erupted radially from the central crater, contributing to the majority of the volcano's mass and building it up to approximately a little more than its present size. This andesite was clearly viscous as the flows are very massive and reach only a little more than 2/3 of the way down the volcano's slopes. A few flows of this eruptive sequence, particularly on the west side, either had a sufficient force or low gradient or both to create ramping structures. These second andesite flows have definitely been eroded. Ravines that create a radial pattern on the volcano resulted from the down cutting of water along the edges and contacts of adjacent flows. Apparent dip directions measured near the sides of the flows indicate a downward direction toward the ravines. Most of the erosion occurred at the flow sides and only a moderate amount of surface appears to have been removed. Late eruptions of this andesite, small blocky flows that appear to have erupted from the base and sides of the volcano's summit, indicate that this sequence chronologically extends into the next stage.

Stage 4 the summit

The previous flows of Sierra Grande could be identified as successive and distinct. At the summit, however, it is more complex and any interpretation based on field interpretation is in part speculative. The topographic features of the summit are the two peaks, a slightly lower saddle region connecting the peaks and two (cirque-like) depressions on either side of the saddle. The slopes of the summit are relatively steeper than those lower on the volcano.

The formation of the summit was the final activity of the volcano and began near the end of the previous stage. The age relationship between the remaining lithologic/flow units of the summit is not as clear. The following is one possible scenario from field interpretation.

The summit formed as eruptions of the summit andesite accumulated at the crater or central vent. This andesite is the first and dominant lava of this stage. The accumulating material

concentrated at both the east and west sides of the crater rim, forming the peaks of the volcano. A transition from the preceding stage and this stage is evident from a few late flows of the second andesite, which erupted from the lower slopes and sides of the summit. Between the peaks, an area of least accumulation above the central vent was the source vent for some of the late second andesite extrusions. The final event was an explosive one that produced the andesitic breccias, filled in the central vent and the crater area not occupied by the peaks, and created the saddle region. Any ash expelled has long been eroded away, although it is possible that the soil covering much of the summit and even other portions of the volcano could be from such ash. The andesitic plug and saddle andesite squeezed up through minor fissures within the summit and andesitic breccia, respectively, as the last extrusions of the volcano. The summit has been subsequently modified by erosion, the extent of which is uncertain, but more so than most of the earlier flows. The two (cirque-like) depressions are topographic features that resulted from the erosion of the side of the saddle.

Stage 5 the peripheral cinder cones and vents

The features of this stage are definitely younger than the previous lithologic/flow units. The cinder cones, which are located around the perimeter of Sierra Grande, overlie one or more of the earlier flows (i.e., the basaltic andesites and the early andesites) and have experienced only moderate to very little erosion; they are nearly intact. It is possible, therefore, that these cones may be contemporaneous with Mount Capulin, which would give them an age of about 10,000 yrs. The composition of the cones is either basaltic scoria or basalt and basaltic scoria. The composition difference and both the apparent and possible age difference between the cones and volcano suggest that the cones may be unrelated to Sierra Grande. The relationship between the volcano and the cones will be discussed later in the paper.

The basaltic vents are the center remnants of much smaller undeveloped cones. These vents are located in the second andesite on the lower slopes of the volcano. The age relationship to the larger cones is uncertain; however, it is likely that they are contemporaneous and therefore have been

considered as such.

The smallest cone formed in an isolated ravine or valley on the west side. A rim of more fused cinder rock is present at the top as a nearly complete circle. Located on the east side, the second largest cone has experienced very little erosion. The top of this cone still retains some rim like features. The largest cone, located on the west-northwest side, has experienced only a moderate amount of erosion and there is a general outline of the central vent still present. Prior to any erosional modification, this third cone experienced an explosive event. This is inferred from an opening on its west-southwest side and a widening shape of the cone trending west-southwest.

The dikes

Dikes were found on the main volcano and two of the peripheral cinder cones. Their ages could only be inferred by their crosscutting relationships to the associated flows or the cones. Several andesitic dikes intrude the main volcano at mid-slope, lower slope and just below the summit. These dikes crosscut the flows of the first or second andesite and are in some places exposed less than a foot above the flows, indicating that some of the andesite has been removed. These dikes appear to be of similar composition and are all very mafic, more so than the host rock. The basaltic dikes of the peripheral cinder cones apparently are related to cone formation as possible feeder dikes. The dikes found on the east cone and the west-northwest cone have trends that parallel the shape of the cones.

PETROGRAPHY

There is some degree of variation between samples within lithologic/flow units. This resulted in separating many of the litologic/flow units into subunits. In unit 4, the samples are subdivided on the basis of field lithologies. For unit 5, subdivisions were made solely on three distinct textures determined petrographically, however, they were mapped as a single unit. Based on distinct, separate outcrops and some lithologic differences, unit 6 was divided up into four lithologic units, each a separate mapping unit. In addition, unit 6b was further subdivided into three separate subunits based on color and textural distinctions, differences between angular fragments, fragment sizes, intersertial material and mineralogy. In unit 7, the samples are divided into four textural and lithologic subunits, determined by both field and petrographic observations. The samples of unit 8 have been subdivided into two subunits on the basis of field observation, field location, petrographic textures and lithology.

Most of the plagioclase in the samples of lithologic/flow units occur in three generations. However, in some samples only one or two generation(s) is present and in a few samples of the basaltic scoria and basalt none are present at all. The three generations consist of: 1) a few unstable phenocryst or microphenocryst with inclusions and irregular or corroded margins, 2) stable phenocryst and/or microphenocryst subhedral laths with zoning, and 3) groundmass microlites. If only two generations are present they are the subhedral laths and groundmass microlites. One generation of plagioclase consists of only groundmass microlites. The majority of phenocrysts to microphenocrysts, are either olivine and clinopyroxene, clinopyroxene, or clinopyroxene and orthopyroxene. These minerals are euhedral to subhedral, nearly equidimensional crystals. The samples have varying degrees of pyroxene clustering and this variable glomeroporphyritic texture is responsible for the extent of porphyritic texture in the hand specimens. Some olivines and pyroxenes exhibit skeletal growth. The plagioclase microlites mostly dominate the groundmass and show either a subparallel to parallel alignment or a random orientation. The other principle groundmass constituent is glass

which varies in color and abundance.

First basaltic andesite (unit 1)

This andesite has a hypocrystalline, microporphyritic to slightly porphyritic, slightly to moderately glomeroporphyritic, slightly trachytic and vesicular texture. Plagioclase occurs in three generations, the microphenocryst to phenocryst subhedral laths amount to about 3 modal percent and have either normal or reverse zoning. Olivines and clinopyroxenes (augite) amount to less than 5 modal percent with some of the olivines exhibiting skeletal growth; and some of the pyroxenes being clustered. There is also a trace amount of quartz which appears to be either secondary mineralization or a xenocryst; slightly irregular to rounded shaped grains. The groundmass is dominated by the plagioclase microlites, about 65 percent, with some subparallel to parallel alignment. Also anhedral grains of olivine and pyroxene, and a trace amount of anhedral Fe-Ti oxide are present. The remaining groundmass is brown glass comprising approximately 25-30 percent.

Second basaltic andesite (unit 2)

The texture of this andesite is holo- to hypocrystalline, microporphyritic to slightly porphyritic, moderately glomeroporphyritic, trachytic to microlitic and vesicular. Three generations of plagioclase are present and microphenocryst to phenocryst subhedral laths (5-10 modal percent) appear to have either normal or reverse zoning. Clinopyroxenes (augite) are the dominant microphenocrysts and phenocrysts amounting to approximately 10-15 modal percent. Olivine microphenocrysts and phenocrysts are also present and amount to less than 5 modal percent. The pyroxenes are highly to moderately clustered and the glomeroporphyritic texture is responsible for this andesite being the most porphyritic appearing lithologic/flow unit. Both the olivines and pyroxenes exhibit some skeletal growth. The groundmass is dominated by parallel aligned plagioclase microlites, about 80-85 percent. Also present in the groundmass is anhedral pyroxene and olivine, a trace amount of anhedral Fe-Ti oxide and less than 5 percent brown glass.

Third basaltic andesite (unit 3)

This andesite has a holo- to slightly hypocrystalline, microporphyritic to slightly porphyritic, slightly to moderately glomeroporphyritic, trachytic to microlitic and vesicular texture. The plagioclase is present in three generations with stable microphenocryst to phenocryst subhedral laths amounting to less than 5 modal percent. Clinopyroxenes (augite) and olivines are the primary microphenocrysts and phenocrysts, amounting to less than 5 modal percent each. Some of the pyroxenes and olivines show skeletal growth and a few of the pyroxenes are clustered. Plagioclase microlites dominate the groundmass comprising about 80-90 percent and show some parallel alignment. Anhedral pyroxenes and olivines are present along with a minor amount of anhedral Fe-Ti oxides. The remaining groundmass is gray and brown glass and is less than 5 percent.

First andesite (unit 4)

There are six subdivisions of this andesite derived from differences in hand specimen textures and colors, however they are grouped together based on a common stratigraphic position. The petrographic textures vary largely due to the amount of glass present and the degree of plagioclase microlite alignment. Variation in mineralogy is primarily due to the presence or absence of plagioclase remnants and quartz.

The texture of the andesite is holocrystalline or holo- to hypocrystalline or hypocrystalline, microporphyritic to very slightly porphyritic, slightly to moderately glomeroporphyritic, slightly trachytic to trachytic to microlitic, and moderately vesicular to vesicular. In two subunits plagioclase occurs in three generations and the stable microphenocryst subhedral laths comprise about 2 modal percent. The remaining samples have two generations of plagioclase, microphenocrysts and groundmass. The dominant microphenocrysts and few phenocrysts are clinopyroxenes (augite), ranging from less than 5 percent to between 5 and 10 modal percent with many of them clustered and a few exhibiting skeletal growth. In the samples that contain remnant plagioclase, there is also present traces of quartz which appear to be either secondary or a xenocryst; they are slightly irregular

to rounded grains. Plagioclase microlites dominate the groundmass, vary from 50-90 percent and have either a random or subparallel alignment. Present also are anhedral grains of pyroxene and Fe-Ti oxide. Some Fe-Ti oxides occur as coronas around a few microphenocryst pyroxenes or as partial replacement of a few pyroxenes having formed prior to groundmass plagioclase. The remaining groundmass is glass, ranging in color from gray to brown to red and in percentage from less than 1 to 42.

Second andesite (unit 5)

The second andesite has three subdivisions based on textural differences, however there is no correlation between texture and stratigraphic position. These textures imply a variation in crystallization both prior to and during extrusion. The textural variation is primarily due to the amount of glass present.

The textures are hypocrystalline or hypo- to holocrystalline or holocrystalline, microporphyritic to moderately porphyritic, slightly to moderately glomeroporphyritic, moderately trachytic to trachytic and/or microlitic, and moderately vesicular to vesicular. Plagioclase is found as three generations in all but the holocrystalline rock. Phenocrysts or microphenocrysts of plagioclase amount to less than 5 modal percent. A few of the second generation plagioclases in the hypocrystalline textures exhibit cuneiform crystal growth. The holocrystalline samples have plagioclases as microphenocrysts to phenocrysts and as groundmass microlites. The dominant microphenocrysts and phenocrysts in the hypocrystalline and hypo- to holocrystalline samples are clinopyroxene (augite) and orthopyroxene. In the holocrystalline texture, only clinopyroxene (augite) is present. The amount of clinopyroxene increases and orthopyroxene decreases with increasing crystallinity (hypocrystalline: cpx < 5 percent and opx 5 - 10 percent, hypo- to holocrystalline: cpx 5 - 10 percent and opx < 5 percent, and holocrystalline: cpx 5 - 10 percent and opx 0). In one sample of hypocrystalline rock, a rare stable euhedral to subhedral olivine phenocryst was identified and since no others were found it is presumed to be a xenocryst. The pyroxenes, mostly augite, are

clustered together and the degree of clustering varies between and within textural types. A few of the pyroxenes, again mostly augite, exhibit skeletal growth. There is also a trace amount of quartz present, except for in the holocrystalline samples, and this appears to be secondary mineralization, having slightly irregular to rounded shapes that fully or partially occupy vesicles. The groundmass in the hypocrystalline and hypo- to holocrystalline samples is dominated by the plagioclase microlites, 53 - 85 percent respectively, with a subparallel to parallel alignment. The holocrystalline rocks have a groundmass which is at least 90 percent plagioclase microlites. Gray and brown glass, present only in the hypocrystalline and hypo- to holocrystalline rocks, amount to 8 - 21 percent and less than 5 percent respectively. Present also, in all samples, are anhedral pyroxenes and anhedral Fe-Ti oxides.

Andesite dike (unit 8a)

The andesitic dike has a hypocrystalline, microporphyritic to slightly porphyritic, slightly glomeroporphyritic, and very vesicular texture. Plagioclase occurs in two generations and the microphenocryst to phenocryst subhedral laths amount to less than 5 modal percent. Clinopyroxene (augite) and orthopyroxene are the dominant microphenocrysts and phenocrysts, amounting to 5 percent and less than 2 modal percent respectively. Many of the clinopyroxenes are clustered together and a few exhibit skeletal growth. The groundmass is dominated by the plagioclase microlites (50 percent). Present also are anhedral grains of pyroxene, and trace amounts of anhedral Fe-Ti oxides. The remaining groundmass is brown glass (40 percent).

Summit andesite (unit 6a)

This andesite has a hypocrystalline to hypohyaline, microporphyritic to very slightly porphyritic, slightly to moderately glomeroporphyritic, and moderately vesicular to vesicular texture. Plagioclase occurs in three generations with stable microphenocryst to phenocryst subhedral laths amounting to less than 2 modal percent. Clinopyroxenes (augite) are the dominant microphenocrysts and are less than 5 modal percent. Some of the pyroxenes are clustered and some exhibit skeletal growth. The groundmass is dominated by plagioclase microlites, ranging from 30 to 50 percent, in

a relatively random arrangement. Present also is anhedral pyroxene and a trace amount of anhedral Fe-Ti oxide. The remaining groundmass is brown and gray glass ranging from 30 to 50 percent.

Andesitic breccia (unit 6b)

There are three distinct breccias identified at the summit of the volcano and definitely indicate a disruption of earlier andesitic material, the identification of which is uncertain. The breccias vary in block sizes and color and have minor differences in petrographic textures and constituents.

The first andesitic breccia has clasts of two different textures: holocrystalline, microporphyritic and very slightly glomeroporphyritic and hypocrystalline, microporphyritic and slightly glomeroporphyritic. There is a general vesicularity to the clasts which are surrounded by intersertal material that has a hypocrystalline to microcrystalline, microporphyritic, very slightly glomeroporphyritic and very slightly trachytic texture. The second breccia has clasts that are hypocrystalline, moderately glomeroporphyritic, microlitic, vesicular and either microporphyritic or microporphyritic to very slightly porphyritic with intersertal material that is hypohyaline to hypocrystalline, microporphyritic and moderately glomeroporphyritic. The clasts and intersertal material of the third breccia have a hypocrystalline to microcrystalline, microporphyritic, slightly to moderately glomeroporphyritic and vesicular texture. The first breccia has plagioclase in three generations, with less than 5 modal percent microphenocryst. The second and third breccia have only groundmass plagioclase.

The dominant microphenocrysts of the first breccia are clinopyroxenes (augite) amounting to less than 5 modal percent and there is about 2 modal percent olivine also present. Some of the pyroxenes are clustered and a few olivines and pyroxenes exhibit skeletal growth. Both the second and third breccia are dominated by similar pyroxenes and in approximately the same amount, and neither has olivine present. However, in the second breccia, the pyroxenes range from microphenocryst to near phenocryst with many appearing altered or replaced by Fe-Ti oxides and

none exhibiting skeletal growth. This suggests either a different crystallization path or later alteration in situ.

The groundmass of the first breccia (clasts and intersertal material) is dominated by the plagioclase microlites (about 65 percent). These microlites have a relatively random orientation within the clasts and a subparallel alignment within the intersertal material. This suggests two stages: 1) early crystallization followed by a disruption and 2) later crystallization prior to extrusion. Also present is anhedral pyroxene and olivine, a minor amount of anhedral Fe-Ti oxide and about 10 percent clear to gray glass. The groundmass of the second breccia is dominated by either plagioclase microlites (40 - 85 percent), or red and red to brown glass (10 - 55 percent). The crystallization of the microlites is identical to the first breccia. Present also in the groundmass are anhedral pyroxenes and Fe-Ti oxides. The third breccia has a groundmass that is dominated by the plagioclase microlites (about 60 percent) which have a random orientation both in the clasts and intersertal material. The remainder is composed of anhedral pyroxenes, trace amounts of Fe-Ti oxides and 30 percent gray and brown glass.

Andesitic plug (unit 6c)

This andesite has a hypo- to holocrystalline, microporphyritic to slightly porphyritic, slightly to moderately glomeroporphyritic, and vesicular texture. The plagioclase occurs in three generations with less than 2 modal percent stable microphenocryst to phenocryst subhedral laths. The dominant microphenocrysts and few phenocrysts are clinopyroxenes (augite) and amount to about 5 - 10 modal percent. Some pyroxenes are clustered together and a few exhibit skeletal growth. The groundmass, slightly microcrystalline, is dominated by plagioclase microlites, about 90 percent, in a relatively random arrangement. Present also is anhedral pyroxene, a trace amount of anhedral Fe-Ti oxide and less than 5 percent gray glass.

Saddle andesite (unit 6d)

The texture of this andesite is hypo- to holocrystalline, microporphyritic, slightly to

moderately glomeroporphyritic, and slightly vesicular. The plagioclase occurs in two generations and the stable microphenocryst subhedral laths amount to less than 2 modal percent. Clinopyroxenes (augite) are the dominant microphenocrysts, amounting to about 5 modal percent with some clustered together and some exhibiting skeletal growth. In a microcrystalline groundmass, fine plagioclase microlites (85 - 90 percent) dominate and occur in a relatively random arrangement. Also present is anhedral pyroxene, a trace amount of anhedral Fe-Ti oxide and a trace to less than 5 percent gray glass.

Basaltic scoria and basalt (unit 7)

The red scoria from the small cinder cone on the west side of the volcano has a hypocrystalline to hypohyaline, microporphyritic to slightly porphyritic, slightly to moderately glomeroporphyritic, and very vesicular texture. Plagioclase occurs in three generations with less than 5 modal percent subhedral laths. The dominant microphenocrysts to phenocrysts are clinopyroxenes (augite)(5 - 10 modal percent) and olivines (< 5 modal percent). Skeletal growth is exhibited by both the pyroxenes and olivines and a number of pyroxenes are clustered together. The groundmass is composed of plagioclase microlites (40 - 60 percent) and brown and red glass (20 - 50 percent). The microlites have a somewhat random orientation. Present also are anhedral pyroxenes and olivines and minor amounts of Fe-Ti oxides, some of which formed coronas around a few of the olivines.

The red to black scoria, from the east cone, has a texture that is hypo- to holohyaline, cryptocrystalline, microporphyritic and very vesicular. Present are stable microphenocrysts of pyroxene and olivine amounting to less than 5 percent each. All of the pyroxenes and olivines have coronas of Fe-Ti oxide which appears to have occurred during extrusion. The groundmass is dominated by red to brown glass (70 - 75 percent). Also present in the groundmass are anhedral pyroxenes and olivines, anhedral Fe-Ti oxides and traces of plagioclase.

Glassy scoria, also from the east cinder cone, has a holo- to slightly hypohyaline, cryptocrystalline, microporphyritic and vesicular texture. The microphenocrysts are olivines (about

10 percent) and pyroxene laths (< 2 percent). The olivines have been altered or resorbed with inclusions of opaques suggesting some instability prior to extrusion. The groundmass is composed of about 90 percent brown to black glass. Also present are anhedral olivines and pyroxenes. The glass, which likely contains a fair percentage of Fe-Ti oxide, has a convoluted structure suggesting turbulent flow during crystallization.

The basalt forming the base of the east cone has a hypocrystalline, partially microcrystalline, microporphyritic, very slightly glomeroporphyritic and vesicular texture. The minerals present are olivine (10 percent) and pyroxene (< 2 percent) microphenocrysts. The olivines are rimmed by Fe-Ti oxide, which occurred prior to extrusion. The groundmass is composed of microcrystalline olivine and pyroxene (about 40 percent) and anhedral plagioclase (about 30 percent). There is also anhedral Fe-Ti oxide and green glass, each about 15 percent. The oxides are generally opaque, however there are a few red and translucent needle-like crystals that may be rutile.

Basaltic dikes (unit 8b)

The textures of the basaltic dikes are: 1) hypocrystalline, cryptocrystalline, microporphyritic to slightly porphyritic, slightly glomeroporphyritic and moderately vesicular, 2) hypocrystalline, cryptocrystalline to microcrystalline, microporphyritic and vesicular and 3) holocrystalline to hypocrystalline, microcrystalline, microporphyritic to slightly porphyritic, and slightly glomeroporphyritic. Olivines and clinopyroxenes (augite) are the dominant microphenocrysts and phenocrysts. The mineral abundance ranges from 5-15 modal percent for olivines and less than 2 to 5 modal percent for pyroxenes. In one dike, some of the pyroxenes are clustered together. The olivines may exhibit skeletal growth and a few olivines and pyroxenes have alteration coronas of Fe-Ti oxides. The groundmass is dominated by either microcrystalline olivine and/or pyroxene, or glass. There is no crystalline orientation, which would follow with crystallization occurring during intrusion. The glass ranges from a trace amount to 40 percent of the groundmass. Also present is plagioclase (15 - 20 percent) and a minor amount of anhedral Fe-Ti oxide.

PARAGENESIS

The basaltic andesites, andesites and andesitic dike

Field interpretations indicate a series of lithologic/flow units that emanated from a common central vent. The petrographic analysis indicates that the successive lithologic/flow units exhibit a changing mineralogy, from olivine and clinopyroxene to clinopyroxene to clinopyroxene and orthopyroxene as the dominant phenocrysts and microphenocrysts. It can be infered from this changing mineralogy that a differentiating parent magma was present. Therefore, without any evidence to suggest multiple magma chambers or multiple batch melts, the Sierra Grande volcano was the product of successive extrusions from a single differentiating magma.

The first mineral phase to crystallize in the magma was the corroded plagioclase phenocrysts to microphenocrysts found in both the basaltic andesites and andesites. These are interpreted as remnants of an early crystallization in the magma at higher pressure, which remained dispersed throughout the chamber and had begun to readjust to equilibrium prior to extrusion. The plagioclases are single, rather sparse and are some of the largest crystals, which originally had nearly euhedral shapes but had been subsequently resorbed, as inferred from their irregular or corroded margins.

The mineral phases to crystallize next were: in the basaltic andesites - olivine, clinopyroxene and a second generation of plagioclase; in the first andesite - clinopyroxene and a second generation of plagioclase; and in the second andesite - clinopyroxene, orthopyroxene and a second generation of plagioclase. Crystallization of the olivines and clinopyroxenes in the basaltic andesites and of the clinopyroxenes and orthopyroxenes in the second andesite were contemporaneous, respectively, as euhedral to subhedral and equidimensional phenocrysts to microphenocrysts. The skeletal forms of several olivines and clinopyroxenes in the basaltic andesites and of several clinopyroxenes in the andesites, which are intergrown with the groundmass and groundmass plagioclase, suggests a period

of rapid crystallization that continued to just prior to extrusion. The clustering of many clinopyroxenes in the lithologic/flow units would indicate the onset of accumulation. The second generation of plagioclase was nearly contemporaneous with the olivines and/or pyroxenes, as stable nearly equidimensional and less abundant subhedral phenocrysts to microphenocrysts. The first crystallization phases of clinopyroxene, orthopyroxene and a second generation of plagioclase in the andesitic dike would suggest a co-genetic relationship with the second andesite.

The last mineral phases to crystallize in the basaltic andesites, andesites and the andesitic dike were the groundmass plagioclases (microlites), anhedral olivines and/or pyroxenes, and Fe-Ti oxide minerals. The olivine and/or pyroxene, and the plagioclase are nearly contemporaneous, as inferred from their approximately equal size. The parallel, subparallel or random orientation or the plagioclase microlites, in the basaltic andesites and andesites, indicate that they formed just prior to, during or after extrusion respectively. The Fe-Ti oxide minerals were either contemporaneous as anhedral grains surrounded by plagioclase, slightly later as intersertal grains between plagioclase crystals or much later as partial alteration or replacement of earlier olivines and/or pyroxenes. The interstitial glass was the last to form as the lavas and dikes cooled upon extrusion and intrusion, respectively.

The basaltic scoria, basalt and basaltic dikes

The composition of the cones and associated dikes (based on petrographic analyses) and the spatial and age relationship to the volcano (based on field interpretation) would suggest that the peripheral volcanics are unrelated to the magma chamber of Sierra Grande. Therefore, the basaltic cinder cones and associated basaltic dikes formed from a separate magma or magmas that extruded and intruded, respectively, around the perimeter of Sierra Grande.

The mineral phases to crystallize first were: in the basalt - olivine; in the basaltic scoria and basaltic dikes - olivine, clinopyroxene and in a few samples a minor amount of plagioclase. The olivines and pyroxenes of the scoria and dikes are nearly contemporaneous, as inferred from their

euhedral to subhedral shape and equidimensional size. Some of the olivines and clinopyroxenes in the basaltic scoria and basaltic dikes exhibit skeletal growth suggesting a period of rapid crystallization prior to extrusion. The basaltic scoria, basalt, and basaltic dikes have very little if any plagioclase phenocrysts to microphenocrysts; in those samples that do, the plagioclase is nearly contemporaneous with the olivine and pyroxene, as subhedral and nearly equidimensional crystals. A trace amount of a remnant plagioclase is present in one sample of basaltic scoria from the west cinder cone and is not found in the remaining basaltic scoria nor the basalt or basaltic dikes. This could support the possibility that each cone and associated dike(s) are from separate magmas.

The last mineral phases to form in the basalt, basaltic dikes, and most of the basaltic scoria were the groundmass plagioclases, anhedral olivines and pyroxenes, and Fe-Ti oxide minerals. The plagioclase, olivine and pyroxene are nearly contemporaneous, as equidimensional grains. The Fe-Ti oxide minerals mostly form late alteration coronas around some of the olivines, particularly in the basalt. The last to form upon extrusion in these lithologic/flow units was glass, which is the dominant and only other constituent, besides the earlier phenocrysts and microphenocrysts in the most glassy scoria.

MINERALOGY

Microprobe analyses of the lithologic/flow units support the petrographic interpretation that the lavas of Sierra Grande originated from a source different than that for the peripheral cones and associated dikes. Further, compositional changes between mineral phases of successive lithologic/flow units indicate that the parent magma of the volcano experienced a degree of differentiation.

Sierra Grande lavas and andesitic dike

olivine

Olivine crystals are present as phenocrysts and microphenocrysts, as well as in the groundmass of several lithologic/flow units of Sierra Grande in contrast to the findings of Stormer (1972b). They occur in the basaltic andesites, but in the andesites and andesitic dike none were observed petrographically or detected by microprobe analyses, with the exception of one crystal in one sample of the second andesite, which has been proposed as being a xenocryst. The olivines of the basaltic andesites (units 1, 2 and 3) are very Mg-rich (Fo_{79-91}) and the majority of the cores have compositions of Fo_{82} to Fo_{88}. A stratigraphical upward trend of Mg depletion can be inferred between the successive basaltic andesites and a plot of core averages supports this fractionation trend, at least between the first and third basaltic andesites (Figure 3). The single olivine in one second andesite sample is nearly identical to the olivines in the first basaltic andesite and is considered to be an oddity and will not be discussed further.

pyroxene

Although references to Sierra Grande by Stormer (1972b & 1987) would suggest that most of the volcano is composed of a two-pyroxene andesite (augite and orthopyroxene), only the largest and apparently the most viscous flow, the second andesite, contains two pyroxenes. Analyses indicate that the andesites contain either augite or augite and enstatite. Pyroxene compositions were

Figure 3. Olivine forsterite (Fo) values vs. lithologic/flow units of Sierra Grande and the peripheral volcanics in stratigraphic succession.

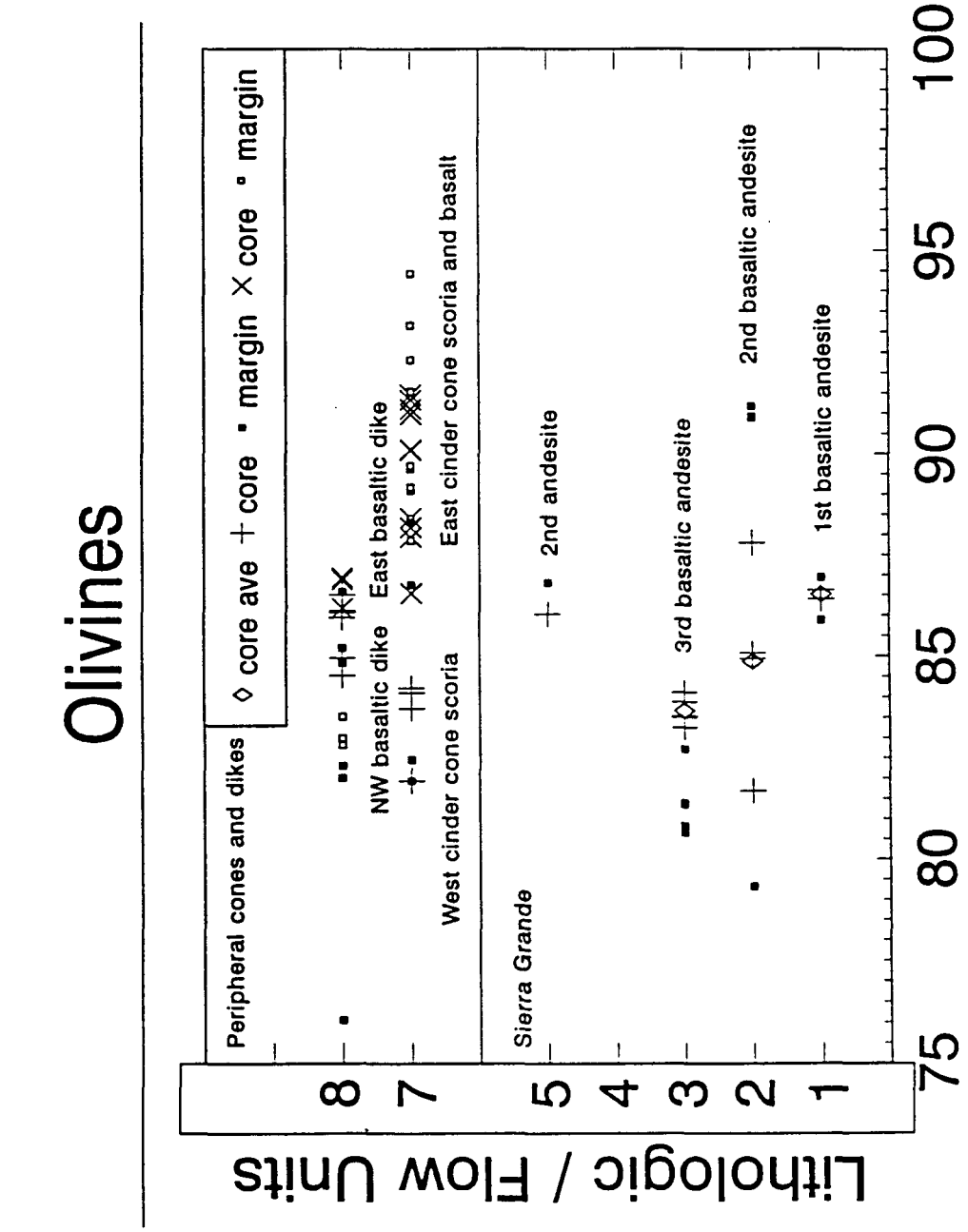
Olivines
Peripheral cones and dikes
◊ core ave + core ▪ margin × core ▫ margin
NW basaltic dike
East basaltic dike
West cinder cone scoria
East cinder cone scoria and basalt
Sierra Grande
2nd andesite
3rd basaltic andesite
2nd basaltic andesite
1st basaltic andesite
Lithologic / Flow Units
8
7
5
4
3
2
1
75
80
85
90
95
100
Fo

Figure 3

Figure 4. Pyroxene enstatite (En) values vs. lithologic/flow units of Sierra Grande and the peripheral volcanics in stratigraphic succession.

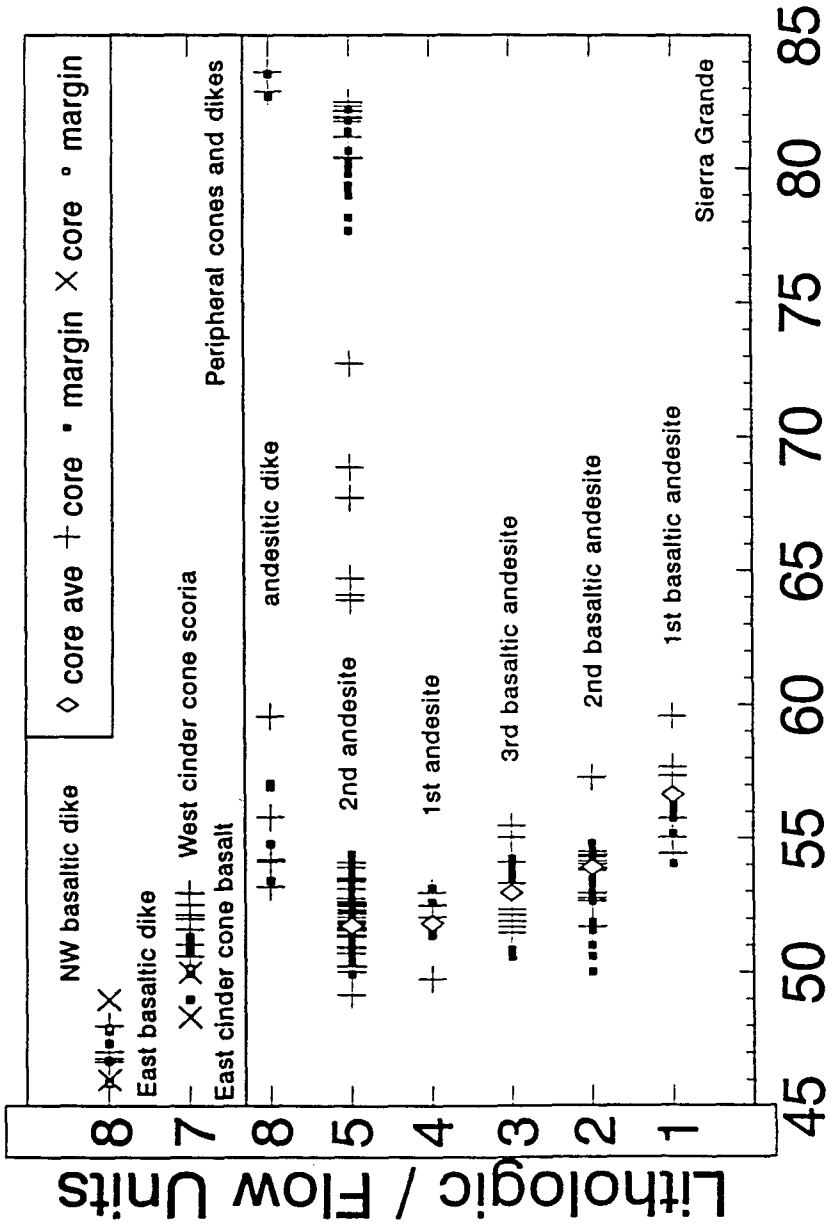
Pyroxenes
◊ core ave + core ▪ margin × core ▫ margin
NW basaltic dike
East basaltic dike
West cinder cone scoria
East cinder cone basalt
Peripheral cones and dikes
andesitic dike
2nd andesite
1st andesite
3rd basaltic andesite
2nd basaltic andesite
1st basaltic andesite
Sierra Grande
Lithologic / Flow Units
8
7
8
5
4
3
2
1
45
50
55
60
65
70
75
80
85
En

Figure 4

calculated, in mole percent, using the method of Lindsley and Anderson (1983). This method accounts for the effects of non-quadrilateral components allowing compositions to be expressed as mole fractions of En, Wo and Fs. The non-quadrilateral components such as Ti and Al were relatively low, .2 - .7 mol% and 1 - 3 mol% respectively, and have essentially no effect on end member composition.

Augites are the dominant phenocrysts in the basaltic andesites and andesites. The compositions of cores and margins range between En_{49-60}, Wo_{34-44} and Fs_{5-11}, with most augites averaging around En_{53}, Wo_{39} and Fs_{8}. The augites of the first basaltic andesite and the andesitic dike are much more Mg-rich than the flows that followed or preceded, respectively (Figure 4). There is a stratigraphic upward trend of Mg depletion between the successive basaltic andesites and andesites and from a plot of core averages for the lithologic/flow units (Figure 4) a fractionation trend between the first basaltic andesite and the third basaltic andesite can be distinguished. An overall trend for the successive flows is probable, albeit slight.

Enstatite phenocrysts occur only in a few samples of the second andesite and in the andesitic dike (Figure 4). The enstatites have a large variation in composition (En_{63-84}, Wo_{1-4}, Fs_{13-35}). Most of the cores and margins of the enstatites have nearly the same composition (En_{80-84}, Wo_{2-4}, Fs_{13-17}) while a few have cores that are slightly to very Fe-rich compared to their margins, (En_{63-73}, Wo_{1-2}, Fs_{25-35} and En_{78-80}, Wo_{3}, Fs_{17-19} respectively). These few enstatites with pronounced reverse zoning occur in only two samples of the second andesite; the cores are hypersthene to bronzite, based on the classification of Deer, Howie and Zussman (1983).

plagioclase

The plagioclase is the least abundant phenocryst in the basaltic andesites and andesites. The majority of plagioclase crystals occur as groundmass microlites. The relatively few phenocrysts identified by petrography are; some sparsely distributed crystals slightly larger than the microlites and the much larger and sparsely distributed remnant crystals with irregular shapes and corroded

Figure 5. Plagioclase anorthite (An) values vs. lithologic/flow units of Sierra Grande in stratigraphic succession.

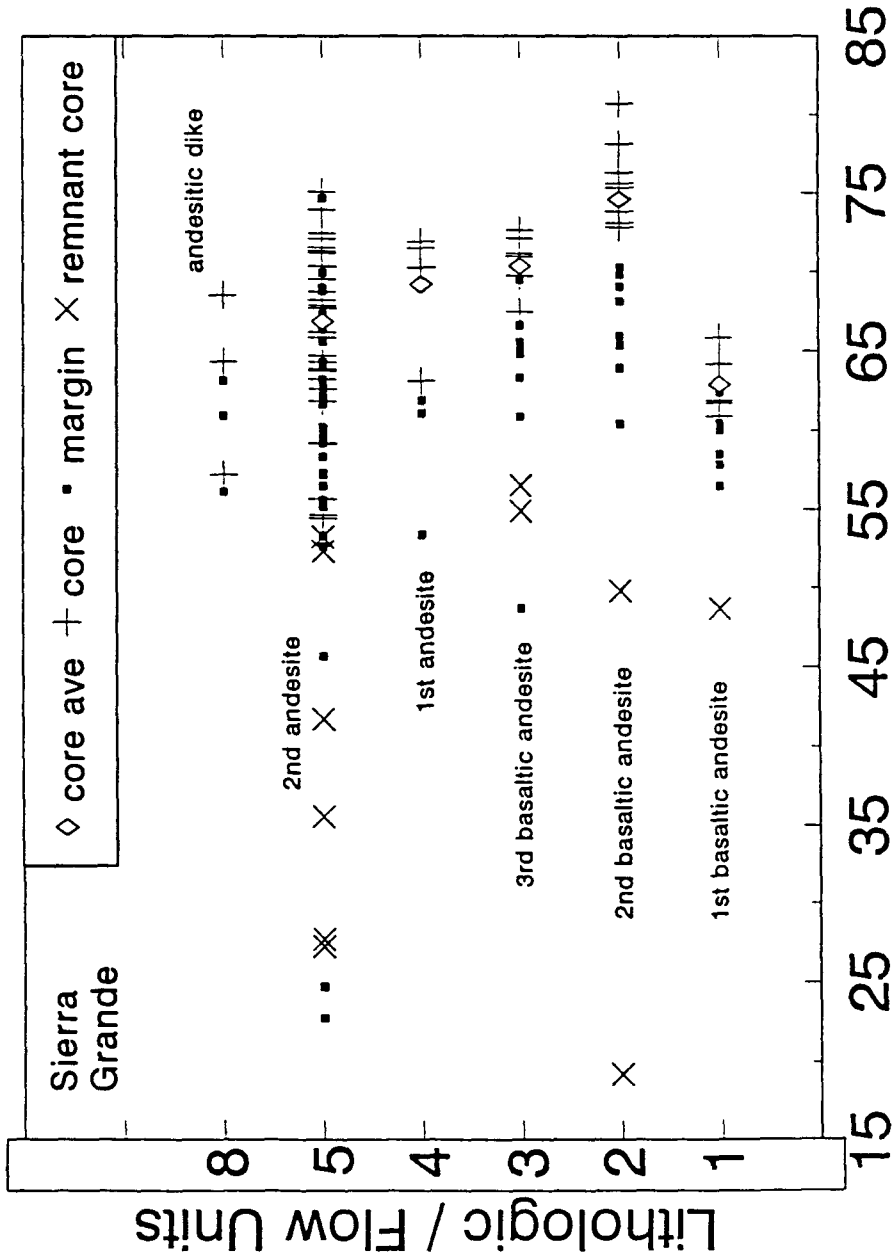
Plagioclase
Sierra Grande
◇ core ave + core ▪ margin × remnant core
andesitic dike
2nd andesite
1st andesite
3rd basaltic andesite
2nd basaltic andesite
1st basaltic andesite
Lithologic / Flow Units
8
5
4
3
2
1
15
25
35
45
55
65
75
85
An

Figure 5

margins. Microprobe analyses show very little compositional difference between non-remnant plagioclase phenocrysts and groundmass microlites. The first basaltic andesite contains labradorite (An_{61-66}) while the remaining basaltic andesite and the andesite plagioclases have cores that range from labradorite to bytownite (An_{54-81}). A stratigraphic upward trend in Ca depletion is evident and a fractionation trend is supported by a plot of core averages, excluding the remnant phenocrysts/microphenocrysts (Figure 5). This fractionation trend, however, is apparent only from the second basaltic andesite through the second andesite, while between the first and second basaltic andesite there is a substantial enrichment of Ca; this will be discussed later. The remnant plagioclases in the basaltic andesites and andesites have cores that range from oligioclase to labradorite (An_{19-57}).

quartz

Quartz was identified in a few samples of each lithologic/flow unit and are isolated, translucent and rounded grains that appear to be either secondary mineralization or inclusions (xenoliths). The quartz grains are considered unrelated to the parent magma, particularly in relation to the olivines of the basaltic andesites. It can be inferred from the petrography that there is the possibility of contamination from the intruded sedimentary country rock, most likely the Dakota Sandstone.

Fe-Ti oxide

Microprobe analyses of the Fe-Ti oxides indicate some variation between and within samples. There were no oxide phases found to be in equilibrium contact. All analyses recorded all Fe as FeO. A method to adjust wt% and determine FeO and Fe_2O_3 was accomplished from a procedure outlined by Stormer (1983). The result changed the weight percent totals from 90 - 95 percent to 96 - 101 percent. The Fe-Ti oxides analyzed were primarily ilmenite and magnetite with some gradation in composition to hematite and ulvospinel, respectively.

Peripheral cones and the dikes

There is a problem with a limited stratigraphic correlation between peripheral cones and associated dikes. Therefore, extending any trend between the cones and dikes is difficult and subjective.

olivine and pyroxene

The Mg content of the olivine cores from the east cinder cone scoria and basalt is generally higher than those of Sierra Grande (Figure 3). Olivines of the basaltic dike associated with the east cone have a lower Mg content indicating that the dike may be younger than the cone. The west cinder cone scoria and the NW basaltic dikes have olivine cores with a Mg content similar to those in the lavas of Sierra Grande. The olivines of the scorias and basalt of the east cone have cores with substantially higher MgO/FeO ratios than the olivines in the lavas of Sierra Grande; most of the cores range between Fo_{88} and Fo_{92}. The dikes, however, have cores with compositions between Fo_{84} and Fo_{87} similar to the lavas of the volcano.

Augites are the second most abundant phenocrysts in the basaltic scoria, basalt, and basaltic dikes. Microprobe analyses show that the augites of the scoria and basalt have a Mg content similar to the augites of all but the earliest flow of Sierra Grande (Figure 4); they have a lower Mg content than the augites in the first basaltic andesite. The basaltic dikes have augites that are generally lower in Mg than those in the lavas of Sierra Grande (Figure 4). In addition, the augites of the scoria, basalt, and basaltic dikes were found to be generally more Ca-rich than the augites in the Sierra Grande andesitic lavas. The difference in the Mg content of the augites between the scoria and basalt, and the associated basaltic dike of the east cinder cone indicates that the dike may be younger that the cone, and may suggest a stratigraphic upward trend of fractionation.

plagioclase and Fe-Ti oxide

The scoria and basaltic dikes have even fewer plagioclase phenocrysts and groundmass microlites than the lithologic/flow units of the volcano, and any stratigraphic trend is inconclusive due

to the correlation problem. However, the plagioclases from the cones and associated dikes are generally Ca-rich. The composition of the plagioclase is bytownite (An_{71-76}) in the scoria, and is either labradorite (An_{56-68}) to bytownite (An_{81-82}) in the basaltic dikes.

The Fe-Ti oxides have the same range of composition as those in the lithologic/flow units of Sierra Grande: mostly ilmenite and magnetite with a gradation to hematite and ulvospinel respectively. Several of the magnetites in the basaltic dikes are Cr-rich (4 - 7 wt% Cr_2O_3) and a few are very Cr-rich (13 and 19 wt% Cr_2O_3).

GEOTHERMOMETRY

Microprobe analyses resulted in the evaluation of two geothermometers, using Fe-Ti oxides and coexisting pyroxenes, for the lavas of Sierra Grande. The only lithologic/flow units with both geothermometers present are the second andesite and the andesitic dike. Temperatures, using Fe-Ti oxides, were calculated by a method outlined by Stormer (1983). In the second andesite, only one pair of ilmenite and magnetite was found to be touching. Therefore an assumption was made, based on the petrography, that the majority of Fe-Ti oxides appear to have formed during the crystallization of the groundmass in relative equilibrium. Few samples from the lithologic/flow units contained both ilmenite and magnetite. Most analyses gave data that could not be plotted or plotted accurately, therefore either the assumption was in error, the Fe-Ti oxide minerals have been altered or the analyses were invalid. A couple of data points from Fe-Ti oxides in the second andesite that could be plotted on a Spencer-Lindsley diagram gave late crystallization temperatures between 820-880 °C. The geothermometry evaluation of the Fe-Ti oxides for second andesite of Sierra Grande was therefore incomplete and questionable.

The most useful geothermometry data was from the two pyroxenes in several of the samples of the second andesite and in the andesitic dike. Two-pyroxene geothermometry calculations were made using two separate methods: one outlined by Lindsley (1983) and the other proposed by Kretz (1981). The procedure by Lindsley (1983) uses the projection of pyroxene end-members, allowing for the effect of non-quadrilateral components, and applies them to natural systems. This is an empirical method, which is useful for pyroxenes with a total of quadrilateral components greater than 90%, appropriate for the pyroxenes of Sierra Grande. The procedure of Kretz (1981) uses two thermometry equations (temperature dependence): one based on the distribution coefficient of Mg-Fe, and the other using the transfer reaction/exchange of Ca between clinopyroxenes and orthopyroxenes. The second set of equations was used for the Sierra Grande samples because of a

Figure 6. Temperature comparison diagram of two pyroxene geothermometry calculations (Kretz vs. Lindsley). The data points are from the pyroxene cores in the second andesite and the most andesitic dike rock of Sierra Grande.

Two Pyroxene Geothermometry Comparison

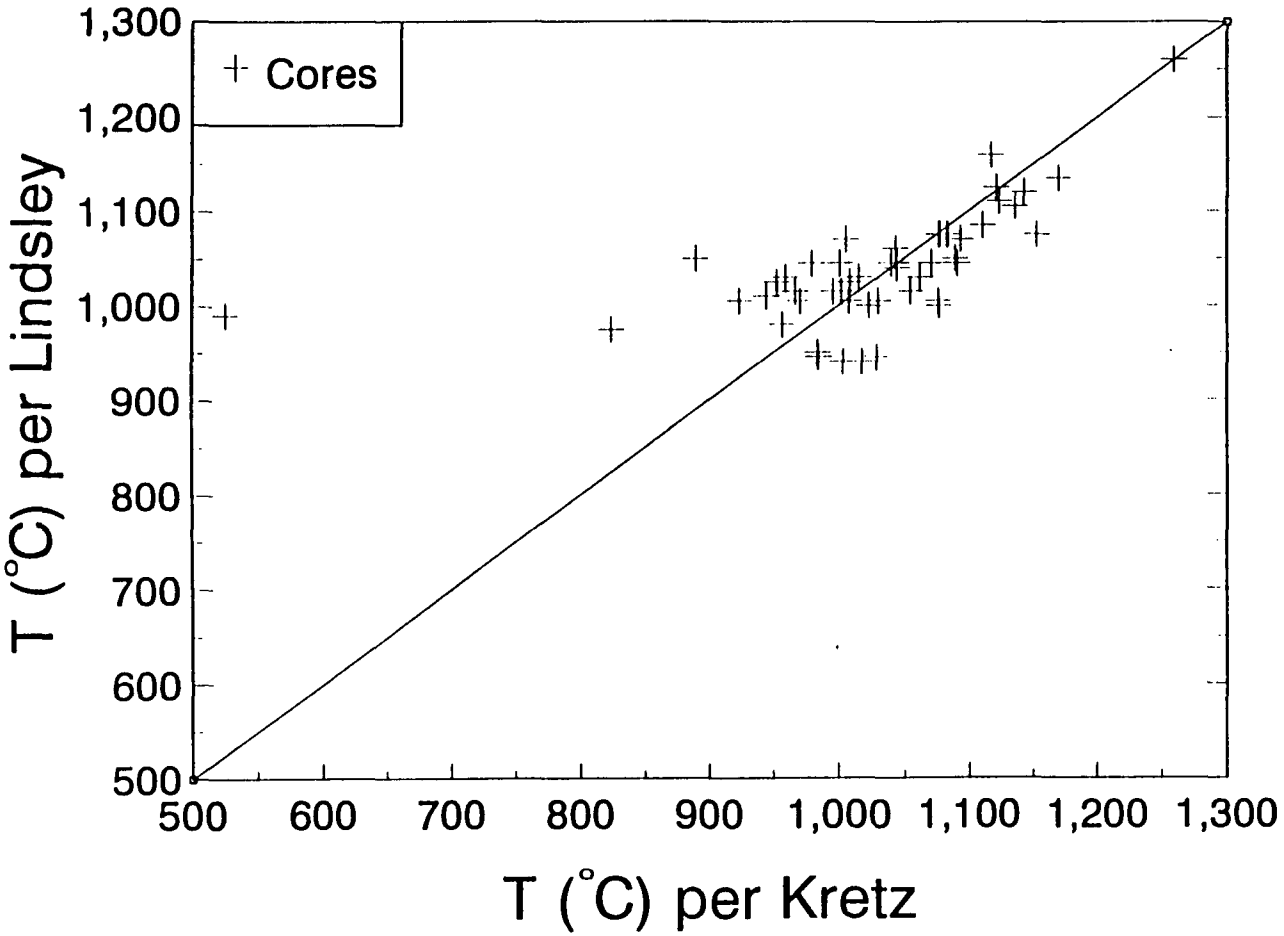

Figure 6

Figure 7. Temperature comparison diagram of two pyroxene geothermometry calculations (Kretz vs. Lindsley). The data points are from the pyroxene margins in the second andesite and the most andesitic dike rock of Sierra Grande.

Two Pyroxene Geothermometry Comparison

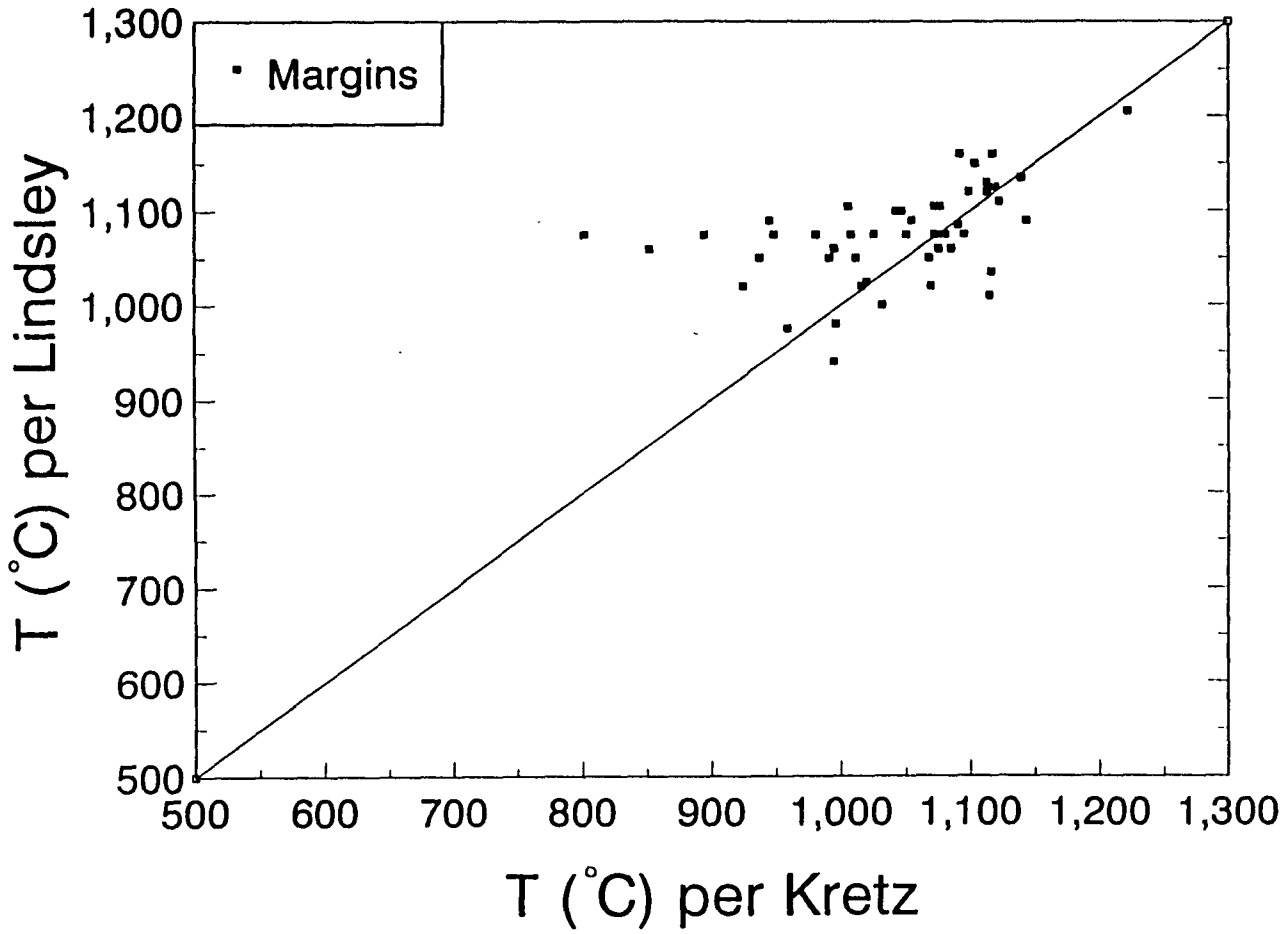

Figure 7

potential for the over estimation of temperature in the first thermometry equation, as suggested by Lindsley (1983) and confirmed in preliminary calculations. The resulting temperatures from the clinopyroxenes at 1 atmosphere were plotted as Kretz vs. Lindsley (Figure 6 and 7). The correlation between the two methods was relatively good and the scatter can be attributed primarily to the difficulty in making temperature determinations from Lindsley's empirical graphs and the fact that the Kretz calculations were based on Fe-free pyroxenes; the pyroxenes of the analyzed samples were very low in Fe but not Fe-free. Temperatures for the second andesite, based on either calculation method, were found to range generally from 1160 °C to 960 °C for the cores and 1140 °C to 960 °C for the margins. A margin of error for either method is approximately +/- 50 °C. These ranges are acceptable temperatures for andesitic lavas, although they are rather broad, and using 1-atmosphere results in at least a minimum temperature range. Further geothermometry calculations will be required to narrow the range for the crystallization temperatures of the mineral phases (olivines, pyroxenes, and plagioclase). This will require whole rock chemical analyses of the other lithologic/flow units as well as the second andesite. At present the core temperatures can be used as a reasonable approximation of crystallization temperatures.

DISCUSSION

Mineralogical interpretation

Successive olivine compositions suggest a fractionating trend among the early lithologic/flow units of Sierra Grande. Mafic rocks, such as peridotite are characterized by very Mg-rich olivines (Fo_{88}) (Deer et al., 1983). Common basaltic lavas, which are typically Mg-rich, have olivines $Fo_{65\text{-}80}$ (Carmichael et al., 1974). Basalts, basaltic andesites, and andesites of orogenic low K and calc-alkaline suites have olivines that range $Fo_{70\text{-}85}$, and basaltic andesites and andesites of orogenic high K and shoshonite suites have olivines that can be either as Mg-rich or more Fe-rich (Ewart, 1976). Olivines with $<Fo_{55}$ are rarely found in orogenic andesites, except for occasional margins, but are often found in anorogenic andesites (Gill, 1981). According to Gill, the absence of such Fe-rich olivines in orogenic andesites suggests insufficient magmatic Fe enrichment. The basaltic andesite lavas of Sierra Grande therefore have olivine compositions that would suggest a magmatic source rich to very rich in Mg and similar in composition to the sources for orogenic volcanics. However, the tectonic environment of the volcano is not of an orogenic style and therefore some parameter of the magma source or generation must be limited to this volcano of the Raton-Clayton field. The completely andesitic composition of the volcano would suggest a differentiated magma with only the siliceous melt extruded. There is also no direct correlation in terms of olivine and pyroxene compositions between the basaltic andesites of the volcano and the scoria, basalt, and basaltic dikes of the cinder cones. In fact, the peripheral volcanics are not only stratigraphically younger but contain pyroxenes and some olivines that are more Mg-rich which infers a more mafic source. It could be suggested, therefore, that the cones and associated dikes originated from either a separate source altogether, an influx of the original parental magma with very little fractionation, or a more mafic residual of the originally fractionated source; this will require further investigation.

The majority of the augites and enstatites analyzed in the lithologic/flow units of the volcano

have compositions that fall within the general parameters for clinopyroxenes (En_{40-55}, Wo_{38-50}, Fs_{7-20}) and orthopyroxenes (En_{70-85}, Wo_{2-5}) respectively, in orogenic andesites as described by Gill (1981). The pyroxenes of each stratigraphically younger unit become generally more depleted in Mg (enriched in Ca and slightly enriched in Fe). The overall variation and scattering of data between flow units within larger lithologic/flow units is a function of individual flow composition and was not investigated in this study. Such a variation are the hypersthene cores in the second andesite which are similar to those reported by Stormer (1972b) but were not consistently found throughout the andesite. The presence of two pyroxenes (augite and orthopyroxene) in an andesite would indicate a change in pressure during one stage of differentiation from a basaltic magma. An increase in pressure, under anhydrous conditions, on a basaltic magma causes the olivine phase volume to grow smaller while the augite and orthopyroxene phase volumes are enlarged (Grove and Kinzler, 1986). This allows the pyroxene minerals to coexist during differentiation and accounts for the eventual absence of olivine, typical of andesites in an orogenic environment. Under hydrous conditions the effect of increasing pressure is just the opposite; olivine becomes more dominant and the pyroxenes phase volumes grow farther apart (Grove and Kinzler, 1986). The petrographic analyses of the two-pyroxene andesite of Sierra Grande showed that the augites and orthopyroxenes were contemporaneous and that olivine is absent as phenocrysts and in the groundmass. The initial presence of early formed plagioclase, which is discussed later, and the partial dominance of olivine in the basaltic andesites compared to the subsequent one- and two-pyroxene andesites would suggest an upper mantle source initially under a hydrous condition.

The andesitic lavas of Sierra Grande do not contain a majority of plagioclase phenocrysts with compositions less than An_{50}, characteristic of anorogenic andesites (Gill, 1981). The change in the plagioclase An composition between the first and second basaltic andesites and the successively younger flows suggests three possible causes; 1) that there was contamination from the country rock by assimilation after the extrusion of the first basaltic andesite, 2) that there was a different source

for the first basaltic andesite than that for the later basaltic andesites and andesites, or 3) that after the differentiation of the parent magma which produced the first basaltic andesite, the residual was left enriched in Ca prior to further differentiation and subsequent extrusion of successive flows. The first case it is very unlikely. Such an increase would require a lot of assimilated rock (without being superheated), which would depress the melting temperature of the remaining magma, induce crystallization and stop fractionation. The second case may be possible, however, the good correlation for the fractionation trends of the olivines and pyroxenes in the older units would tend to contradict this possibly. Finally, the third case could be possible if there was an appreciable water loss after an initial fractionation. That is, that the magma experienced a decline in hydrostatic pressure associated with its ascension. This is a major factor in magmatic resorption of plagioclase (Vance, 1965). The presence of the remnant plagioclases in most all samples and their lower An values would suggest that with the loss of hydrostatic pressure after the fractionation of the first basaltic andesite the subsequent residual magma became Ca enriched followed by a normal trend of Ca depletion with each subsequent flow unit. The few plagioclases in the scoria, basalt and basaltic dikes of the peripheral volcanics are either more Ca-rich or as Ca-rich as the first basaltic andesite of Sierra Grande. This could also suggest, as previously mentioned concerning the olivines, a second magma source or the introduction of new or residual material.

A possible scenario for the lavas of Sierra Grande would be as follows; first an upper mantle source, Mg rich and under a hydrous condition which began to differentiate with the crystallization of early plagioclases, with lower An values, Mg-rich olivine and augite (first basaltic andesite), then a drop in hydrostatic pressure and change over to a anhydrous condition under relatively moderate pressure with the crystallization of olivine, augite and more An-rich plagioclase (second and third basaltic andesites), next the absence of olivine, the dominance of augite and the crystallization of increasingly less An-rich plagioclase (first andesite), and finally the crystallization of coexisting augite and orthopyroxene and less An-rich plagioclase (second andesite).

Comparisons to the surrounding volcanics

Based on the composition comparison of olivine, pyroxene and plagioclase in this study with those found in the other volcanics of the Raton-Clayton field it is suggested that the lithologic/flow units of Sierra Grande and peripheral cones originated from different sources than those of the surrounding field.

A comparison of olivine compositions was made between those analyzed by Stormer(1972b) for the Raton-Clayton field and those analyzed in this study. The FeO and CaO wt% values of representative olivines of the basaltic andesites of Sierra Grande and the peripheral volcanics were plotted along with three representative trends for the surrounding volcanics. The trends for the surrounding volcanics were taken from Figure 2 in Stormer (1972b). Stormer's data are from phenocryst centers, phenocryst rims, and groundmass compositions while the Sierra Grande data are from matching cores and margins. The Sierra Grande lavas (Figure 8) show that the basaltic andesites have a trend similar to the Raton-Clayton and Capulin basalts, although they are lower in FeO content and subsequently are more Mg-rich. The scorias and basalt have olivines (Figure 9) which exhibit either an Fe enrichment trend similar to the Raton-Clayton and Capulin basalts or a Ca enrichment and slight Fe depletion trend. The latter has no similarities to any of the surrounding volcanics analyzed by Stormer (1972b). The basaltic dikes have olivines that exhibit two trends; one similar to the Raton-Clayton and Capulin basalts, and another having the same Ca enrichment and slight Fe enrichment as the Feldspathoidal lavas. It should be noted that the samples of this study did not contain any feldspathoids.

The pyroxenes of Sierra Grande appear to be different than those of the surrounding field. There was no direct comparison made between the pyroxenes of this study and those analyzed by Stormer (1972b) for the Raton-Clayton field because the microprobe data are in depository and were not obtained. Also, Stormer reported that many of the pyroxenes he analyzed, in the surrounding volcanics, had high amounts of Al and Ti (9.9 and 2.8 percent respectively) which required the

Figure 8. FeO vs. CaO wt% diagrams for representative olivines of Sierra Grande. Lithologic/flow unit identification shown by the symbols indicated in the key. The typical trends of a few of the surrounding volcanics are labeled on the diagrams: the Raton-Clayton basalts, the Capulin basalts and the Feldspathoidal lavas.

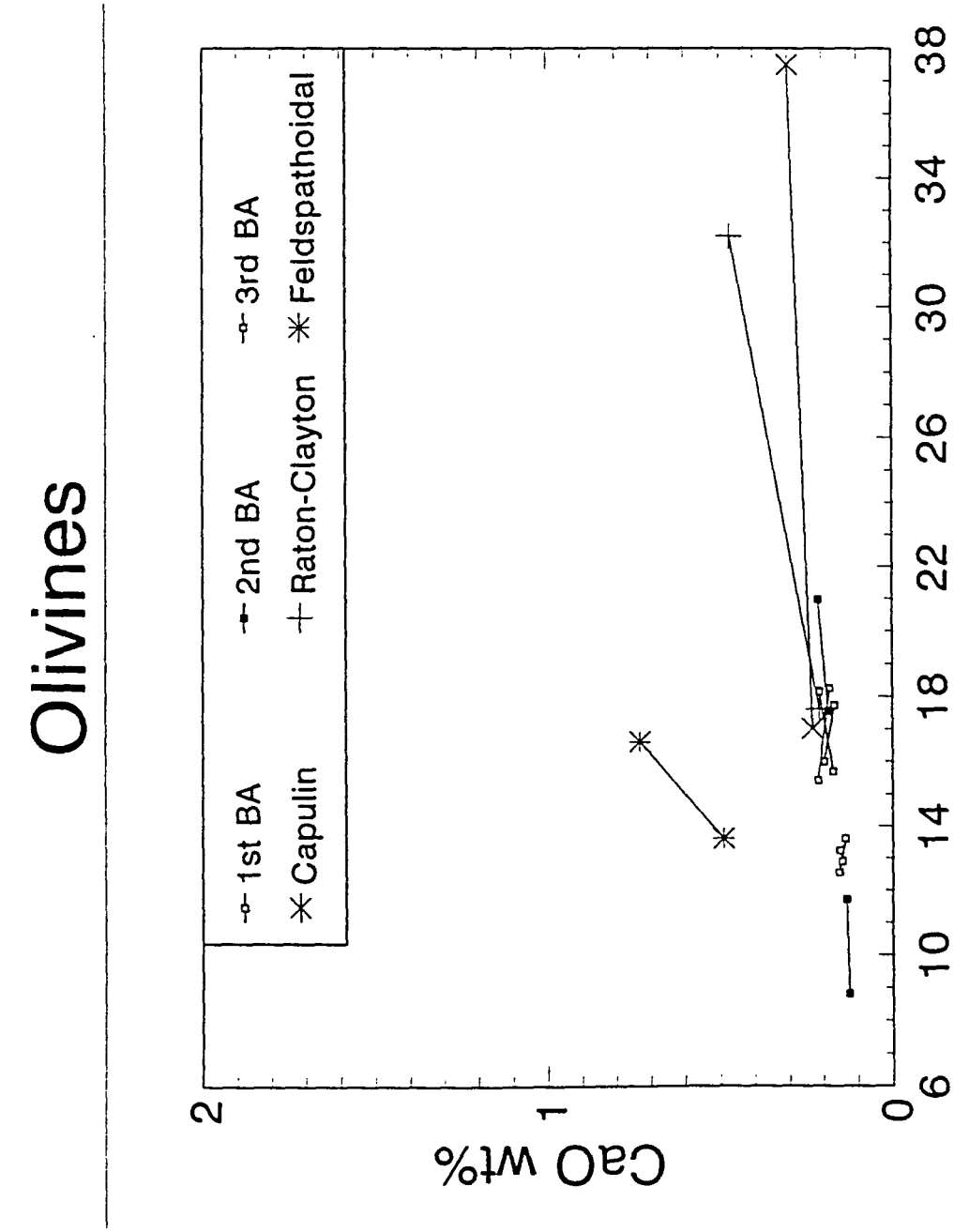
Olivines
1st BA
2nd BA
3rd BA
Capulin
Raton-Clayton
Feldspathoidal
CaO wt%
FeO wt%
0
1
2
6
10
14
18
22
26
30
34
38

Figure 8

Figure 9. FeO vs. CaO wt% diagrams for representative olivines of the peripheral cinder cone and dikes. Lithologic/flow unit identification shown by the symbols indicated in the key. The typical trends of a few of the surrounding volcanics are labeled on the diagrams: the Raton-Clayton basalts, the Capulin basalts and the Feldspathoidal lavas.

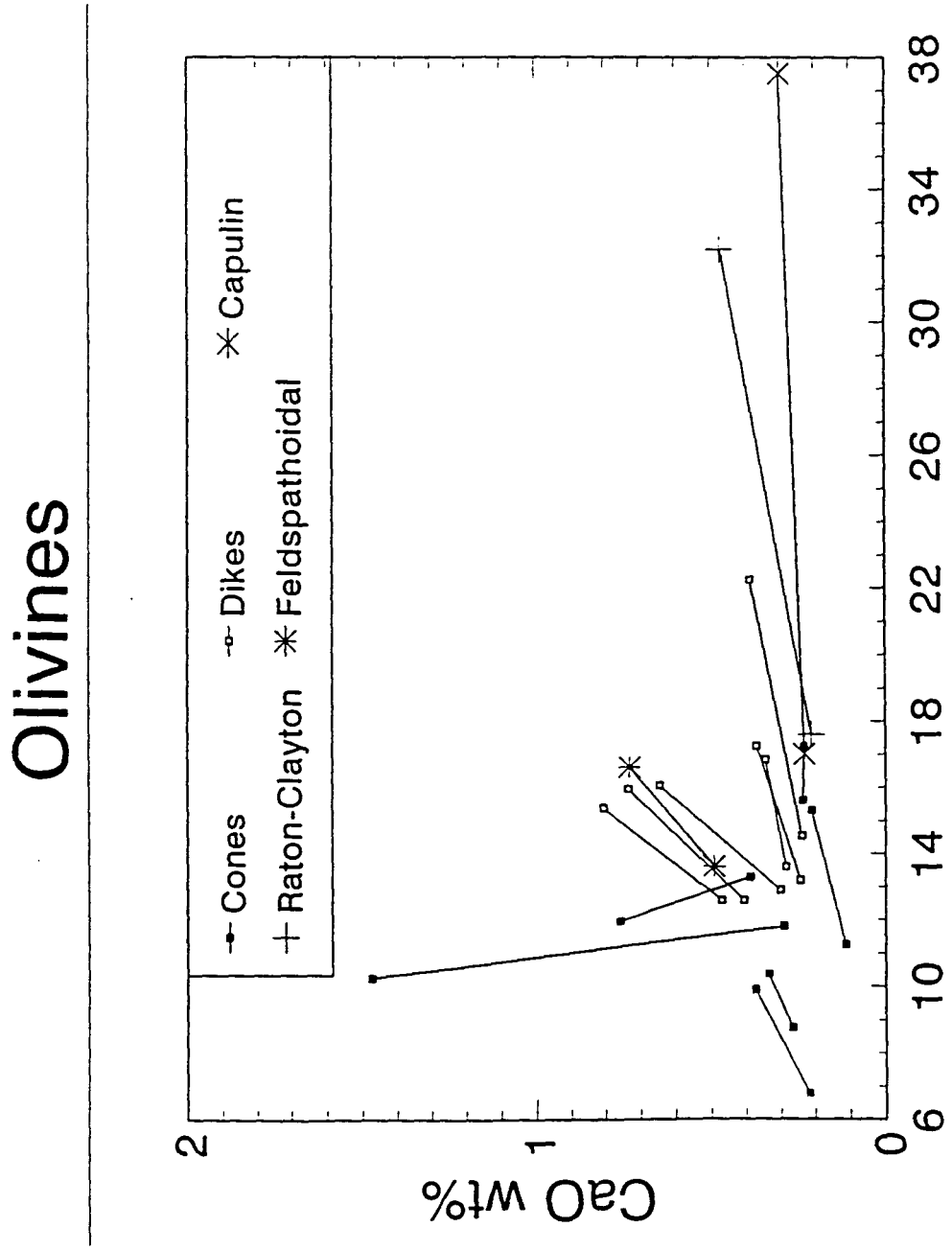
Olivines
Cones
Dikes
Capulin
Raton-Clayton
Feldspathoidal
CaO wt%
FeO wt%
0
1
2
6
10
14
18
22
26
30
34
38

Figure 9

Figure 10. Comparison of the range in plagioclase anorthite (An) values for the lithologic/flow units of Sierra Grande and the peripheral volcanics, and those of the surrounding volcanics taken from a Figure 4 in Stormer (1972b) [JCS].

Plagioclase

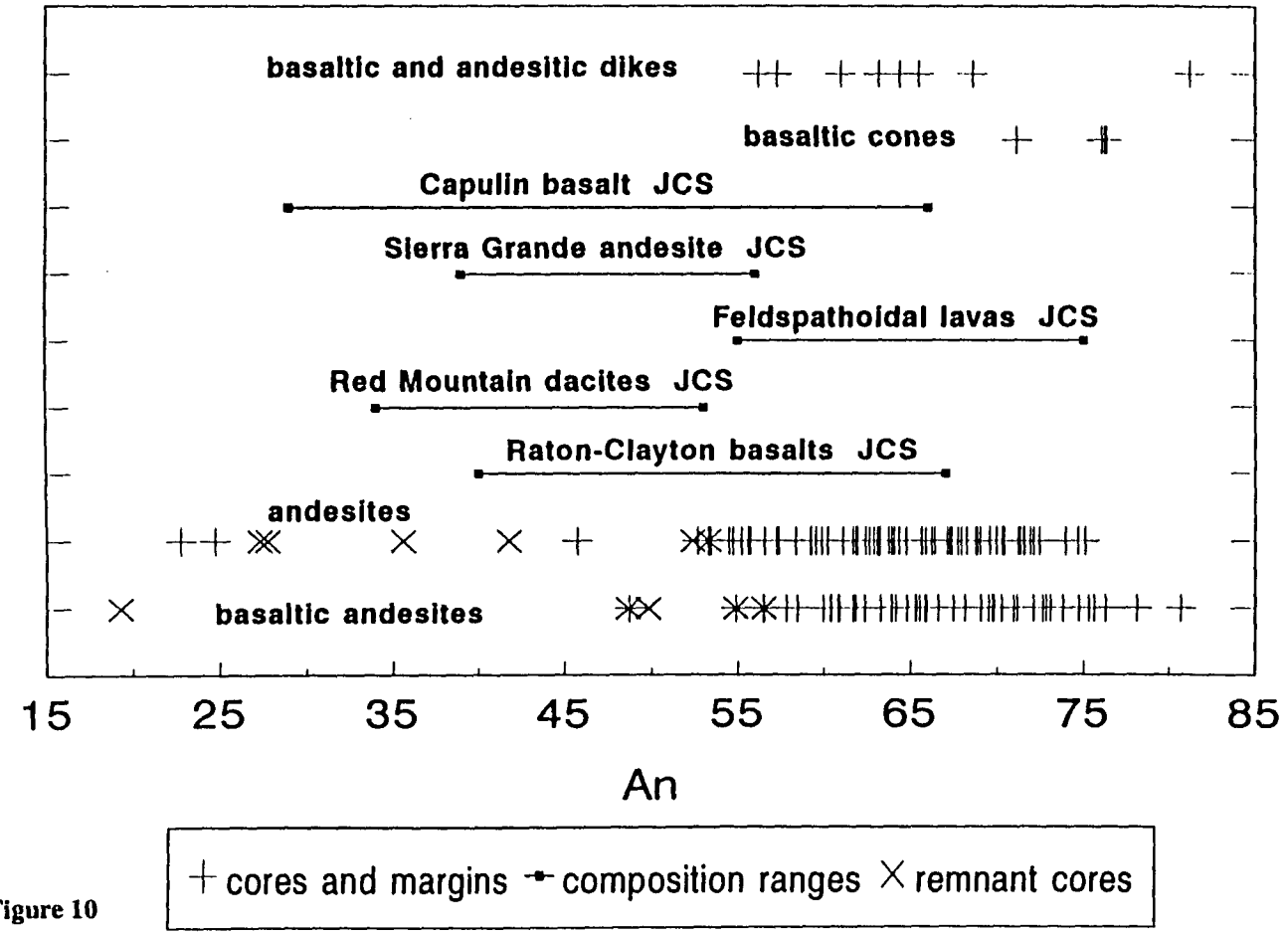

Figure 10

plotting of recalculated values of Mg, Ca and Fs, and Stormer stated that the proportions were inconsistent with molecular proportions for principle components. The augites of this study, however, had less Al and Ti (1 - 5 and .2 - 1.2 wt% respectively) and there was no difficulty with non-quadrilateral components in calculating end-member compositions. Therefore any direct comparison would be questionable. In comparing the quadrilateral position of the augites, those in the lavas of the surrounding field (Stormer, 1972b) are more Fe-rich than those analyzed in this study for Sierra Grande. Those that Stormer analyzed for Sierra Grande are less Ca-rich that those in this study. The augites of the peripheral volcanics are less Fe-rich but as calcic as those of the Raton-Clayton basalt, the Red Mountain dacites and the Felspathoidal lavas.

A composition diagram, based on An mol% values for the plagioclase groundmass and phenocrysts cores and margins, were compared to general compositional ranges of plagioclase groundmass and phenocryst rims, taken from Figure 4 in Stormer (1972b) for the Raton-Clayton field (Figure 10). What was found to be most interesting was that the plagioclases of the lithologic/flows units of Sierra Grande are generally more Ca-rich than most of those of the surrounding volcanics. Those closest in content are the feldspathoidal lavas, however, again no feldspathoids were identified by petrographic or microprobe analyses in the samples of this study. Also, from Stormer's diagram, the compositional range of plagioclase of Sierra Grande should be somewhere between An_{39} and An_{56}. However, from the more complete sampling of the present study it was found that a majority of plagioclase phenocrysts fall within a range of An_{50-76} and only a few are below An_{56} (Figure 10). Those that do fall within the compositional range adapted from Stormer, are primarily a few plagioclase phenocrysts that exhibit reverse zoning and the plagioclase remnants discussed previously.

SUMMARY

A comparison in olivines, pyroxenes and plagioclases between successive lithologic/flow units of Sierra Grande indicate a general fractionation trend of one magmatic source and a separate source for the peripheral volcanics. Without information from bulk chemical analyses, the mineralogy determined by the microprobe has shown to be the most useful aid in distinguishing rock types and a classification has been made using petrography, microprobe data and field observation.

The closest analogy to the lavas of Sierra Grande are the basaltic andesites and andesites of the low K and calc-alkaline suites. The general composition of the basaltic andesites and andesites in orogenic calc-alkaline suites is: calcic plagioclase, augite, orthopyroxene, titanomagnetite and +/- Mg olivine, with hornblende and biotite becoming frequent in the andesites and plagioclase being less Ca rich in the basaltic rocks (Ewart, 1976). Yet, unlike typical orogenic lavas, those of Sierra Grande are modally closer to anorogenic equivalents in the abundance of phenocrysts. In anorogenic basalts, basaltic andesites, and andesites, phenocrysts are generally 4 to 10% by volume while phenocrysts of orogenic rocks tend to be > 20% by volume (Ewart, 1976). The phenocrysts in the Sierra Grande basaltic andesites and andesites are on average 5- 10% modal. Therefore, mineralogically Sierra Grande lavas appear orogenic, while modally and tectonically they are anorogenic.

Sierra Grande, therefore, is an andesitic volcano (basaltic andesites, andesites and andesitic breccia), composed of transitional (anorogenic/orogenic) calc-alkaline lava formed by the partial melting of an upper mantle source (peridotite) that experienced differentiation with the most siliceous melt extruding to the surface. The minimum temperature for the andesites during extrusion or intrusion, based on two-pyroxene geothermometry, was found to be between 1160 and 960 °C +/- 50 °C. The conduit for these extrusions may coincide with the older vent for the Clayton basalts. The basaltic andesites are porphyritic and trachytic and composed of phenocrysts of augite, Mg-rich olivines and calcic or very calcic plagioclase. The andesites are porphyritic and trachytic, and composed of augite or augite and enstatite, and calcic plagioclase. The end of the volcano's activity

is marked by an event of andesite accumulation and pyroclastic extrusions which modified the summit.

The peripheral cinder cones and associated dikes are calc-alkaline basaltic rocks derived from either a completely separate source, a secondary pulse of the parent magma that had not experienced the previous path of differentiation or the mafic residual melt after fractionation. This magma for the peripheral volcanics was likely obstructed by the earlier andesitic magma chamber and extruded around the perimeter of the volcano through fractures in the underlying sedimentary strata and Precambrian basement.

REFERENCES

Atwater, T., 1970, Implications of plate tectonics for the Cenozoic evolution of western North America. G.S.A. Bull., 81, 3513-3536.

Baldridge, W. S., 1979, Petrology and petrogenesis of Plio-Pleistocene basaltic rocks from central Rio Grande rift, New Mexico, and their relation to rift structure. In; Riecker, R. E. (ed) Rio Grande rift: Tectonics and Magnetism. A. G. U., Washington, DC, 323-353.

Baldridge, W. S., Olsen, K. H., and Callender, J. F., 1984, Rio Grande rift: problems and perspectives. In; Rio Grande Rift: Northern New Mexico. New Mexico Geo. Soc. Guidebook 35th Field Conf., 1-12.

Baldwin, B. and Muehlberger, W. R., 1959, Geologic studies of Union County, New Mexico. New Mexico Bur. Mines Bull., 63, 171p.

Basaltic Volcanism Study Project, 1981, Basaltic Volcanism on the Terrestrial Planets. Lunar and Planetary Inst., Pergamon Press Inc., New York, 1286p.

Bence, A. E. and Albee, A. L., 1968, Empirical correction factors for electron microanalysis of silicates and oxides. Jour. Geol., 76, 382-403.

Carmichael, I. S. E., Turner, F. J., and Veerhoogan, J. 1974, Igneous Petrology. McGraw-Hill Book Co., New York, 739p.

Clark, F. W., 1915, Analysis of rocks and minerals. U.S.G.S. Bull., 591, 376p.

Collins, R. F., 1949, Volcanic rocks of northeastern New Mexico. G.S.A. Bull., 60, 1017-1040.

Coney, P. J., 1971, Cordilleran tectonic transitions and motion of the North American plate. Nature, 233, 462-465.

Coney, P. J., 1978, Mesozoic-Cenozoic cordilleran plate tectonics, In; Smith, R. B. and Eaton, G. I. (eds) Cenozoic Tectonics and Regional Geophysics of the Western Cordillera. G.S.A. Memoir, 152, 33-50.

Coney, P. J., 1987, The regional tectonic setting and possible causes of the Cenozoic extension in the North American Cordillera. In; Coward, M. P., Dewey, J. F., and Hancock, P. L. (eds) Continental Extensional Tectonics. G.S.A. Spec. Pub., 28, 177-186.

Coney, P. J. and Reynolds, S. J., 1977, Cordilleran benioff zones. Nature, 270, 403-406.

Cross, T. A., 1986, Tectonic controls of foreland basin subsidence and Laramide style deformation, western United States. Spec. Pubs. Int. Ass. Sediment, 8, 15-39.

Deer, W. A., Howie, R. A., and Zussman, J., 1983, An Introduction to the Rock Forming Minerals (14th ed.). Longman Group Ltd., England, 528p.

Eaton, G. P., 1979, A plate-tectonic model for the late Cenozoic crustal spreading in the western United States. In; Riecker, R. E. (ed) Rio Grande: Tectonics and Magnetism. A.G.U., Washington, D.C., 7-32.

Eaton, G. P., 1986, A tectonic redefinition of the southern Rocky Mountains. Tectonophysics, 132, 163-193.

Elston, W. E., 1984, Subduction of young oceanic lithosphere and extensional orogeny in southwestern North America during mid-Tertiary time. Tectonics, 3(2), 229-250.

Elston, W. E. and Bornhorst, T. J., 1979, The Rio Grande rift in context of regional post-40 m.y. volcanic and tectonic events. In; Riecker, R. E. (ed) Rio Grande: Tectonics and Magnetism. A.G.U., Washington, D.C., 416-438.

Ewart, A., 1982, The mineralogy and petrology of Tertiary-Recent orogenic volcanic rocks; with special reference to the andesitic-basaltic composition range. In; Thorpe, R. S. (ed) Andesites; Orogenic Andesites and Related Rocks. John Wiley and Sons Pub., New York, 25-95.

Gardner, J. N. and Goff, F., 1984, Potassium-argon dates from the Jemez volcanic field; implications for tectonic activity in the north-central Rio Grande rift. In; Rio Grande Rift: Northern New Mexico, New Mexico Geo. Soc. Guidebook 35th Field Conf., 75-81.

Gill, J., 1981, Orogenic Andesites and Plate Tectonics. Springer-Verlag, New York, 370p.

Gornitz, V., 1982, Volcanism and the tectonic development of the Rio Grande rift and environs, New Mexico-Colorado, from analysis of petrochemical data. Mountain Geologist, 19(2), 41-58.

Grove, T.L. and Kinzler, R.J., 1986, Petrogenesis of Andesite. Ann. Rev. Earth Planet. Sci., 14, 417-454.

Jones, L. M., Walker, R. L., and Stormer, J. C., 1974, Isotopic composition of strontium and origin of the volcanic rocks of the Raton-Clayton district, northeastern New Mexico. G.S.A. Bull., 85, 33-36.

Kerr, R. A., 1985, Plate tectonics goes back 2 Ga.. Science, 230, 1364-1367.

Kretz, R., 1982, Transfer and exchange equilibria in a portion of the pyroxene quadrilateral as deduced from natural and experimental data. Geochem. Cosmochem. Atca, 46, 411-421.

Laughlin, A. W., Rehrig, W. A., and Mauger, R. L., 1969, K-Ar chronology and sulfur and strontium isotope ratios of the Questa Mine, New Mexico. Econ. Geol., 64, 903-909.

Lee, W. T., 1912, Extinct volcanoes of northeastern New Mexico. Am. Forestry, 18, 357-365.

Lee, W. T., 1922, Description of the Raton, Brilliant and Koehler quadrangles. U.S.G.S. Atlas, Folio 214.

Lindsley, D. H., 1983, Pyroxene thermometry. Am. Min., 68, 477-493.

Lindsley, D. H. and Andersen, D. J., 1983, A two pyroxene thermometer. J.G.R., 88, supp., A887-A906.

Lipman, P. W., 1969, Alkalic and tholeiitic basaltic volcanism related to the Rio Grande depression, southern Colorado and northern New Mexico. G.S.A. Bull., 80, 1343-1354.

Lipman, P. W., 1980, Cenozoic volcanism in the western United States. Implication for continental tectonics. In; Studies in Geophysics; Continental Tectonics. Nat. Acad. Sci., Washington, D.C., 161-174.

Lipman, P. W. and Mehnert, H. W., 1975, Late Cenozoic basaltic volcanism and development of the Rio Grande depression in the southern Rocky Mountains. In; Curtis, B. F. (ed) Cenozoic History of the Southern Rocky Mountains. G.S.A. Memoir, 144, 119-154.

Morgan, P. and Golombek, M. P., 1984, Factors controlling the phases and styles of extension in the northern Rio Grande rift. In; Rio Grande Rift: Northern New Mexico. New Mexico Geo. Soc. Guidebook 35th Field Conf., 13-19.

Phelps, P. W., Gust, D. A., and Wooden, J. L., 1983, Petrogenesis of the mafic feldspathoidal lavas of the Raton-Clayton volcanic field, New Mexico. Contrib. Mineral. Petrol., 84, 182-190.

Potter, L. S., 1988, Petrology and petrogenesis of Tertiary igneous rock, Chico Hills, New Mexico. M.S. Thesis, Iowa State Univ., Ames, IA., 179p.

Ragland, D. C., 1989, Basic Analytical Petrology. Oxford Univ. Press, New York, 269p.

Scott, G. R., 1986, Geologic and structural contour map of the Springer 30 x 60 quadrangle, Colfax, Hardin, Mora and Union counties, New Mexico. U.S.G.S. Misc. Invest. Series, Map I-1705.

Spencer, K. J. and Lindsley, D. H., 1981, A solution model for coexisting iron-titanium oxides. Am. Min., 66, 1189-1201.

Staatz, M. H., 1985, Geology and description of the thorium and rare-earth veins in the Laughlin peak area, Colfax County, New Mexico. U.S.G.S. Prof. Paper, 1049-E, 31p.

Stobbe, H. R., 1949, Petrology of volcanic rocks of northeastern New Mexico. G.S.A. Bull., 60, 1041-1093.

Stormer, J. C., 1972a, Ages and nature of volcanic activity of the southern High Plains, New Mexico and Colorado. G.S.A. Bull., 83, 2443-2448.

Stormer, J. C., 1972b, Mineralogy and petrology of the Raton-Clayton volcanic field, northeastern New Mexico. G.S.A. Bull., 83, 3299-3322.

Stormer, J. C., 1983, The effect of recalculation on estimates of temperature and oxygen fugacity from analyses of multicomponent iron-titanium oxides. Am. Min., 68, 586-594.

Stormer, J. C., 1987, Capulin Mountain volcano and the Raton-Clayton volcanic field, northeastern New Mexico. In; G.S.A. Centen. Field Guide, Rocky Mountain Sect., 421-424.

Suppe, J., 1985, Principles of Structural Geology. Prentice-Hall Inc., New Jersey, 537p.

Tanaka, K. L., Shoemaker, E. M., Ulrich, G. E., and Wolfe, H. W., 1986, Migration of volcanism in the San Francisco volcanic field, Arizona. G.S.A. Bull., 97, 129-141.

Taylor, L. W., 1989, Petrological and geochemical study of some igneous rocks from the Raton-Clayton volcanic field, northeastern New Mexico. M.S. Thesis, Iowa State Univ., Ames, IA., 228p.

Vance, J. A., 1965, Zoning in igneous plagioclase: patchy zoning. Jour. Geol., 73, 636-651.

Warner, L. A., 1978, The Colorado lineament: A middle Precambrian wrench fault system. G.S.A. Bull., 89, 161-171.

Washington, H. S., 1917, Chemical analyses of igneous rocks. U.S.G.S. Prof. Paper, 99, 1201p.

Wyllie, P. J., 1971, Role of water in magma generation and initiation of diapiric uprise in the mantle. J.G.R., 76, 1329-1338.

ACKNOWLEDGEMENTS

First and foremost, I wish to thank my wife and life partner Cynthia. I am endeared to her and thankful for her patience and support, particularly during my absence while I conducted my field survey. I also thank my parents for their continued support and encouragement.

Funding for this project was provided in part by a Geological Society of America grant for field research. Additional support was from the Department of Geological and Atmospheric Sciences for petrographical thin section preparation and microprobe analyses.

I would like to thank Dr. Bert E. Nordlie for his time, support, guidance and consultation in this project. Thanks also go out to; Drs. Kenneth E. Windom and Steven M. Richardson for their helpful advice, Bruce Tanner and Alfred Kracher for the help in thin section preparation and the microprobe analyses advice, respectively, my office mate Greg Fuhrmann for his listening and our discussions, and to Felix Oyarzabal for his guiding me through AutoCAD and Harvard Graphics.

I also wish to thank the Office of the Commissioner of Public Lands, State of New Mexico for expediting my permit for entry and collecting on state trust land. During my stay in New Mexico I met a great number of helpful and friendly folk and wish to extend a thank you to all, particularly the people of Des Moines, New Mexico. Next, I wish to thank a select few from the vicinity of Sierra Grande for their support and friendship; Mrs. Patricia Hewitt and Amisdad Ranch clan (Boogie, Johnny, Johnette and Joe). Finally I wish to dedicate this thesis to the memory of Clifford Gilbert, former manager of the Amisdad Ranch, for his support of my field work, his interest in my well being, and the brief friendship we had.

APPENDIX A SEDIMENTARY STRATIGRAPHY

The sedimentary lithology of the Raton Basin and northeastern New Mexico is summarized below. Modified after Potter (1988).

Age	Name or rock type	Thickness (m)	Descriptions
Quaternary	alluvium & colluvium		unconsolidated
Tertiary	Ogallala Formation	0 - 46	poorly consolidated, light brown silt, sand and gravel
Cretaceous Upper	Vermejo Formation	0 - 62	interbedded coal, shale, siltstone and sandstone
	Trinidad Sandstone	15 - 30	light gray to yellowish gray fine to medium quartzose sandstone
	Pierre Shale	542 - 588	olive shale with limestone and sandstone at top
	Niobrara Formation	257 - 288	
	Smokey Hill Shale Mbr.	247 - 277	yellowish-gray to gray, silty calcareous shale, sandy shale and limestone
	Fort Hays Limestone Mbr.	9 - 11	gray, massive, dense limestone 3 - 26 in beds (8 - 66 cm)
	Carlile Shale	51	dark gray, silty, with both calcareous and non-calcareous members
	Greenhorn Limestone	40	massive, dense 1 - 14 in (2.5 - 3.5 cm) thick beds separated by silty shale
	Graneros Shale	23	dark-gray, blocky, noncalcareous shale with bentonite layers and a basal limestone layer

Age	Name or rock type	Thickness (m)	Descriptions
Cretaceous Upper			
	Dakota Sandstone	24 - 40	white to light gray or orange fine to medium grained cross-stratified quartz sandstone with conglomerate and lenticular shale layers
Lower	Purgatoire Formation	23 - 37	dark-gray silty shale (upper) and fine to medium grained crossbedded quartzose sandstone (lower)
Jurassic	Morrison Formation (includes Bell Ranch Formation and Exeter Sandstone)	150	vericolored calcareous siltstone and claystone interbedded with thin fine to medium grained sandstone
Triassic	Dockum Formation	150+	reddish-brown to light brown sandstone with minor conglomerate

APPENDIX B ALTERNATIVE CLASSIFICATION

(Taylor 1989)

Group I Dacites; includes all Miocene and younger dacites and rhyolites.

Group II Alkali olivine basalts and basanites; includes the majority of basalts designated "Raton-Clayton" and some of the Feldspathoidal lavas.

Group III Nephelinites; includes the remaining Feldspathoidal lavas.

Group IV Andesites; includes some Red Mountain Lavas, Sierra Grande Lavas and a Chico Hill latitic andesite.

Group V Saturated basalts; includes some of the Raton-Clayton basalts and the Capulin basalts.

APPENDIX C ORIGINS AND DESCRIPTIONS

Extrusives

Red Mountain lavas

The Red Mountain lavas are a grouping of hornblende andesites and dacites that began erupting about 8.2 Ma (Stormer, 1972a) from several volcanic centers in the western half of the volcanic field (i.e., Red Mountain, Laughlin Peak and Palo Blanco). This rock type also crops out at some of the western mesas (e.g. Johnson, Hunter and Meloche) within the volcanic field in an apparent younger stratigraphic position than the Raton-Clayton basalts. This causes some confusion and suggests that the eruption of the Red Mountain lavas overlaped the extrusion of the late Raton basalts (Stormer, 1972a) and maybe the Clayton basalts. The hornblende andesites are identified by their altered hornblende phenocrysts and amphibole remnants in a fine grained trachytic groundmass of augite and plagioclase laths. The dacite is characterized by amphibole and plagioclase phenocrysts in a glassy to microcrystalline texture (Stormer, 1972b). Stormer suggested that the Red Mountain lavas are similar to intermediate volcanics of calc-alkaline or orogenic suites and proposed that they originated from the partial melting of a basaltic amphibolite in the lower crust with little or no fractional crystallization.

The Raton-Clayton basalt

Stormer's (1972b) Raton-Clayton basalt was derived from the equivalent time relationship between the Clayton basalt and the late Raton basalt which was noted by Baldwin and Muehlberger (1959). The two basalts differ in REE and incompatible element compositions (Phelps et al., 1983). This unit is characterized by an alternating series of low-K olivine basalts with olivine phenocrysts in a holocrystalline groundmass and alkali olivine basalts with olivine and augite phenocrysts (Stormer, 1972b). Collins (1949) proposed that all of the igneous rocks of the region originated from a single magma of approximate olivine basalt composition. Stormer suggested that the typical sample of

Raton-Clayton basalt is equivalent to alkali olivine basalts found elsewhere in the western United States and other continental volcanic regimes which are proposed to have been derived by the partial melting of a peridotite or some other mantle composition. Lower Sr ratios suggest a direct link with an upper mantle source with little or no contamination (Jones et al., 1974). Collins (1949) noted that the stratigraphy of the lava flows was reversed. This is caused by the widespread down cutting of stream erosion into the lava flows followed by subsequent flows that filled the lower areas. This occurred repeatedly and thus created younger formation units below older ones. The eruptive sequence ranges in age from 7.2 to 2.2 Ma (Stormer, 1972a) and are contemporaneous with a late stage of tectonic and associated volcanic activity of the Rio Grande Rift that began about 10 Ma (Baldridge et al., 1984) and which had a major peak in activity at about 5 Ma (Lipman and Mehnert, 1975; Elston, 1984). However, although the basalts of the Raton-Clayton field texturally resemble those within the Rio Grande rift system, they have been reported to be slightly more alkaline by Stormer (1972a). In addition, Stormer noted that even though a symmetrical distribution proposed by Lipman (1969) was apparent (i.e., described basically as tholeiitic basalt within the rift and alkali basalts on either side) the presence of the Raton-Clayton field suggests a more asymmetrical distribution because of the more calc-alkaline nature of the Raton-Clayton basalts compared to those west of the rift. This episodic or asymmetrical distribution is most apparent when viewed within a narrow time interval (Lipman and Mehnert, 1975).

Sierra Grande Lavas (see text)

Feldspathoidal Lavas

The Feldspathoidal lavas are a group of mafic, fine grained, dense basanites and olivine nephelinites characterized by hauyne phenocrysts and/or abundant nepheline. Other phenocrysts are olivine and augite which vary in abundance (Stormer, 1972b). Pyroxenes dominate as phenocrysts in the nephelinites (Phelps et al., 1983). The groundmass is often composed of plagioclase microlites in either a cryptocrystalline texture or glassy matrix (Stormer, 1972b). The extrusion of this group

began about 1.8 Ma (Phelps et al., 1983) and these rocks were initially included with the Clayton basalts by Collins (1949) (Phelps et al., 1983). Phelps and others proposed that the most likely and least objectionable origin of the mafic feldspathoidal volcanics is the partial melting of a garnet peridotite in the upper mantle. This is supported by the discovery of Type I and Type II xenoliths in many of the mafic feldspathoidal lavas (Phelps et al., 1983). Phelps and others describe the Type I (Cr-diopside) and Type II (Ti-Al augite) xenoliths as less than 15 cm in diameter, oxidzed to some extent, partially disaggregated, and exhibiting a remnant metamorphic texture. They report that websterite, wehrlite and harzburgite are present but that spinel iherzolite, which is common in xenoliths of similar western United States locations, is not present.

Capulin basalts

The Capulin basalts are characterized by rounded and resorbed phenocrysts of plagioclase with inclusion rich zones and olivine in a matrix of dark glass and microscopic oxide grains (Stormer, 1972b). The basalt flows and cinder cones of this unit are the youngest in the volcanic field with an age between 10,000 to 4,500 years ago (Baldwin and Muehlberger, 1959). This was based on Carbon 14 dating of material associated with a single flow and the underlying alluvial strata that is associated with the Folsom Man artifact finds. The rocks are olivine basalt, silicic alkali basalt and basaltic andesite (Collins, 1949; Phelps et al., 1983). The suggested source of these basalts, as determined from strontium isotopic signatures, was a magma originating in the upper mantle which then experienced little or no crustal contamination upon its ascent (Jones et al., 1974).

Intrusives

Chico Hill Phonolites

The remaining igneous rocks, in particular the Chico Hills phonolite sill complex, have been proposed to be the oldest in the volcanic field being contemporaneous with the Spanish Peaks of southern Colorado (21.7-25.6 Ma) (Stormer, 1972a). They also may be related to the early period

of tectonic and igneous activity of the Rio Grande Rift around 27-21 Ma (Elston and Bornhorst, 1979). The intrusive rocks of the Raton-Clayton field include sills of trachyandesite, trachyphonolite, phonolite, trachyte and peralkaline phonolite with numerous lamprophyre dikes (Potter, 1988). Potter also stated that chemical variations between samples imply that the peralkaline phonolite was the final product of a complex differentiating sequence of events that involved trachyandesite to trachyte to trachyphonolite to phonolite. In addition, considering the proximity of the phonolite sill complex to the Rio Grande Rift and an associated mantle upwelling, the idea that alkali rich magma produced from small amounts of partial melting of the upper mantle with little or no subsequent crustal contamination is a probable origin and one which is similar to other rifting regimes (Potter, 1988).

APPENDIX D METHODS OF ANALYSIS

Petrographic Analysis

One hundred and two samples of one hundred thirty eight samples returned from the field were initially selected for study. This number was reduced to 84 samples which were cut, mounted and polished. Thin sections were prepared on a Logitec at the Department of Geological and Atmospheric Sciences, Iowa State University and were ground to approximately 30 microns. Final polishing was done by hand using polishing wheels and 6, 3, 1 and 1/4 micron diamond grit. Petrographic analyses were completed on a standard petrographic microscope. Each thin section was analyzed for minerals present, estimated mode percent, size and shape. Textural, fabric and groundmass characteristics were recorded as well as observations pertaining to twinning, zoning and mineral relationships. Phenocryst percents are modal for the whole rock.

Microprobe Analysis

Chemical analyses of olivine, pyroxene, plagioclase and Fe-Ti oxide mineral grains were conducted on 23 thin sections from the petrographic analysis. The thin sections selected were representative samples of units 1, 2, 3, 4, 5, 7 and 8. The analyses were performed using an ARL-SEMQ electron microprobe located at the Department of Geological and Atmospheric Sciences, Iowa State University. The acceleration voltage for the microprobe was set at 15 Kev and the beam current was set at 20 nanoamps on a brass Faraday cup. Standardization counting times were 10 seconds for the peak and 2 seconds for the background. Sample analysis counting times were 20 seconds for the peak and 2 seconds for the background. Two iterations were run for each sample analysis.

Selection of olivine, pyroxene and plagioclase mineral grains was based on size and quality. A limited range for cross sectional area was predetermined from petrographic and hand specimen

analyses to insure adequate core and margin data points. Only those grains with little or no alteration were selected. The resulting minerals grains analyzed were randomly chosen to insure an overall representation of composition. An exception to this random analysis was the olivine occurring in SG513, being the only such grain identified in the second andesite. Fe-Ti oxides were randomly analyzed and consisted of isolated grains and a few minor alteration grains in olivines and pyroxenes.

The elements determined for in the olivines, pyroxenes and plagioclase were Si, Ti, Al, Fe (Total as FeO), Mg, Mn, Ca, Na and K. The Fe-Ti oxide minerals were analyzed for Cr, Ti, Fe (Total as FeO), Mg, Mn, Ca, Si, Al and Zn. The Bence-Albee (1968) correction program was applied and the data expressed as weight percent oxide. The chemical compositions of the olivines, pyroxenes and plagioclases are presented in weight percent oxide and formula units (Appendix G), the later using the method of calculation described by Ragland (1989). The grains analyzed are identified by the field sample numbers followed by a grain number (if given) and the designation as to whether it is a core (C) or margin (M) location. Each standard used is listed below along with the element for which it was used.

<u>For olivines, pyroxenes and plagioclases</u>

Hornblende, Kakanui Si, Mg, Ca, Fe*, Ti, Al
(Smithsonian USNM 143965)

Spessartine-Almandine Garnet Mn

Jadeite Na
(Coleman, 1961)

Microcline K

<u>For Fe-Ti oxide minerals:</u>

Chromite Cr
(Smithsonian USNM 117075)

Ilmenite Fe*, Mn, Ti
(Smithsonian USNM 96189

Hornblende, Kakanui Mg, Ca, Al, Si
(Smithsonian USNM 143965)

Gahnite Zn
(Smithsonian USNM 145883)

Fe* (Total Fe)

APPENDIX E PETROGRAPHIC DESCRIPTIONS

first basaltic andesite (unit 1) (black to very dark gray)

The andesite has a hypocrystalline (intersertal), microporphyritic to slightly porphyritic, slightly to moderately glomeroporphyritic and vesicular texture. A few samples have a slight trachytic texture. Microphenocrysts and phenocrysts range from .25 - 1.25 mm and 3 - 4 mm in size respectively and are euhedral to subhedral pyroxenes (augite) (< 5 percent) and olivines (< 5 percent), and subhedral plagioclases (An_{45-55}) (< 3 percent). Clusters of microphenocrysts occur composed of mostly pyroxene and some have olivine and plagioclase also present. A few pyroxenes exhibit simple twinning and sector and/or multiple zoning. Many of the olivines exhibit some skeletal growth. The plagioclases show either simple carlsbad twinning, albite twinning or both, and some have noticeable multiple zoning (normal and reverse). Present also are a few remnant phenocryst plagioclases with resorption characteristics (irregular or corroded margins) and trace amounts of secondary quartz which are single grains (rounded or slightly irregular shaped). Approximately 87 - 90 percent of the rock is groundmass, of which about 65 - 70 percent is plagioclase microlites, 5 percent is anhedral pyroxene and olivine, less than 1 percent is anhedral Fe-Ti oxide and 25 - 30 percent is brown glass. Some of the plagioclases exhibit simple twinning.

second basaltic andesite (unit 2) (light gray porphyritic)

This andesite has a texture that is a holocrystalline to hypocrystalline (fine grained intergranular to slightly intersertal), trachytic to microlitic, microporphyritic to slightly porphyritic, moderately glomeroporphyritic and vesicular. The microphenocrysts range from .25 - 1 mm and the few phenocrysts are 2 - 3.5 mm in size. They are euhedral to subhedral pyroxenes (augite)(10 - 15 percent) and olivines (< 5 percent), and subhedral plagioclases (An_{55})(5 - 10 percent). Present also are clusters of microphenocrysts (pyroxenes, often with some olivine and plagioclase). A few pyroxenes have simple twinning and/or sector zoning. Some of the pyroxenes and olivines exhibit

skeletal growth. The plagioclases show either simple carlsbad twinning, albite twinning or combination, and some have multiple zoning (normal and reverse). There are also a few remnant phenocryst plagioclases with corroded or irregular margins. The groundmass is 71 - 82 percent of the rock and is composed of about 85 - 90 percent plagioclase microlites, 5 - 10 percent anhedral pyroxene and olivine, about 1 percent anhedral Fe-Ti oxide and 5 percent brown glass. Most of the plagioclase show simple twinning.

third basaltic andesite (unit 3) (dark gray basaltic)

The andesite has a holocrystalline to slightly hypocrystalline (fine grained intergranular to very slightly intersertal), trachytic to microlitic, microporphyritic to slightly porphyritic, slightly to moderately glomeroporphyritic and vesicular to very vesicular texture. Microphenocrysts .25 - 1.25 mm and a few phenocrysts 2 - 3 mm are euhedral to subhedral pyroxenes (augite)(< 5 percent) and olivines (< 5 percent), and subhedral plagioclases (An_{55-60}) (< 5 percent). There are also clusters of microphenocrysts (mostly pyroxenes, a few olivines and fewer plagioclases). Many pyroxenes exhibit simple twinning and sector and/or multiple zoning. A few pyroxenes and olivines show skeletal growth. Twinning in the plagioclases is either simple carlsbad, albite or both, and some have either multiple or convoluted zoning present (normal and reverse). Remnant phenocryst plagioclases are present with resorption characteristics (irregular or corroded margins). The groundmass, which is about 88 - 92 percent of the rock is composed of about 85 - 90 percent plagioclase microlites, 5 - 10 percent anhedral pyroxene and olivine, less than 2 percent anhedral Fe-Ti oxide and less than 5 percent gray and brown glass. The plagioclases show simple twinning.

first andesites (unit 4)

subunit 4a (reddish gray aphanitic tuffaceous andesite)

The texture of this andesite is a hypocrystalline to holocrystalline-hypocrystalline (fine grained intergranular to intersertal), slightly trachytic to trachytic, microporphyritic to very slightly porphyritic, slightly glomeroporphyritic and vesicular to very vesicular. Microphenocrysts and a few phenocrysts

range from .25 - 1.25 mm and 2 - 2.25 mm respectively. They are euhedral to subhedral pyroxenes (augite)(< 5 percent) and subhedral plagioclases (< 2 percent). There are also clusters of microphenocrysts composed of mostly pyroxene, often with olivine and plagioclase present. Some of the pyroxenes have simple twinning and sector and/or multiple zoning while a few exhibit skeletal growth and/or intergrowth relationships with Fe-Ti oxides (alteration coronas and probable replacement). The plagioclases have either simple carlsbad twinning, albite twinning or both, some with multiple zoning. There is also remnant phenocryst plagioclase with resorption characteristics (irregular or corroded margins) and secondary quartz (single, rounded or irregular grains). The groundmass, 93 - 95 percent of the rock, is composed of about 80 - 85 percent plagioclase microlites, 5 - 10 percent anhedral pyroxene, less than 2 percent anhedral Fe-Ti oxide and 5 - 7 percent gray, brown and red glass. Most of the plagioclases show simple twinning.

subunit 4b (light gray slightly porphyritic tuffaceous andesite)

This andesite has a holocrystalline to hypocrystalline, (fine grained intergranular to slightly intersertal), trachytic, microporphyritic, slightly to moderately glomeroporphyritic and vesicular texture. Often clustered together, the microphenocrysts .25 - 1 mm are euhedral to subhedral pyroxenes (augite) (< 5 percent) and subhedral plagioclases (< 2 percent). Some pyroxenes exhibit simple twinning and/or sector zoning while a few have skeletal growth or some alteration. Plagioclase show either simple carlsbad twinning, albite twinning or both, and some have multiple zoning. The groundmass, which is 93 - 95 percent of the rock, is composed of about 85 - 90 percent plagioclase microlites, 5 - 10 percent anhedral pyroxene, about 1 percent anhedral Fe-Ti oxide and about 5 percent brown and red glass. Many of the plagioclase show simple twinning.

subunit 4c (gray porphyritic tuffaceous andesite)

The texture of this andesite is a holocrystalline (fine grained intergranular), trachytic, microporphyritic, moderately glomeroporphyritic and vesicular. Microphenocrysts range from .25 - 2 mm and are euhedral to subhedral pyroxenes (augite)(5 - 10 percent) and subhedral (An_{65-70})

plagioclases (< 2 percent). Many of the pyroxenes are clustered together, often with a few plagioclases. Some of the pyroxenes show simple twinning and either sector and/or multiple zoning. A few exhibit skeletal growth and/or late stage alteration. The plagioclases exhibit twinning that is either simple carlsbad, albite or combination, and a few have multiple or convoluted zoning. The groundmass is 88 - 94 percent of the rock and is composed of about 85 - 90 percent plagioclase microlites, 10 - 15 percent anhedral pyroxene, about 2 percent anhedral Fe-Ti oxide and traces of brown and red glass. Most of the plagioclases show simple twinning and define a flow structure.

subunit 4d (dark gray aphanitic andesite)

This andesite has a texture that is hypocrystalline (fine grained intergranular to intersertal), slightly trachytic to microlitic, microporphyritic, slightly glomeroporphyritic and slightly to moderately vesicular. The microphenocrysts range from .25 - 1.25 mm and are euhedral to subhedral pyroxenes (augite)(5 - 10 percent) and subhedral plagioclases (< 3 percent), often clustered. A few of the pyroxenes exhibit simple twinning and sector or multiple zoning, some show skeletal growth. Some of the plagioclases have either simple carlsbad twinning, albite twinning or both, and a few show either multiple or convoluted zoning. The groundmass, which is 87 - 92 percent of the rock is composed of about 75 - 80 percent plagioclase microlites, 5 - 10 percent anhedral pyroxene, 2 percent anhedral Fe-Ti oxide and about 10 - 15 percent brown and gray glass. Most of the plagioclase has simple twinning.

subunit 4e (red gray aphanitic tuffaceous andesite)

This andesite has a hypocrystalline (fine grained intergranular to intersertal), microlitic, microporphyritic, slightly glomeroporphyritic and moderately vesicular texture. The microphenocrysts .25 - 2 mm, some clustered together are euhedral to subhedral pyroxenes (augite)(5 - 10 percent) and subhedral plagioclases (< 3 percent). Many of the pyroxenes show simple twinning and/or sector zoning, a few show skeletal growth. Some of the plagioclase exhibit either simple carlsbad, albite or combination twinning, a few with multiple zoning. The groundmass, 87 - 94 percent of the rock, is

composed of about 50 - 75 percent plagioclase microlites, 5 - 15 percent anhedral pyroxene, less than 1 percent anhedral Fe-Ti oxide and about 10 - 45 percent brown and gray or brown glass. Some of the plagioclase show simple twinning. Only in the more fine grained intergranular groundmass texture is there a sense of flow structure.

subunit 4f (banded, multicolored aphanitic andesite)

The texture of this andesite is holocrystalline to hypocrystalline (fine grained intergranular to intersertal), slightly trachytic to trachytic, microporphyritic, slightly glomeroporphyritic and vesicular. Microphenocrysts range .25 - 2 mm in size and a few of which are clustered. These are euhedral to subhedral pyroxenes (augite)(< 5 percent) and subhedral plagioclases (< 2 percent). Several pyroxenes have simple twinning and/or sector zoning. A few exhibit skeletal growth or some alteration. The plagioclases have twinning that is either simple carlsbad, albite or both, and some have multiple zoning. There is also a few remnant near phenocryst plagioclases with corroded or irregular margins. There are traces of secondary quartz that are single grains (rounded or slightly irregular). The groundmass, which is 93 - 95 percent of the rock is composed of about 50 - 75 percent plagioclase microlites, 5 - 10 percent anhedral pyroxene, less than 2 percent anhedral Fe-Ti oxide and about 15 - 45 percent brown and gray glass. The groundmass generally has a good sense of flow structure.

second andesite (unit 5)

subunit 5a (dark bluish gray porphyritic andesite)

This andesite has a hypocrystalline (fine grained intergranular to intersertal), moderately trachytic, microporphyritic to moderately porphyritic, moderately to slightly glomeroporphyritic and moderately to very vesicular texture. Microphenocrysts and phenocrysts range from .25 - 2 mm and 2.25 - 4.5 mm respectively. They are euhedral to subhedral pyroxenes (< 5 percent augite and 5 - 10 percent enstatite) and subhedral plagioclases (An_{50-60}) (< 3 percent). Many of the microphenocrysts are clustered together (mostly augites, a few enstatites and fewer plagioclases). In

one sample, an isolated euhedral to subhedral olivine was found. Some of the pyroxenes exhibit skeletal growth, particularly the augites, while a few others show simple twinning and sector or multiple zoning. The plagioclases exhibit either simple carlsbad or albite twinning or both, some with multiple zoning (normal and reverse). One feature found in a few rocks of this subunit is an almost cuniform growth of a few plagioclase microphenocrysts. Present are a few phenocryst plagioclase remnants that show typical resorption characteristics (irregular or corroded margins). There is also some quartz present as secondary mineral which appears to be vugs fillings and can range up to 5 mm in size. The groundmass, comprising 82 - 89 percent of the rock, is composed of about 65 - 85 percent plagioclase microlites, 5 - 10 percent anhedral pyroxene, less than 2 percent anhedral Fe-Ti oxide and about 10 - 25 percent gray and brown glass. Some of the plagioclases show simple twinning. Most all samples showed a sense of flow.

subunit 5b (gray to dark gray porphyritic andesite)

The texture of this andesite is a holocrystalline to hypocrystalline (fine grained to slightly intersertal), moderately trachytic to trachytic to microlitic, microporphyritic to slightly porphyritic, slightly to moderately glomeroporphyritic and vesicular to very vesicular. The microphenocrysts range from .25 - 1.25 mm and the phenocrysts range from 2 - 2.5 mm. These are euhedral to subhedral pyroxenes (about 5 - 10 percent augite and less than 5 percent enstatite) and subhedral plagioclases (An_{50-70}) (< 5 percent). Some of the microphenocrysts are clustered together, mostly pyroxenes. Many of the pyroxenes, both augite and enstatite, exhibit simple twinning, sector or multiple zoning and some show skeletal growth. The plagioclases usually show simple carlsbad twinning, albite twinning or both, and some exhibit multiple zoning. A few remnant phenocryst plagioclases have irregular or corroded margins. Quartz occurs as a secondary mineral as single grains with rounded or slightly irregular shapes. Approximately 82 - 89 percent of the rock is groundmass, of which about 80 - 90 percent is plagioclase microlites, 10 - 15 percent is anhedral pyroxene, less than 1 percent is anhedral Fe-Ti oxide and less than 5 percent is gray and brown glass. The plagioclase show simple

twinning. A sense of flow is evident in the groundmass which decreases with increased glass percentage.

subunit 5c (dark gray aphanitic andesite)

This andesite has a holocrystalline (fine grained intergranular), trachytic, microporphyritic to slightly porphyritic, slightly glomeroporphyritic and vesicular texture. Microphenocrysts are .25 - 1.5 mm and phenocrysts are 2 - 2.25 mm in size. They are euhedral to subhedral pyroxenes (5 - 10 percent augite) and subhedral plagioclases (An_{50-60}) (< 2 percent). Some of the pyroxenes have simple twinning, sector or multiple zoning and some show skeletal growth. Most of the plagioclases show either simple carlsbad twinning, albite twinning or both, some with multiple zoning. The groundmass, which is 88 - 94 percent of the rock, is composed of about 90 percent plagioclase microlite, 10 percent anhedral pyroxene and less than 1 percent anhedral Fe-Ti oxides. Most of the plagioclases show simple twinning. There is a sense of flow to the rock structure.

andesitic dikes (unit 8)

subunit 8a (black porphyritic andesitic dike)

The texture of these dike rocks is hypocrystalline (intersertal), microporphyritic to slightly porphyritic, slightly glomeroporphyritic and very vesicular. Microphenocrysts and phenocrysts are .25 - .1 mm and 1.25 - 5.5 mm respectively. The minerals present are euhedral to subhedral pyroxenes (5 percent augite and less than 2 percent enstatite) and subhedral $An_{(50-60)}$ plagioclases (< 2 percent). Many of the pyroxenes show simple twinning and sector and/or multiple zoning and some exhibit skeletal growth. The plagioclases show simple carlsbad or albite twinning, and some have multiple zoning. The groundmass totals to about 92 percent and is composed of about 50 percent plagioclase microlites, 10 percent anhedral pyroxene, 1 percent anhedral Fe-Ti oxide and about 40 percent brown glass.

upper andesites and andesitic breccias (unit 6)

summit andesite (unit 6a) (red to reddish gray aphanitic tuffaceous)

This andesite has a hypocrystalline to hypohyaline (intersertal to fine grained intergranular, intersertal), microporphyritic to very slightly porphyritic, slightly to moderately glomeroporphyritic and moderately to very vesicular texture. Microphenocrysts range from .25 - 1.25 mm and the few phenocrysts present are 2 - 2.25 mm in size. The microphenocrysts are euhedral to subhedral pyroxenes (augite)(< 5 percent) and subhedral plagioclases (< 2 percent). The phenocrysts are a few subhedral pyroxenes and remnant plagioclases. Most of the pyroxenes have simple twinning and multiple zoning and a few show skeletal growth. The plagioclases exhibit either simple carlsbad twinning, albite twinning or both, and some show multiple zoning. Remnant plagioclases present are ovate, anhedral and have been very resorbed (irregular or corroded margins). The groundmass is 93 - 95 percent of the rock and is composed of about 30 - 50 percent plagioclase microlites, 20 percent anhedral pyroxene, less than 1 percent anhedral Fe-Ti oxide and about 30 - 50 percent brown to gray glass. Very few plagioclase show any twinning.

andesitic breccias (unit 6b)

subunit 6b1 (bluish gray to gray mottled basaltic - andesitic breccia)

This andesitic breccia has clasts with: a holocrystalline (fine grained intergranular), slightly trachytic, microporphyritic and very slightly glomeroporphyritic texture and a hypocrystalline (fine grained intergranular to slightly intersertal), very slightly trachytic, microporphyritic, slightly glomeroporphyritic texture and intersertal material that is hypocrystalline to microcrystalline and microporphyritic. There is an overall slight vesicularity to the samples. The microphenocrysts range from .25 - .75 mm and are euhedral to subhedral pyroxenes (augite)(< 5 percent), subhedral plagioclase (< 2 percent) and subhedral to anhedral olivines (< 2 percent). Some of the pyroxenes show simple twinning and multiple zoning. A few of the pyroxenes and olivines show skeletal growth. The plagioclases exhibit either simple carlsbad or albite twinning or combination and some have

multiple zoning. Also a few plagioclases appear to be remnants which have been well resorbed, with irregular or corroded margins. The groundmass (both clasts and intersertal material) is about 92 - 95 percent of the rock and is composed of about 65 percent plagioclase microlites, 20 percent subhedral to anhedral pyroxene and olivine, 5 percent anhedral Fe-Ti oxide and about 10 percent clear and gray glass. Some of the plagioclase show simple carlsbad twinning.

subunit 6b2 (bluish red to bluish gray mottled andesitic breccia)

The clasts of this breccia have textures that are: hypocrystalline (fine grained intergranular to intersertal), slightly microlitic, microporphyritic to slightly porphyritic, moderately glomeroporphyritic and vesicular, and hypocrystalline (fine grained intergranular), slightly trachytic, microporphyritic, moderately glomeroporphyritic and vesicular surrounded by a matrix that is hypohyaline to holohyaline (intersertal), microporphyritic, very slightly glomeroporphyritic. The microphenocrysts and few phenocrysts are .25 - 1.25 mm and 2 - 2.25 mm respectively. They are euhedral to subhedral pyroxenes (augite)(5 percent) and a few larger anhedral Fe-Ti oxides (< 2 percent). Many of the pyroxenes show simple twinning and some zoning. Also a few are very to slightly altered and some appear to have been replaced. The groundmass (both clasts and matrix) is about 93 percent of the rock. Overall, it is composed of plagioclase microlites ranging from 40 - 85 percent, about 5 percent anhedral pyroxene, less than 1 percent anhedral Fe-Ti oxides, and red and brown glass ranging from 10 to 55 percent. The groundmass of the clasts is either composed of random plagioclase microlites in glass while the intersertal material has slightly trachytic plagioclase microlites. The fabric is somewhat convoluted in the more glassy matrix.

subunit 6b3 (multicolored tuffaceous andesitic breccia)

This breccia is composed of clasts which have a hypocrystalline (very fine grained intergranular to intersertal), microcrystalline, microporphyritic, slightly to moderately glomeroporphyritic and microvesicular texture, surrounded by intersertal material with a similar texture and microcrystalline groundmass. The microphenocrysts are .25 to .5 mm in size with a few

as large as .75 - 1 mm. They are euhedral to subhedral pyroxenes (augite)(5 percent), many of which show simple twinning, sector and/or multiple zoning, other exhibit skeletal growth. The groundmass overall (both within the clasts and between) is about 95 percent of the rock and in both cases is composed of about 60 percent plagioclase microlites, 10 percent anhedral pyroxene, less than 1 percent Fe-Ti oxide and about 30 percent gray and brown glass.

andesitic plug (unit 6c) (dark gray to bluish gray aphanitic)

The texture of this andesite subunit is holocrystalline to hypocrystalline (fine grained intergranular), microlitic, microporphyritic, slightly to moderately glomeroporphyritic and slightly vesicular. The microphenocrysts range from .25 - .75 mm and 1 - 1.75 mm. They are euhedral to subhedral pyroxenes (augite)(5 percent) and subhedral plagioclases (< 2 percent). A few of the pyroxenes show skeletal growth, while some others exhibit simple twinning and sector and/or multiple zoning. Most of the plagioclases show either simple carlsbad or albite twinning and no zoning was observed. The groundmass, which is about 93 - 95 percent of the rock, has a microcrystalline appearance. The groundmass is composed of about 85 - 90 percent plagioclase microlites, 10 percent anhedral pyroxene, less than 1 percent anhedral Fe-Ti oxide and a trace to less than 5 percent gray glass.

saddle andesite (unit 6d) (bluish gray to gray aphanitic)

This andesite has a hypocrystalline to holocrystalline (fine grained intergranular), microlitic, microporphyritic to slightly porphyritic, slightly to moderately glomeroporphyritic and vesicular texture. Microphenocrysts range .25 - 1.00 mm, the few phenocrysts are 2.00 - 2.75 mm. There are euhedral to subhedral pyroxenes (augite)(5 - 10 percent) and subhedral plagioclases (< 2 percent). Some of the pyroxenes exhibit simple twinning and sector and/or multiple zoning, while some others show skeletal growth. Many of the plagioclases show either some simple carlsbad twinning, albite twinning or both, and some have multiple zoning. Present also are a few remnant plagioclases with resorption characteristics (irregular or corroded margins). The groundmass, which is about 88 - 93

percent of the rock, has a microcrystalline appearance and is composed of about 90 percent plagioclase microlites, 5 - 10 percent anhedral pyroxene, less than 1 percent anhedral Fe-Ti oxide and less than 5 percent gray glass. Some of the plagioclases show simple carlsbad twinning.

basaltic scoria and basalt (unit 7)

subunit 7a (dark red porphyritic scoria)

This scoria has a hypohyaline, microporphyritic to slightly porphyritic, slightly to moderately glomeroporphyritic and very vesicular texture. The microphenocrysts and few phenocrysts range from .25 - 1 mm and 1.5 - 3.75 mm respectively. They are euhedral to subhedral pyroxenes (augite)(5 - 10 percent), euhedral olivines (< 5 percent) and subhedral plagioclases (< 5 percent). Many of the pyroxenes show some simple twinning and zoning while some others have skeletal growth. The olivines also show skeletal growth as well as alteration coronas. Plagioclases show twinning that is either simple carlsbad, albite or both, and some zoning. A few plagioclases are probable remnants having been through resorption (irregular shapes). The groundmass is 81 to 88 percent of the rock and is composed of about 40 - 60 plagioclase microlites, 5 - 10 percent anhedral pyroxene and olivine, less than 5 percent anhedral Fe-Ti oxide and 20 - 50 percent brown and red brown glass.

subunit 7b (red and black scoria)

The texture of this scoria is hypohyaline or holohyaline (cryptocrystalline), microporphyritic and very vesicular. Microphenocrysts, which range from .25 - .5 mm, are subhedral to euhedral pyroxenes (augite)(< 5 percent) and euhedral to subhedral olivines (< 5 percent). There is very little indication of zoning or twinning in any microphenocrysts. All the pyroxenes and olivines have alteration coronas of Fe-Ti oxides. The groundmass, 90 - 92 percent of the rock, is composed of about 20 percent anhedral pyroxene and olivine, 5 - 10 percent anhedral Fe-Ti oxide and 70 - 75 percent green, gray and red brown glass. There are traces of plagioclase in the groundmass.

subunit 7c (brown to black glassy scoria)

This scoria has a holohyaline to slightly hypohyaline (cryptocrystalline), microporphyritic and

vesicular texture. The microphenocrysts range from .25 to 1 mm and are anhedral to subhedral pyroxenes (augite)(< 2 percent) and euhedral to subhedral olivines (< 10 percent). The pyroxenes are lath like and some show simple twinning. Most of the olivines have been altered or resorbed and many show intergrowths with opaque minerals. The groundmass, which is 88 percent of the rock, is composed of about 10 percent subhedral to anhedral olivine and pyroxene, and 90 percent brown and black glass. The glass has a convoluted structure. No Fe-Ti oxides were identified.

subunit 7d (greenish black porphyritic basalt)

This basalt has a hypocrystalline (fine grained to partially intersertal), partially microcrystalline, microporphyritic, very slightly glomeroporphyritic and vesicular texture. Microphenocrysts range from .25 - 1 mm and are euhedral to subhedral to anhedral olivines (10 percent) and subhedral pyroxenes (augite) (2 percent). The olivines are rimmed by Fe-Ti oxides. No definite twinning or zoning was observed. The groundmass is 88 percent of the rock and is composed of about 40 percent anhedral olivine and pyroxene, 30 percent anhedral plagioclase, 15 percent anhedral Fe-Ti oxide and 15 percent green and gray green glass. Although most of the oxide minerals are opaque, some are red and translucent.

basaltic dikes (Unit 8)

subunit 8b1 (black porphyritic basaltic dike)

The rock of these dikes has a hypocrystalline, cryptocrystalline to near glassy, microporphyritic to slightly porphyritic, slightly glomeroporphyritic and moderately vesicular texture. The microphenocrysts and the few phenocrysts are .25 - 1 mm and 2 to 3.5 mm respectively. They are euhedral to subhedral olivines (10 - 15 percent) and euhedral to subhedral pyroxenes (augite)(5 percent). Many of the olivines have skeletal growth and some have been partially replaced by Fe-Ti oxides. Some of the pyroxenes exhibit simple twinning and sector and/or multiple zoning and some appear to have been altered. The groundmass which is 80 - 85 percent of the rock is composed of about 20 percent plagioclase microlites, 30 percent anhedral pyroxene, 5 percent subhedral to

anhedral olivine, 5 percent anhedral Fe-Ti oxides and about 40 percent gray glass. The groundmass has a more cryptocrystalline to microcrystalline texture.

subunit 8b2 (dark gray aphanitic basaltic dike (west))

The texture of this dike rock is hypocrystalline (fine grained intergranular to intersertal), cryptocrystalline to microcrystalline, microporphyritic and vesicular. The microphenocrysts are .25 - 1 mm in size and are euhedral to subhedral (a few anhedral) olivines (5 - 10 percent) and euhedral to subhedral pyroxenes (augite)(< 2 percent). Most of the olivines have alteration coronas. Some of the pyroxenes show simple twinning and multiple or sector zoning. There are a few unknowns that appear to be inclusions or xenoliths but were not identifiable. The groundmass is about 83 - 90 percent of the rock and is composed of about 15 percent plagioclase microlites, 70 - 75 percent subhedral to anhedral pyroxene, 2 percent anhedral Fe-Ti oxide and 10 percent glass.

subunit 8b3 (gray to dark gray aphanitic basaltic dike (east))

This dike rock has a texture that is holocrystalline to hypocrystalline (fine grained intergranular), microcrystalline, microporphyritic to slightly porphyritic and slightly glomeroporphyritic. The microphenocrysts and phenocrysts are .25 - 1 mm and 2 - 2.5 mm respectively. There are euhedral to subhedral olivines (15 percent) and euhedral to subhedral pyroxenes (augite)(5 percent). Some of the olivines have either skeletal growth or resorption features (irregular margins). Most pyroxenes exhibit simple twinning and sector or multiple zoning. There are also a few pyroxenes that have Fe-Ti oxide rims. The groundmass, which is about 80 percent of the rock, is composed of about 15 percent plagioclase microlites, 25 percent subhedral to anhedral pyroxene, 5 percent anhedral Fe-Ti oxide, 50 percent microcrystals and a trace of glass. Some of the plagioclase show simple twinning.

APPENDIX F SAMPLE LOCATIONS

	Sample #		Sec	T	R	Unit	Lithologic Rock Type
1	SG2-0-1	NE1/4, NE1/4	23	29N	29E	0	Clayton basalt
2 *	SG2-1-2	SW1/4, NW1/4	19	29N	29E	1	first basaltic andesite
3 *	SG2-1-4	NE1/4, NW1/4	24	29N	28E	"	"
4 *	SG2-1-6	SW1/4, SE1/4	35	29N	28E	"	"
5 *	SG2-1-8	NW1/4, SW1/4	15	29N	29E	"	"
6 **	SG2-1-9	NE1/4, SE1/4	18	29N	29E	"	"
7 *	SG2-2-1	SE1/4, NE1/4	2	28N	28E	2	second basaltic andesite
8 **	SG2-2-2	NW1/4, NW1/4	1	28N	28E	"	"
9 **	SG2-2-4	NE1/4, NW1/4	1	28N	28E	"	"
10 *	SG2-3-2	SW1/4, NE1/4	26	29N	29E	3	third basaltic andesite
11 **	SG2-3-3	SW1/4, NE1/4	26	29N	29E	"	"
12 *	SG2-3-5	SE1/4, NW1/4	35	29N	29E	"	"
13 **	SG2-3-6	SW1/4, NW1/4	26	29N	29E	"	"
14 *	SG2-3-7	NW1/4, SE1/4	15	29N	29E	"	"
15 *	SG2-4A-1	NE1/4,NW1/4	25	29N	28E	4a	first andesite
16 **	SG2-4A-2	NW1/4, SE1/4	34	29N	29E	"	"
17 *	SG2-4A-3	SE1/4, NE1/4	28	29N	29E	"	"
18 *	SG2-4B-2	SW1/4, SW1/4	21	29N	29E	4b	"
19 *	SG2-4B-3	SW1/4, SW1/4	36	29N	28E	"	"
20 *	SG2-4C-1	SW1/4, SW1/4	19	29N	29E	4c	"
21 *	SG2-4C-3	SW1/4, SW1/4	36	29N	28E	"	"

* petrographic thin section

** petrographic and microprobe thin section

	Sample #		Sec	T	R	Unit	Lithologic Rock Type
22 *	SG2-4C-4	SW1/4, NE1/4	27	29N	29E	4c	first andesite
23 *	SG2-4C-6	NW1/4, NE1/4	22	29N	29E	"	"
24 *	SG2-4D-1	NE1/4, NW1/4	25	29N	28E	4d	"
25 *	SG2-4D-2	SE1/4, SW1/4	26	29N	29E	"	"
26 *	SG2-4D-3	NE1/4, SW1/4	26	29N	29E	"	"
27 *	SG2-4E-1	SW1/4, NW1/4	19	29N	29E	4e	"
28 *	SG2-4E-3	SE1/4, SW1/4	24	29N	28E	"	"
29 *	SG2-4E-4	SE1/4, SW1/4	21	29N	29E	"	"
30 *	SG2-4E-5	NE1/4, NE1/4	26	29N	29E	"	"
31 *	SG2-4E-6	NW1/4, SW1/4	26	29N	29E	"	"
32 *	SG2-4F-1	NW1/4, SE1/4	24	29N	28E	4f	"
33 *	SG2-4F-2	NE1/4, NW1/4	25	29N	28E	"	"
34 *	SG2-4F-3	NE1/4, SW1/4	31	29N	29E	"	"
35 *	SG2-4F-5	NE1/4, NE1/4	19	29N	29E	"	"
36 *	SG2-4F-6	SE1/4, NE1/4	28	29N	29E	"	"
37 *	SG2-4F-7	SE1/4, SW1/4	28	29N	29E	"	"
38 *	SG2-5-1	SW1/4, SW1/4	19	29N	29E	5a	second andesite
39 **	SG2-5-2	NW1/4, NE1/4	25	29N	28E	"	"
40 *	SG2-5-4	NE1/4, NW1/4	25	29N	28E	"	"
41 *	SG2-5-5	NW1/4, MW1/4	36	29N	28E	5b	"
42 *	SG2-5-6	NE1/4, NE1/4	30	29N	29E	5a	"
43 **	SG2-5-8	SE1/4, NW1/4	31	29N	29E	5c	"
44 *	SG2-5-9	NE1/4, SE1/4	21	29N	29E	5a	"

* petrographic thin section

** petrographic and microprobe thin section

	Sample #		Sec	T	R	Unit	Lithologic Rock Type
45 **	SG2-5-10	NW1/4, SE1/4	21	29N	29E	5a	second andesite
46 *	SG2-5-11	NE1/4, SE1/4	30	29N	29E	5c	"
47 **	SG2-5-13	SE1/4, SW1/4	21	29N	29E	5a	"
48 *	SG2-5-14	SE1/4, SE1/4	20	29N	29E	"	"
49 *	SG2-5-15	SE1/4, NE1/4	19	29N	29E	"	"
50 *	SG2-5-16	SW1/4, SW1/4	17	29N	29E	5b	"
51 **	SG2-5-17	NW1/4, SE1/4	34	29N	29E	"	"
52 **	SG2-5-18	SE1/4, NW1/4	1	28N	28E	5a	"
53 *	SG2-5-20	NW1/4, NW1/4	1	28N	28E	"	"
54 *	SG2-5-21	SW1/4, SW1/4	16	29N	29E	"	"
55 **	SG2-5-22	NW1/4, NE1/4	33	29N	29E	"	"
56 *	SG2-5-23	SE1/4, NE1/4	28	29N	29E	"	"
57 *	SG2-5-24	NE1/4, SE1/4	32	29N	29E	5b	"
58 **	SG2-5-25	SW1/4, NW1/4	32	29N	29E	5a	"
59 *	SG2-5-28	SE1/4, SE1/4	17	29N	29E	"	"
60 **	SG2-5-29	SW1/4, SE1/4	20	29N	29E	"	"
61 *	SG2-5-30	SE1/4, NW1/4	29	29N	29E	"	"
62 *	SG2-5-31	SE1/4, NW1/4	29	29N	29E	5b	"
63 **	SG2-5-32	NE1/4, NE1/4	32	29N	29E	"	"
64 *	SG2-5-33	NE1/4, NW1/4	32	29N	29E	"	"
65 *	SG2-5-34	NW1/4, SW1/4	26	29N	29E	5a	"
66 *	SG2-5-35	NW1/4, SE1/4	32	29N	29E	5b	"
67 *	SG2-6-0	NE1/4, SE1/4	32	29N	29E	6a	summit andesite

* petrographic thin section

** petrographic and microprobe thin section

	Sample #		Sec	T	R	Unit	Lithologic Rock Type
68 *	SG2-6-2	SW1/4, SE1/4	32	29N	29E	6a	summit andesite
69 *	SG2-6-3	NW1/4, SE1/4	32	29N	29E	6c	andesitic plug
70 *	SG2-6-4	NW1/4, SE1/4	32	29N	29E	6b	andesitic breccia
71 *	SG2-6-5	NE1/4, SW1/4	32	29N	29E	6d	saddle andesite
72 *	SG2-6-6	NE1/4, SW1/4	32	29N	29E	6b	andesitic breccia
73 *	SG2-6-7	SE1/4, NW1/4	32	29N	29E	"	"
74 *	SG2-6-8	NE1/4, SW1/4	32	29N	29E	"	"
75 *	SG2-6-10	NE1/4, SW1/4	32	29N	29E	"	"
76 *	SG2-7-1	SW1/4, NW1/4	36	29N	28E	7a	basaltic scoria
77 **	SG2-7-2	NE1/4, NE1/4	35	29N	28E	"	"
78 *	SG2-7-4	SW1/4, NW1/4	36	29N	29E	7b	"
79 **	SG2-7-7	SW1/4, NW1/4	36	29N	29E	7c	basaltic scoria (glassy)
80 **	SG2-7-11	SE1/4, NE1/4	35	29N	29E	7d	basalt
81 **	SG2-8-1	SE1/4, NE1/4	26	29N	28E	8b	basaltic dike
82 **	SG2-8-5	SE1/4, SE1/4	20	29N	29E	8a	andesitic dike
83 **	SG2-8-8	SW1/4, NW1/4	36	29N	29E	8b	basaltic dike
84 *	SG2-8-10	SW1/4, NE1/4	26	29N	29E	8b	"
85 **	SG2-8-13	NW1/4, SE1/4	26	29N	28E	8b	"

* petrographic thin section

** petrographic and microprobe thin section

APPENDIX G MICROPROBE DATA

TABLE 1 Olivine Composition

	SG219-1C	SG219-1M	SG219-2M	SG219-2C	SG222-1C	SG222-1M	SG224-1M	SG224-1C
SiO2	39.5470	39.7910	39.6900	39.4960	38.9460	38.2780	40.7990	39.0560
TiO2	0.0260	0.0000	0.0320	0.0000	0.0000	0.0280	0.0250	0.0410
Al2O3	0.0260	0.0160	0.0210	0.0210	0.0210	0.0450	0.0520	0.0590
FeO	12.5440	13.5940	12.8850	13.2350	17.5310	19.1240	8.8000	11.7070
MnO	0.3850	0.3280	0.3640	0.2580	0.2680	0.4440	0.2910	0.4810
MgO	46.8250	46.4180	46.8290	47.1920	43.9000	41.1690	50.9540	47.2390
CaO	0.1540	0.1360	0.1450	0.1520	0.1850	0.2130	0.1250	0.1330
K2O	0.0000	0.0000	0.0000	0.0000	0.0000	0.0000	0.0000	0.0000
Na2O	0.0250	0.0000	0.0000	0.0000	0.0000	0.0000	0.0160	0.0000
SUM	99.5320	100.2830	99.9660	100.3540	100.8510	99.3010	101.0620	98.7160
Si	0.9889	0.9912	0.9892	0.9824	0.9832	0.9902	0.9865	0.9824
Ti	0.0005	0.0000	0.0006	0.0000	0.0000	0.0005	0.0005	0.0008
Al	0.0008	0.0005	0.0006	0.0006	0.0006	0.0014	0.0015	0.0017
Fe	0.2623	0.2832	0.2686	0.2753	0.3701	0.4137	0.1780	0.2463
Mn	0.0082	0.0069	0.0077	0.0054	0.0057	0.0097	0.0060	0.0102
Mg	1.7449	1.7232	1.7394	1.7494	1.6517	1.5871	1.8362	1.7709
Ca	0.0041	0.0036	0.0039	0.0041	0.0050	0.0059	0.0032	0.0036
K	0.0000	0.0000	0.0000	0.0000	0.0000	0.0000	0.0000	0.0000
Na	0.0012	0.0000	0.0000	0.0000	0.0000	0.0000	0.0008	0.0000
	SG224-2M	SG224-2C	SG224-3M	SG224-3C	SG233-1M	SG233-1C	SG233-2M	SG233-2C
SiO2	40.7280	39.6040	40.1780	38.9600	38.4420	39.9570	38.9020	39.6210
TiO2	0.0070	0.0050	0.0290	0.0120	0.0240	0.0490	0.0000	0.0000
Al2O3	0.0290	0.0460	0.0470	0.1890	0.0630	0.0500	0.0230	0.0230
FeO	8.9730	14.5560	9.0960	14.3240	18.1330	15.6840	18.2450	15.4060
MnO	0.4430	0.5010	0.4060	0.5540	0.2780	0.2450	0.3090	0.1610
MgO	50.3720	46.0720	50.8240	45.8210	42.4140	44.5560	43.1690	45.0160
CaO	0.1320	0.1740	0.1280	0.1870	0.2100	0.1710	0.1810	0.2140
K2O	0.0000	0.0000	0.0000	0.0000	0.0000	0.0000	0.0000	0.0000
Na2O	0.0000	0.0060	0.0170	0.0000	0.0000	0.0000	0.0160	0.0000
SUM	100.6840	100.9640	100.7250	100.0470	99.5640	100.7120	100.8450	100.4410
Si	0.9897	0.9855	0.9780	0.9788	0.9865	0.9990	0.9854	0.9929
Ti	0.0001	0.0001	0.0005	0.0002	0.0005	0.0009	0.0000	0.0000
Al	0.0008	0.0013	0.0013	0.0056	0.0019	0.0015	0.0007	0.0007
Fe	0.1824	0.3029	0.1852	0.3010	0.3892	0.3280	0.3865	0.3229
Mn	0.0091	0.0106	0.0084	0.0118	0.0060	0.0052	0.0066	0.0034
Mg	1.8242	1.7086	1.8437	1.7157	1.6222	1.6602	1.6297	1.6812
Ca	0.0034	0.0046	0.0033	0.0050	0.0058	0.0046	0.0049	0.0057
K	0.0000	0.0000	0.0000	0.0000	0.0000	0.0000	0.0000	0.0000
Na	0.0000	0.0003	0.0008	0.0000	0.0000	0.0000	0.0008	0.0000

TABLE 1 continued

	SG233-3C	SG233-3M	SG233-4M	SG233-4C	SG236-2M	SG236-2C	SG2513-1M	SG2513-1C
SiO2	39.5040	39.4380	38.9780	39.7690	39.8430	39.9070	40.4060	39.9820
TiO2	0.0000	0.0280	0.0010	0.0010	0.0200	0.0000	0.0000	0.0000
Al2O3	0.0750	0.0180	0.0180	0.0770	0.0480	0.0580	0.0450	0.0130
FeO	16.6270	17.6880	17.7200	15.9850	15.2760	15.7590	12.6870	13.4180
MnO	0.1630	0.3100	0.3390	0.1770	0.4220	0.3530	0.4310	0.4770
MgO	44.6980	43.3270	43.4960	44.6240	45.4250	44.8950	46.8970	46.4330
CaO	0.1540	0.1850	0.1670	0.1970	0.1750	0.1650	0.1600	0.1440
K2O	0.0000	0.0000	0.0000	0.0000	0.0000	0.0000	0.0000	0.0000
Na2O	0.0000	0.0000	0.0000	0.0000	0.0030	0.0110	0.0000	0.0000
SUM	101.2210	100.9940	100.7190	100.8300	101.2120	101.1480	100.6260	100.4670
Si	0.9878	0.9936	0.9862	0.9948	0.9910	0.9946	0.9981	0.9935
Ti	0.0000	0.0005	0.0000	0.0000	0.0004	0.0000	0.0000	0.0000
Al	0.0022	0.0005	0.0005	0.0023	0.0014	0.0017	0.0013	0.0004
Fe	0.3477	0.3727	0.3749	0.3344	0.3178	0.3285	0.2621	0.2789
Mn	0.0035	0.0066	0.0073	0.0038	0.0089	0.0075	0.0090	0.0100
Mg	1.6657	1.6267	1.6401	1.6635	1.6838	1.6676	1.7265	1.7196
Ca	0.0041	0.0050	0.0045	0.0053	0.0047	0.0044	0.0042	0.0038
K	0.0000	0.0000	0.0000	0.0000	0.0000	0.0000	0.0000	0.0000
Na	0.0000	0.0000	0.0000	0.0000	0.0001	0.0005	0.0000	0.0000
	SG272-1M	SG272-1C	SG272-2M	SG272-2C	SG272-3M	SG272-3C	SG272-4M	SG272-4C
SiO2	40.2900	39.9380	39.4050	39.8680	40.4270	39.0150	39.5050	39.4470
TiO2	0.0240	0.0000	0.0000	0.0130	0.0230	0.0300	0.0450	0.0000
Al2O3	0.0080	0.0330	0.0260	0.0650	0.0380	0.0230	0.0350	0.0370
FeO	12.8760	15.1550	17.2300	15.5950	11.2490	15.2960	16.6880	17.3370
MnO	0.3730	0.1150	0.3670	0.2490	0.3400	0.3500	0.1900	0.3030
MgO	47.3730	45.4230	43.8880	45.0260	47.6940	45.4250	44.0360	44.1560
CaO	0.1600	0.2090	0.2310	0.2340	0.1130	0.2100	0.2070	0.2080
K2O	0.0000	0.0000	0.0000	0.0000	0.0000	0.0000	0.0000	0.0000
Na2O	0.0060	0.0000	0.0000	0.0000	0.0000	0.0000	0.0150	0.0000
SUM	101.1100	100.8730	101.1470	101.0500	99.8840	100.3490	100.7210	101.4880
Si	0.9918	0.9946	0.9899	0.9937	0.9991	0.9807	0.9931	0.9877
Ti	0.0004	0.0000	0.0000	0.0002	0.0004	0.0006	0.0009	0.0000
Al	0.0002	0.0010	0.0008	0.0019	0.0011	0.0007	0.0010	0.0011
Fe	0.2651	0.3156	0.3620	0.3251	0.2325	0.3216	0.3508	0.3631
Mn	0.0078	0.0024	0.0078	0.0053	0.0071	0.0075	0.0040	0.0064
Mg	1.7379	1.6858	1.6431	1.6726	1.7567	1.7017	1.6498	1.6478
Ca	0.0042	0.0056	0.0062	0.0062	0.0030	0.0057	0.0056	0.0056
K	0.0000	0.0000	0.0000	0.0000	0.0000	0.0000	0.0000	0.0000
Na	0.0003	0.0000	0.0000	0.0000	0.0000	0.0000	0.0007	0.0000

TABLE 1 continued

	SG277-1M	SG277-1C	SG277-2M	SG277-2C	SG277-3M	SG277-3C	SG277-4M	SG277-4C
SiO2	39.1330	40.0300	39.6550	40.3000	40.0990	39.9750	39.2660	39.5110
TiO2	0.0620	0.0540	0.0250	0.0400	0.0140	0.0260	0.0270	0.0150
Al2O3	0.0590	0.1300	0.0450	0.0510	0.0490	0.0560	0.1270	0.0130
FeO	8.4930	8.8510	5.7600	8.8720	10.3580	8.7570	10.2720	11.7870
MnO	0.4470	0.2980	0.3670	0.3400	0.3740	0.2960	0.3670	0.2350
MgO	51.5520	50.0320	54.7490	50.9860	50.6360	51.7250	49.7980	49.3710
CaO	1.5530	1.7240	0.1950	0.6320	0.3350	0.2660	1.4740	0.2900
K2O	0.0000	0.0000	0.0000	0.0000	0.0000	0.0000	0.0000	0.0000
Na2O	0.0380	0.0020	0.0000	0.0050	0.0140	0.0080	0.0220	0.0190
SUM	101.3370	101.1210	100.7960	101.2260	101.8790	101.1090	101.3530	101.2410
Si	0.9517	0.9737	0.9535	0.9762	0.9714	0.9688	0.9605	0.9694
Ti	0.0011	0.0010	0.0005	0.0007	0.0003	0.0005	0.0005	0.0003
Al	0.0017	0.0037	0.0013	0.0015	0.0014	0.0016	0.0037	0.0004
Fe	0.1727	0.1801	0.1158	0.1797	0.2098	0.1775	0.2102	0.2419
Mn	0.0092	0.0061	0.0075	0.0070	0.0077	0.0061	0.0076	0.0049
Mg	1.8685	1.8138	1.9619	1.8407	1.8281	1.8683	1.8155	1.8053
Ca	0.0405	0.0449	0.0050	0.0164	0.0087	0.0069	0.0386	0.0076
K	0.0000	0.0000	0.0000	0.0000	0.0000	0.0000	0.0000	0.0000
Na	0.0018	0.0001	0.0000	0.0002	0.0007	0.0004	0.0010	0.0009

	SG277-5M	SG277-5C	SG277-6M	SG277-6C	SG277-7M	SG277-7C	SG2711-1M	SG2711-1C
SiO2	40.9350	39.5490	39.0290	39.9620	40.5190	39.2560	39.7780	39.4190
TiO2	0.0370	0.0080	0.0040	0.0320	0.0470	0.0030	0.0140	0.0320
Al2O3	0.1800	0.0490	0.0510	0.0000	0.0710	0.0580	0.0540	0.0360
FeO	6.7770	9.8870	10.7970	9.9910	7.7470	8.6470	10.6250	11.5360
MnO	0.4680	0.1360	0.2780	0.2330	0.0880	0.1750	0.8340	0.6370
MgO	51.7620	50.5500	49.9140	50.9170	52.2160	51.9560	48.7330	49.4310
CaO	0.2170	0.3720	0.3540	0.3680	0.1810	0.2260	0.7050	0.4610
K2O	0.0000	0.0000	0.0000	0.0000	0.0000	0.0000	0.0000	0.0000
Na2O	0.0150	0.0220	0.0000	0.0050	0.0110	0.0340	0.0000	0.0000
SUM	100.3910	100.5730	100.4270	101.5080	100.8800	100.3550	100.7430	101.5520
Si	0.9882	0.9685	0.9626	0.9699	0.9775	0.9592	0.9783	0.9656
Ti	0.0007	0.0001	0.0001	0.0006	0.0009	0.0001	0.0003	0.0006
Al	0.0051	0.0014	0.0015	0.0000	0.0020	0.0017	0.0016	0.0010
Fe	0.1368	0.2025	0.2227	0.2028	0.1563	0.1767	0.2185	0.2363
Mn	0.0096	0.0028	0.0058	0.0048	0.0018	0.0036	0.0174	0.0132
Mg	1.8622	1.8449	1.8346	1.8417	1.8773	1.8920	1.7861	1.8045
Ca	0.0056	0.0098	0.0094	0.0096	0.0047	0.0059	0.0186	0.0121
K	0.0000	0.0000	0.0000	0.0000	0.0000	0.0000	0.0000	0.0000
Na	0.0007	0.0010	0.0000	0.0002	0.0005	0.0016	0.0000	0.0000

TABLE 1 continued

	SG2711-2M	SG2711-2C	SG2711-3M	SG2711-3C	SG281-1M	SG281-1C	SG281-2M	SG281-2C
SiO2	39.5520	40.1950	39.3060	40.0930	39.5350	39.9530	39.3120	39.7020
TiO2	0.0070	0.0430	0.0320	0.0110	0.0080	0.0000	0.0340	0.0120
Al2O3	0.0590	0.0540	0.1550	0.0630	0.0600	0.0750	0.0780	0.0750
FeO	11.3960	11.8760	11.9390	13.2730	12.8970	13.4980	17.2360	13.1910
MnO	0.7090	0.4460	0.8180	0.2140	0.1620	0.1650	0.4490	0.1510
MgO	48.7660	48.5970	48.4770	47.9510	46.7350	47.0510	44.1280	47.4750
CaO	0.5340	0.3510	0.7580	0.3860	0.2270	0.1760	0.3680	0.2420
K2O	0.0000	0.0000	0.0000	0.0000	0.0000	0.0000	0.0000	0.0000
Na2O	0.0170	0.0090	0.0470	0.0000	0.0270	0.0000	0.0000	0.0590
SUM	101.0400	101.5710	101.5320	101.9910	99.6510	100.9180	101.6050	100.9070
Si	0.9729	0.9823	0.9662	0.9810	0.9882	0.9879	0.9842	0.9816
Ti	0.0001	0.0008	0.0006	0.0002	0.0002	0.0000	0.0006	0.0002
Al	0.0017	0.0016	0.0045	0.0018	0.0018	0.0022	0.0023	0.0022
Fe	0.2344	0.2427	0.2455	0.2716	0.2696	0.2791	0.3609	0.2728
Mn	0.0148	0.0092	0.0170	0.0044	0.0034	0.0035	0.0095	0.0032
Mg	1.7877	1.7700	1.7760	1.7486	1.7409	1.7338	1.6465	1.7493
Ca	0.0141	0.0092	0.0200	0.0101	0.0061	0.0047	0.0099	0.0064
K	0.0000	0.0000	0.0000	0.0000	0.0000	0.0000	0.0000	0.0000
Na	0.0008	0.0004	0.0022	0.0000	0.0013	0.0000	0.0000	0.0028
	SG281-3M	SG281-3C	SG281-4M	SG281-4C	SG281-6M	SG281-6C	SG288-1M	SG288-1C
SiO2	40.0220	39.6760	40.3480	39.8420	39.5150	39.6440	39.3410	40.3540
TiO2	0.0300	0.0000	0.0290	0.0180	0.0390	0.0380	0.0600	0.0470
Al2O3	0.1300	0.1850	0.0950	0.0980	0.0850	0.0750	0.0650	0.0790
FeO	14.6740	14.9330	14.4000	13.4940	16.8330	13.5890	15.3560	12.5760
MnO	0.2260	0.3020	0.2000	0.0950	0.3310	0.2160	1.1130	0.2540
MgO	46.0940	45.8030	46.5460	46.8340	43.9780	46.6940	43.6950	46.9670
CaO	0.3010	0.3710	0.2580	0.2280	0.3430	0.2840	0.8050	0.4690
K2O	0.0000	0.0000	0.0000	0.0000	0.0430	0.0000	0.0000	0.0000
Na2O	0.0100	0.0170	0.0390	0.0460	0.0380	0.0190	0.0030	0.0000
SUM	101.4870	101.2870	101.9150	100.6550	101.2050	100.5590	100.4380	100.7460
Si	0.9894	0.9851	0.9913	0.9878	0.9905	0.9853	0.9918	0.9955
Ti	0.0006	0.0000	0.0005	0.0003	0.0007	0.0007	0.0011	0.0009
Al	0.0038	0.0054	0.0028	0.0029	0.0025	0.0022	0.0019	0.0023
Fe	0.3034	0.3101	0.2959	0.2798	0.3529	0.2825	0.3238	0.2595
Mn	0.0047	0.0064	0.0042	0.0020	0.0070	0.0045	0.0238	0.0053
Mg	1.6982	1.6949	1.7044	1.7305	1.6429	1.7296	1.6418	1.7267
Ca	0.0080	0.0099	0.0068	0.0061	0.0092	0.0076	0.0217	0.0124
K	0.0000	0.0000	0.0000	0.0000	0.0014	0.0000	0.0000	0.0000
Na	0.0005	0.0008	0.0019	0.0022	0.0018	0.0009	0.0001	0.0000

TABLE 2 Pyroxene Composition

	SG219-4M	SG219-4C	SG219-7M	SG219-7C	SG219-8M	SG219-8C	SG219-9M	SG219-9C
SiO2	49.6540	52.4690	50.5390	52.4550	50.5380	50.1260	51.0440	52.5620
TiO2	0.8990	0.3230	0.6010	0.2500	0.5320	0.7300	0.5980	0.3180
Al2O3	3.7550	1.3130	2.9730	1.1500	2.4860	2.8110	2.1520	1.2130
FeO	8.2820	7.0470	6.7510	7.1830	6.9040	7.1420	6.6710	6.0120
MnO	0.2980	0.1850	0.2900	0.1580	0.1540	0.2330	0.2400	0.2460
MgO	16.5600	19.3120	17.0310	19.9010	17.3240	17.4780	17.2760	18.5130
CaO	20.3480	18.2130	20.4310	17.5430	19.8170	20.1000	20.5690	19.9570
K2O	0.0020	0.0000	0.0040	0.0000	0.0000	0.0000	0.0240	0.0000
Na2O	0.4720	0.2100	0.4790	0.2170	0.3940	0.3470	0.5800	0.2820
SUM	100.2700	99.0720	99.0990	98.8570	98.1490	98.9670	99.1540	99.1030
Si	1.8456	1.9398	1.8849	1.9412	1.8998	1.8749	1.9030	1.9440
Ti	0.0251	0.0090	0.0169	0.0070	0.0150	0.0205	0.0168	0.0088
Al	0.1645	0.0572	0.1307	0.0502	0.1102	0.1240	0.0946	0.0529
Fe	0.2575	0.2179	0.2106	0.2223	0.2171	0.2234	0.2080	0.1860
Mn	0.0094	0.0058	0.0092	0.0050	0.0049	0.0074	0.0076	0.0077
Mg	0.9173	1.0640	0.9467	1.0976	0.9705	0.9743	0.9599	1.0204
Ca	0.8104	0.7215	0.8165	0.6957	0.7982	0.8056	0.8217	0.7909
K	0.0001	0.0000	0.0002	0.0000	0.0000	0.0000	0.0011	0.0000
Na	0.0340	0.0151	0.0346	0.0156	0.0287	0.0252	0.0419	0.0202
	SG219-11M	SG219-11C	SG219-12M	SG219-12C	SG222-1M	SG222-1C	SG222-2C	SG222-2M
SiO2	50.8250	51.9850	50.7590	52.6600	48.3470	49.0350	50.9610	49.6620
TiO2	0.4590	0.3130	0.7890	0.3000	0.9000	0.9460	0.4790	0.9000
Al2O3	2.1860	1.6860	2.1880	1.3140	4.7480	4.8470	2.7870	4.8920
FeO	5.9380	5.3090	6.7540	5.9500	7.8000	7.6870	7.3760	7.4880
MnO	0.0800	0.1280	0.3680	0.1660	0.2140	0.1380	0.1220	0.1320
MgO	16.9150	17.5300	16.7640	18.1900	14.5510	14.8250	17.1070	15.0140
CaO	21.4770	21.3690	20.7330	20.7500	21.0590	21.2940	20.0320	21.2210
K2O	0.0000	0.0000	0.0110	0.0000	0.0000	0.0000	0.0000	0.0000
Na2O	0.3390	0.4080	0.6140	0.3120	0.5090	0.4680	0.3560	0.4530
SUM	98.2190	98.7280	98.9800	99.6420	98.1280	99.2400	99.2200	99.7620
Si	1.9084	1.9327	1.8995	1.9401	1.8372	1.8391	1.8974	1.8478
Ti	0.0130	0.0088	0.0222	0.0083	0.0257	0.0267	0.0134	0.0252
Al	0.0968	0.0739	0.0965	0.0571	0.2127	0.2143	0.1223	0.2146
Fe	0.1865	0.1651	0.2114	0.1833	0.2479	0.2411	0.2297	0.2330
Mn	0.0025	0.0040	0.0117	0.0052	0.0069	0.0044	0.0038	0.0042
Mg	0.9466	0.9713	0.9349	0.9988	0.8241	0.8287	0.9493	0.8326
Ca	0.8641	0.8512	0.8313	0.8191	0.8575	0.8558	0.7992	0.8460
K	0.0000	0.0000	0.0005	0.0000	0.0000	0.0000	0.0000	0.0000
Na	0.0247	0.0294	0.0446	0.0223	0.0375	0.0340	0.0257	0.0327

TABLE 2 continued

	SG222-3M	SG222-3C	SG222-4M	SG222-4C	SG222-5M	SG222-5C	SG222-6M	SG222-6C
SiO2	50.6210	49.4000	50.4820	51.7900	51.1960	49.4380	49.7340	51.4870
TiO2	0.6340	0.8650	0.6570	0.4140	0.4710	0.7320	0.6630	0.4060
Al2O3	2.7550	4.4180	3.5260	2.3280	2.4440	3.9590	4.0770	2.1570
FeO	7.5650	7.5330	6.8210	6.6220	6.7280	6.9270	7.0320	6.0720
MnO	0.2130	0.1380	0.1360	0.0940	0.1120	0.1910	0.1540	0.1970
MgO	17.0750	15.5890	16.2870	17.5050	16.9970	16.0240	16.0160	17.2620
CaO	19.6690	21.0620	21.2540	20.6150	21.0170	21.2270	21.0560	20.9070
K2O	0.0020	0.0000	0.0040	0.0000	0.0000	0.0000	0.0000	0.0000
Na2O	0.3890	0.4590	0.3840	0.2460	0.2650	0.4460	0.3910	0.2960
SUM	98.9230	99.4640	99.5510	99.6140	99.2300	98.9440	99.1230	98.7840
Si	1.8927	1.8458	1.8763	1.9140	1.9049	1.8540	1.8593	1.9181
Ti	0.0178	0.0243	0.0184	0.0115	0.0132	0.0206	0.0186	0.0114
Al	0.1214	0.1946	0.1545	0.1014	0.1072	0.1750	0.1797	0.0947
Fe	0.2366	0.2354	0.2120	0.2047	0.2094	0.2173	0.2199	0.1892
Mn	0.0067	0.0044	0.0043	0.0029	0.0035	0.0061	0.0049	0.0062
Mg	0.9514	0.8681	0.9022	0.9641	0.9425	0.8956	0.8923	0.9584
Ca	0.7880	0.8433	0.8465	0.8163	0.8379	0.8530	0.8434	0.8345
K	0.0001	0.0000	0.0002	0.0000	0.0000	0.0000	0.0000	0.0000
Na	0.0282	0.0333	0.0277	0.0176	0.0191	0.0324	0.0283	0.0214
	SG222-8M	SG222-8C	SG222-9M	SG222-9C	SG222-7M	SG222-7C	SG222-10M	SG222-10C
SiO2	49.9470	49.3570	51.0960	51.7580	49.0830	49.6390	49.2990	50.0590
TiO2	0.7550	0.7600	0.5070	0.4870	0.8020	0.6920	0.8960	0.6030
Al2O3	4.1520	4.1430	3.1170	2.3750	4.6740	3.9960	4.8620	3.6860
FeO	7.6530	6.7890	7.1460	6.3510	7.4520	6.9130	7.6470	6.5740
MnO	0.1980	0.1780	0.1790	0.1590	0.1630	0.1320	0.1890	0.1750
MgO	15.4960	16.0240	16.7780	17.3630	15.4100	16.1330	15.4850	15.9430
CaO	21.3550	21.1280	20.8810	21.0960	21.5670	21.2780	21.0330	21.6710
K2O	0.0000	0.0000	0.0000	0.0000	0.0000	0.0000	0.0000	0.0000
Na2O	0.4100	0.3760	0.4450	0.3310	0.4480	0.4370	0.4370	0.4010
SUM	99.9660	98.7550	100.1490	99.9200	99.5990	99.2200	99.8480	99.1120
Si	1.8578	1.8521	1.8877	1.9088	1.8347	1.8551	1.8357	1.8707
Ti	0.0211	0.0214	0.0141	0.0135	0.0225	0.0194	0.0251	0.0169
Al	0.1821	0.1833	0.1358	0.1033	0.2060	0.1761	0.2134	0.1624
Fe	0.2381	0.2131	0.2208	0.1959	0.2330	0.2161	0.2381	0.2055
Mn	0.0062	0.0057	0.0056	0.0050	0.0052	0.0042	0.0060	0.0055
Mg	0.8590	0.8961	0.9238	0.9543	0.8584	0.8986	0.8593	0.8879
Ca	0.8511	0.8495	0.8266	0.8336	0.8638	0.8521	0.8392	0.8677
K	0.0000	0.0000	0.0000	0.0000	0.0000	0.0000	0.0000	0.0000
Na	0.0296	0.0274	0.0319	0.0237	0.0325	0.0317	0.0316	0.0291

TABLE 2 continued

	SG224-1M	SG224-1C	SG224-2M	SG224-2C	SG224-3M	SG224-3C	SG224-5M	SG224-5C
SiO2	50.7680	49.6220	49.1800	50.8590	51.5810	47.6000	50.7360	49.9160
TiO2	0.4900	0.8720	0.8720	0.5450	0.5360	0.8590	0.5880	0.6550
Al2O3	3.0460	4.7090	4.4090	2.8100	2.5430	5.0400	2.7320	3.4480
FeO	7.0550	7.5540	8.1450	7.2970	7.1590	7.9710	7.1480	6.9290
MnO	0.1640	0.0600	0.1680	0.1510	0.2010	0.1450	0.1820	0.1020
MgO	16.7630	15.4640	15.1910	16.8060	16.8810	15.5710	16.8740	16.0270
CaO	20.2790	21.1770	21.0150	20.5100	20.5840	20.9550	21.2590	21.2860
K2O	0.0000	0.0000	0.0020	0.0000	0.0000	0.0000	0.0000	0.0000
Na2O	0.3430	0.4330	0.4700	0.3830	0.4020	0.5330	0.3020	0.3390
SUM	98.9080	99.8910	99.4520	99.3610	99.8870	98.6740	99.8210	98.7020
Si	1.8950	1.8446	1.8438	1.8938	1.9077	1.8034	1.8845	1.8740
Ti	0.0138	0.0244	0.0246	0.0153	0.0149	0.0245	0.0164	0.0185
Al	0.1340	0.2064	0.1949	0.1234	0.1109	0.2251	0.1196	0.1526
Fe	0.2202	0.2348	0.2554	0.2272	0.2214	0.2526	0.2220	0.2176
Mn	0.0052	0.0019	0.0053	0.0048	0.0063	0.0047	0.0057	0.0032
Mg	0.9325	0.8567	0.8488	0.9326	0.9305	0.8792	0.9341	0.8967
Ca	0.8111	0.8435	0.8442	0.8183	0.8157	0.8507	0.8461	0.8563
K	0.0000	0.0000	0.0001	0.0000	0.0000	0.0000	0.0000	0.0000
Na	0.0248	0.0312	0.0342	0.0277	0.0288	0.0392	0.0218	0.0247
	SG224-8M	SG224-8C	SG233-AM	SG233-AC	SG233-BM	SG233-BC	SG233-1M	SG233-1C
SiO2	50.6260	50.4310	50.0010	48.9020	50.3160	51.5620	50.4120	50.4750
TiO2	0.5250	0.5500	0.8140	1.1910	0.6480	0.5670	0.7070	0.7210
Al2O3	2.6430	2.9730	3.7570	4.4410	3.3030	2.7980	3.4290	3.3960
FeO	7.3080	7.2570	8.4630	8.6990	7.4010	7.2830	7.8330	6.8790
MnO	0.1760	0.2100	0.2040	0.1940	0.1330	0.2220	0.1070	0.1190
MgO	16.8590	16.6660	15.3800	15.2130	16.0950	16.5050	15.7880	16.1640
CaO	20.2130	20.4950	20.7860	20.8670	21.1100	20.4770	20.8090	20.9250
K2O	0.0000	0.0000	0.0020	0.0000	0.0010	0.0200	0.0210	0.0000
Na2O	0.3580	0.3920	0.4460	0.3810	0.4570	0.3920	0.3510	0.3730
SUM	98.7080	98.9740	99.8530	99.8880	99.4640	99.8260	99.4570	99.0520
Si	1.8972	1.8868	1.8663	1.8305	1.8775	1.9081	1.8814	1.8838
Ti	0.0148	0.0155	0.0228	0.0335	0.0182	0.0158	0.0198	0.0202
Al	0.1168	0.1311	0.1653	0.1960	0.1453	0.1221	0.1509	0.1494
Fe	0.2290	0.2271	0.2642	0.2723	0.2310	0.2254	0.2445	0.2147
Mn	0.0056	0.0067	0.0064	0.0062	0.0042	0.0070	0.0034	0.0038
Mg	0.9416	0.9293	0.8555	0.8487	0.8950	0.9103	0.8781	0.8991
Ca	0.8116	0.8216	0.8313	0.8370	0.8440	0.8120	0.8321	0.8368
K	0.0000	0.0000	0.0001	0.0000	0.0000	0.0009	0.0010	0.0000
Na	0.0260	0.0284	0.0323	0.0277	0.0331	0.0281	0.0254	0.0270

TABLE 2 continued

	SG233-2C	SG233-3M	SG233-3C	SG233-4M	SG233-4C	SG236-1M	SG236-1C	SG236-2M
SiO2	50.6970	49.0540	51.7570	49.7730	52.8530	50.8010	52.7590	51.8500
TiO2	0.8450	0.9910	0.7220	0.7750	0.3850	0.7110	0.3020	0.4140
Al2O3	3.4100	4.0730	3.0440	3.7050	1.7700	3.3070	1.1280	2.0940
FeO	7.0290	8.3960	6.6930	7.7280	6.2810	7.3580	6.2810	6.0690
MnO	0.0790	0.2390	0.2030	0.1790	0.2010	0.1730	0.1950	0.1670
MgO	16.2980	15.6450	16.7860	15.8460	17.6210	16.5990	18.4310	17.4880
CaO	21.2900	21.0430	20.9530	21.4710	21.1740	21.0660	20.2600	20.4270
K2O	0.0000	0.0030	0.0000	0.0000	0.0040	0.0130	0.0000	0.0000
Na2O	0.3610	0.4190	0.3850	0.4390	0.3530	0.4600	0.2260	0.3690
SUM	100.0090	99.8630	100.5430	99.9160	100.6420	100.4880	99.5820	98.8780
Si	1.8766	1.8361	1.8983	1.8557	1.9321	1.8748	1.9447	1.9257
Ti	0.0235	0.0279	0.0199	0.0217	0.0106	0.0197	0.0084	0.0116
Al	0.1488	0.1797	0.1316	0.1629	0.0763	0.1439	0.0490	0.0917
Fe	0.2176	0.2628	0.2053	0.2410	0.1920	0.2271	0.1936	0.1885
Mn	0.0025	0.0076	0.0063	0.0057	0.0062	0.0054	0.0061	0.0053
Mg	0.8991	0.8727	0.9175	0.8805	0.9600	0.9129	1.0125	0.9680
Ca	0.8444	0.8440	0.8234	0.8578	0.8294	0.8330	0.8002	0.8129
K	0.0000	0.0001	0.0000	0.0000	0.0002	0.0006	0.0000	0.0000
Na	0.0259	0.0304	0.0274	0.0317	0.0250	0.0329	0.0162	0.0266
	SG236-2C	SG236-3M	SG236-3C	SG236-4M	SG236-4C	SG236-5M	SG236-5C	SG24A2-1M
SiO2	51.5370	49.7060	49.6070	52.2830	52.2630	49.7080	51.6690	49.9940
TiO2	0.5600	1.0100	0.9730	0.3800	0.3730	0.9030	0.5070	0.8510
Al2O3	2.5320	3.9520	3.6660	1.9870	2.1330	4.1060	2.1690	3.7820
FeO	6.8090	7.8410	8.7870	6.2040	5.4420	7.9240	7.2200	7.5840
MnO	0.1200	0.2210	0.2150	0.1100	0.0790	0.1200	0.2050	0.0440
MgO	16.7300	15.1970	16.3560	17.6290	17.1680	15.9640	17.5740	15.5350
CaO	21.0280	21.4740	19.9020	20.7420	21.2620	21.0690	20.1560	21.3260
K2O	0.0000	0.0000	0.0000	0.0000	0.0000	0.0000	0.0000	0.0110
Na2O	0.3890	0.4090	0.5580	0.4190	0.3710	0.3370	0.2210	0.4760
SUM	99.7050	99.8100	100.0640	99.7540	99.0910	100.1310	99.7210	99.6030
Si	1.9084	1.8556	1.8495	1.9264	1.9332	1.8472	1.9119	1.8654
Ti	0.0156	0.0284	0.0273	0.0105	0.0104	0.0252	0.0141	0.0239
Al	0.1105	0.1739	0.1611	0.0863	0.0930	0.1799	0.0946	0.1664
Fe	0.2109	0.2448	0.2740	0.1912	0.1684	0.2463	0.2234	0.2367
Mn	0.0038	0.0070	0.0068	0.0034	0.0025	0.0038	0.0064	0.0014
Mg	0.9233	0.8455	0.9088	0.9681	0.9464	0.8841	0.9691	0.8638
Ca	0.8343	0.8590	0.7951	0.8189	0.8427	0.8389	0.7992	0.8526
K	0.0000	0.0000	0.0000	0.0000	0.0000	0.0000	0.0000	0.0005
Na	0.0279	0.0296	0.0403	0.0299	0.0266	0.0243	0.0159	0.0344

TABLE 2 continued

	SG24A2-1C	SG24A2-2M	SG24A2-2C	SG24A2-3M	SG24A2-3C	SG24A2-5M	SG24A2-5C	SG252-AM
SiO2	48.7850	49.3780	53.8390	50.0300	52.5550	49.9350	51.1830	50.7530
TiO2	0.9870	0.9260	0.2220	0.8500	0.3730	0.7480	0.4600	0.5080
Al2O3	4.3700	4.0950	0.4820	3.7330	1.7440	3.3450	2.2010	2.4960
FeO	8.2340	7.7790	7.1970	8.0230	6.1330	7.1650	6.2780	7.2150
MnO	0.1730	0.2110	0.1390	0.1430	0.1750	0.0870	0.1540	0.2230
MgO	15.2170	15.7000	17.4150	16.0530	17.1370	15.8150	16.7880	16.3000
CaO	21.1500	20.6530	20.3750	20.7970	21.3590	21.0150	21.0890	21.5320
K2O	0.0000	0.0070	0.0060	0.0000	0.0000	0.0000	0.0000	0.0000
Na2O	0.4300	0.4050	0.2730	0.4340	0.3790	0.3540	0.3700	0.3850
SUM	99.3460	99.1540	99.9480	100.0630	99.8550	98.4640	98.5230	99.4120
Si	1.8343	1.8517	1.9811	1.8599	1.9366	1.8795	1.9157	1.8956
Ti	0.0279	0.0261	0.0061	0.0238	0.0103	0.0212	0.0129	0.0143
Al	0.1937	0.1810	0.0209	0.1636	0.0758	0.1484	0.0971	0.1099
Fe	0.2589	0.2440	0.2215	0.2494	0.1890	0.2255	0.1965	0.2254
Mn	0.0055	0.0067	0.0043	0.0045	0.0055	0.0028	0.0049	0.0071
Mg	0.8527	0.8774	0.9550	0.8894	0.9411	0.8871	0.9364	0.9073
Ca	0.8521	0.8299	0.8034	0.8284	0.8433	0.8476	0.8458	0.8617
K	0.0000	0.0003	0.0003	0.0000	0.0000	0.0000	0.0000	0.0000
Na	0.0314	0.0294	0.0195	0.0313	0.0271	0.0258	0.0269	0.0279
	SG252-AC	SG252-2M	SG252-2C	SG252-3AM	SG252-3AC	SG252-3M	SG252-3C	SG252-4M
SiO2	49.1960	49.5610	49.4650	50.0740	49.5210	50.0450	49.5170	52.6670
TiO2	0.2710	0.8280	0.7180	0.7810	0.8090	0.6910	1.0240	0.4080
Al2O3	4.3840	3.4620	3.4590	3.4140	3.4100	3.2090	3.9330	1.7060
FeO	12.5050	8.0920	7.9780	7.8990	7.8650	7.9230	7.9760	7.1820
MnO	0.2400	0.1580	0.1600	0.1980	0.1220	0.1870	0.1390	0.1190
MgO	11.3260	15.3020	15.4970	15.8190	15.7960	15.7190	14.9500	17.2010
CaO	20.1460	20.9320	21.0130	20.9430	21.1950	20.8380	21.4110	20.6100
K2O	0.0000	0.0040	0.0000	0.0120	0.0000	0.0000	0.0000	0.0000
Na2O	1.1440	0.3340	0.3590	0.4190	0.3340	0.3800	0.3270	0.2960
SUM	99.2120	98.6730	98.6490	99.5590	99.0520	98.9920	99.2770	100.1890
Si	1.8826	1.8708	1.8679	1.8712	1.8623	1.8801	1.8585	1.9377
Ti	0.0078	0.0235	0.0204	0.0219	0.0229	0.0195	0.0289	0.0113
Al	0.1978	0.1541	0.1540	0.1504	0.1512	0.1421	0.1740	0.0740
Fe	0.4002	0.2555	0.2519	0.2469	0.2474	0.2489	0.2504	0.2210
Mn	0.0078	0.0051	0.0051	0.0063	0.0039	0.0060	0.0044	0.0037
Mg	0.6459	0.8608	0.8721	0.8810	0.8853	0.8801	0.8363	0.9432
Ca	0.8261	0.8466	0.8502	0.8386	0.8541	0.8388	0.8611	0.8125
K	0.0000	0.0002	0.0000	0.0006	0.0000	0.0000	0.0000	0.0000
Na	0.0849	0.0244	0.0263	0.0304	0.0244	0.0277	0.0238	0.0211

TABLE 2 continued

	SG252-4C	SG252-5M	SG252-5C	SG252-6M	SG252-6C	SG252-6AM	SG252-6AC	SG258-1M
SiO2	52.5980	49.6970	52.8030	50.4590	51.5690	50.5900	52.2490	52.8140
TiO2	0.2880	0.7020	0.3310	0.6650	0.3770	0.6150	0.3110	0.3320
Al2O3	1.8380	3.5970	1.8660	3.3350	1.9100	2.9420	1.7690	1.4440
FeO	5.8800	8.0680	6.0830	7.6440	5.9610	7.3660	5.9240	5.8930
MnO	0.1820	0.0970	0.1060	0.1710	0.1420	0.1830	0.1440	0.1440
MgO	16.7190	16.0400	16.9060	15.7850	16.9170	16.0590	16.8970	17.1620
CaO	21.4050	20.5400	21.3110	21.7010	21.4960	21.8030	21.6900	21.5430
K2O	0.0000	0.0000	0.0000	0.0000	0.0000	0.0030	0.0000	0.0000
Na2O	0.3620	0.3940	0.4400	0.3420	0.3380	0.3660	0.3260	0.2860
SUM	99.2720	99.1350	99.8460	100.1020	98.7100	99.9270	99.3100	99.6180
Si	1.9462	1.8644	1.9432	1.8751	1.9247	1.8821	1.9362	1.9480
Ti	0.0080	0.0198	0.0092	0.0186	0.0106	0.0172	0.0087	0.0092
Al	0.0802	0.1591	0.0810	0.1461	0.0840	0.1290	0.0773	0.0628
Fe	0.1820	0.2531	0.1872	0.2376	0.1861	0.2292	0.1836	0.1818
Mn	0.0057	0.0031	0.0033	0.0054	0.0045	0.0058	0.0045	0.0045
Mg	0.9220	0.8968	0.9272	0.8742	0.9410	0.8904	0.9332	0.9434
Ca	0.8487	0.8257	0.8404	0.8641	0.8597	0.8691	0.8613	0.8514
K	0.0000	0.0000	0.0000	0.0000	0.0000	0.0001	0.0000	0.0000
Na	0.0260	0.0287	0.0314	0.0246	0.0245	0.0264	0.0234	0.0205
	SG258-1C	SG258-2M	SG258-2C	SG2510-1M	SG2510-1C	SG2510-2M	SG2510-2C	SG2510-3M
SiO2	52.1830	49.5710	50.4740	50.8550	51.9330	52.5600	52.4240	50.7850
TiO2	0.3080	0.7020	0.5650	0.6240	0.3820	0.3900	0.3900	0.5770
Al2O3	1.7420	3.2460	3.0470	2.0360	2.0510	1.6020	1.7250	2.9570
FeO	5.7350	8.2370	7.4330	6.9490	5.7160	6.8850	7.0740	7.2720
MnO	0.0710	0.1800	0.1390	0.2430	0.0860	0.2830	0.1120	0.2400
MgO	16.8620	16.4530	15.6820	16.2250	16.8070	18.0090	17.4880	16.4050
CaO	21.5140	19.5410	20.9930	21.9560	21.5690	19.8720	20.2830	20.4730
K2O	0.0000	0.0010	0.0000	0.0000	0.0000	0.0050	0.0000	0.0050
Na2O	0.3690	0.2670	0.4300	0.5340	0.3900	0.2960	0.2350	0.4100
SUM	98.7840	98.1980	98.7630	99.4220	98.9340	99.9020	99.7310	99.1240
Si	1.9410	1.8742	1.8951	1.9012	1.9299	1.9352	1.9354	1.8957
Ti	0.0086	0.0200	0.0160	0.0175	0.0107	0.0108	0.0108	0.0162
Al	0.0764	0.1447	0.1349	0.0897	0.0899	0.0695	0.0751	0.1301
Fe	0.1784	0.2605	0.2334	0.2173	0.1776	0.2120	0.2184	0.2270
Mn	0.0022	0.0058	0.0044	0.0077	0.0027	0.0088	0.0035	0.0076
Mg	0.9347	0.9271	0.8775	0.9040	0.9308	0.9882	0.9622	0.9126
Ca	0.8575	0.7916	0.8446	0.8795	0.8588	0.7840	0.8024	0.8189
K	0.0000	0.0000	0.0000	0.0000	0.0000	0.0002	0.0000	0.0002
Na	0.0266	0.0196	0.0313	0.0387	0.0281	0.0211	0.0168	0.0297

TABLE 2 continued

	SG2510-3C	SG2510-AM	SG2510-AC	SG2510-5M	SG2510-5C	SG2513-1M	SG2513-1M	SG2513-1C
SiO2	52.1100	53.2640	55.4290	51.4030	52.6570	54.8720	54.9860	54.5930
TiO2	0.4030	0.1100	0.1580	0.5760	0.4140	0.1970	0.1900	0.2170
Al2O3	1.9490	1.5190	0.9290	2.4090	1.8670	1.1210	1.0350	1.1840
FeO	6.6900	14.2690	10.5200	6.7190	6.2590	10.9890	12.0320	10.9170
MnO	0.1700	0.4160	0.2680	0.1780	0.1810	0.1700	0.2590	0.2330
MgO	17.5810	28.1300	30.6060	17.0320	16.9270	30.2670	29.8020	30.4900
CaO	19.8830	1.0450	1.4210	20.9810	21.2140	1.6780	1.2310	1.5800
K2O	0.0000	0.0000	0.0000	0.0030	0.0000	0.0000	0.0000	0.0000
Na2O	0.3520	0.0010	0.0000	0.3090	0.4920	0.0550	0.0460	0.0110
SUM	99.1380	98.7540	99.3310	99.6100	100.0110	99.3490	99.5810	99.2250
Si	1.9317	1.9403	1.9691	1.9054	1.9376	1.9560	1.9621	1.9489
Ti	0.0112	0.0030	0.0042	0.0161	0.0115	0.0053	0.0051	0.0058
Al	0.0852	0.0652	0.0389	0.1053	0.0810	0.0471	0.0435	0.0498
Fe	0.2074	0.4347	0.3125	0.2083	0.1926	0.3276	0.3591	0.3259
Mn	0.0053	0.0128	0.0081	0.0056	0.0056	0.0051	0.0078	0.0070
Mg	0.9713	1.5272	1.6204	0.9409	0.9282	1.6080	1.5848	1.6221
Ca	0.7898	0.0408	0.0541	0.8333	0.8364	0.0641	0.0471	0.0604
K	0.0000	0.0000	0.0000	0.0001	0.0000	0.0000	0.0000	0.0000
Na	0.0253	0.0001	0.0000	0.0222	0.0351	0.0038	0.0032	0.0008
	SG2513-1C	SG2513-2M	SG2513-2C	SG2513-3M	SG2513-3C	SG2513-4C	SG2513-4M	SG2513-5M
SiO2	55.0920	55.7110	55.2840	51.1500	51.8620	51.2410	50.8330	51.7820
TiO2	0.1900	0.2150	0.1780	0.5500	0.6200	0.6140	0.5990	0.6770
Al2O3	1.0910	0.9490	1.0500	2.8610	2.4910	2.4160	2.4840	2.9060
FeO	10.6240	10.6040	10.7030	7.0460	6.7990	6.7270	7.1340	7.1560
MnO	0.2610	0.2740	0.3380	0.1690	0.2280	0.1190	0.1860	0.1220
MgO	30.4000	30.5650	30.5820	16.6740	16.6320	16.7040	17.2420	16.3590
CaO	1.6050	1.4520	1.3690	20.7810	21.1290	21.2860	19.8050	20.9180
K2O	0.0000	0.0000	0.0000	0.0160	0.0100	0.0000	0.0000	0.0000
Na2O	0.0000	0.0150	0.0190	0.4650	0.4090	0.3230	0.3110	0.3790
SUM	99.2630	99.7850	99.5230	99.7120	100.1800	99.4300	98.5940	100.2990
Si	1.9614	1.9704	1.9628	1.8968	1.9117	1.9046	1.9026	1.9064
Ti	0.0051	0.0057	0.0048	0.0153	0.0172	0.0172	0.0169	0.0187
Al	0.0458	0.0396	0.0440	0.1251	0.1083	0.1059	0.1096	0.1261
Fe	0.3163	0.3137	0.3178	0.2185	0.2096	0.2091	0.2233	0.2203
Mn	0.0079	0.0082	0.0102	0.0053	0.0071	0.0037	0.0059	0.0038
Mg	1.6130	1.6111	1.6182	0.9215	0.9137	0.9253	0.9618	0.8976
Ca	0.0612	0.0550	0.0521	0.8257	0.8345	0.8478	0.7943	0.8252
K	0.0000	0.0000	0.0000	0.0008	0.0005	0.0000	0.0000	0.0000
Na	0.0000	0.0010	0.0013	0.0334	0.0292	0.0233	0.0226	0.0271

TABLE 2 continued

	SG2513-5C	SG2513-7M	SG2513-7C	SG2513-8M	SG2513-8C	SG2517-1C	SG2517-1M	SG2517-2M
SiO2	51.9700	52.5450	52.6580	52.4330	52.3180	52.5050	52.5800	50.2330
TiO2	0.5070	0.3700	0.3750	0.3990	0.4380	0.3000	0.4840	0.7800
Al2O3	2.1670	1.5680	1.4860	1.7260	1.7630	1.9250	2.1030	3.4770
FeO	6.3580	7.1640	6.6530	6.6740	6.7330	5.6170	7.3480	7.6400
MnO	0.1150	0.2370	0.2030	0.1870	0.2110	0.1440	0.1550	0.1920
MgO	17.0990	17.7030	17.4730	17.6630	17.1240	17.1210	17.2120	16.0720
CaO	20.9160	20.3260	21.0240	20.0560	21.1750	21.1330	20.7230	21.3480
K2O	0.0000	0.0000	0.0000	0.0120	0.0000	0.0000	0.0000	0.0100
Na2O	0.2950	0.3480	0.2780	0.2780	0.3660	0.4630	0.3170	0.4220
SUM	99.4270	100.2610	100.1500	99.4280	100.1280	99.2080	100.9220	100.1740
Si	1.9233	1.9328	1.9374	1.9378	1.9283	1.9411	1.9231	1.8653
Ti	0.0141	0.0102	0.0104	0.0111	0.0121	0.0083	0.0133	0.0218
Al	0.0945	0.0680	0.0645	0.0752	0.0766	0.0839	0.0907	0.1522
Fe	0.1968	0.2204	0.2047	0.2063	0.2075	0.1737	0.2248	0.2373
Mn	0.0036	0.0074	0.0063	0.0059	0.0066	0.0045	0.0048	0.0060
Mg	0.9431	0.9705	0.9581	0.9729	0.9406	0.9433	0.9382	0.8894
Ca	0.8294	0.8011	0.8288	0.7942	0.8363	0.8372	0.8121	0.8494
K	0.0000	0.0000	0.0000	0.0006	0.0000	0.0000	0.0000	0.0005
Na	0.0212	0.0248	0.0198	0.0199	0.0262	0.0332	0.0225	0.0304

	SG2517-2C	SG2517-3M	SG2517-3C	SG2517-4A	SG2517-4AC	SG2517-5M	SG2517-5C	SG2517-9M
SiO2	52.0370	51.2490	52.1990	52.7650	52.6950	52.9280	52.9100	51.9380
TiO2	0.5400	0.7110	0.4220	0.3970	0.3880	0.3360	0.3610	0.6130
Al2O3	2.2700	3.0880	2.4170	2.0810	2.0790	1.9060	1.9100	2.5990
FeO	6.5610	7.2570	5.7930	6.1240	5.7820	5.8280	5.8430	7.4720
MnO	0.1080	0.1490	0.1670	0.1390	0.1180	0.0940	0.1270	0.2080
MgO	16.6300	16.7630	16.7830	17.2630	17.1200	17.6690	17.3330	17.0050
CaO	21.4860	20.5500	21.7400	21.4980	21.7230	21.3360	21.6550	20.8860
K2O	0.0000	0.0000	0.0000	0.0000	0.0000	0.0000	0.0000	0.0000
Na2O	0.4240	0.3920	0.4220	0.4400	0.3910	0.3890	0.4400	0.3580
SUM	100.0560	100.1590	99.9430	100.7070	100.2960	100.4860	100.5790	101.0790
Si	1.9190	1.8910	1.9213	1.9277	1.9307	1.9334	1.9334	1.9015
Ti	0.0150	0.0197	0.0117	0.0109	0.0107	0.0092	0.0099	0.0169
Al	0.0987	0.1343	0.1049	0.0896	0.0898	0.0821	0.0823	0.1122
Fe	0.2024	0.2239	0.1783	0.1871	0.1772	0.1780	0.1786	0.2288
Mn	0.0034	0.0047	0.0052	0.0043	0.0037	0.0029	0.0039	0.0065
Mg	0.9140	0.9218	0.9206	0.9399	0.9348	0.9619	0.9439	0.9278
Ca	0.8490	0.8125	0.8574	0.8415	0.8528	0.8351	0.8479	0.8193
K	0.0000	0.0000	0.0000	0.0000	0.0000	0.0000	0.0000	0.0000
Na	0.0303	0.0280	0.0301	0.0312	0.0278	0.0276	0.0312	0.0254

TABLE 2 continued

	SG2517-9C	SG2517-10	SG2517-10C	SG2517-11C	SG2517-11C	SG2517-12	SG2517-12C	SG2518-1M
SiO2	52.4330	49.9080	52.4910	51.4820	51.9620	51.5070	53.3830	51.8530
TiO2	0.6330	0.8970	0.4550	0.6710	0.7140	0.9460	0.3570	0.5420
Al2O3	2.4420	3.9480	1.8440	2.2790	2.3040	2.8080	1.3150	2.2310
FeO	8.0870	8.1060	6.8960	9.0530	9.2150	8.7020	6.9850	7.4840
MnO	0.2890	0.1230	0.2300	0.3350	0.2720	0.2840	0.2300	0.2330
MgO	16.3450	15.7550	17.2580	16.7830	16.6430	16.0810	18.1460	17.4840
CaO	20.6050	20.8230	20.7150	19.2880	19.1940	20.8430	20.1880	19.9890
K2O	0.0000	0.0000	0.0020	0.0000	0.0000	0.0000	0.0000	0.0000
Na2O	0.4840	0.3890	0.3230	0.5530	0.5660	0.4930	0.2670	0.3590
SUM	101.3180	99.9490	100.2140	100.4440	100.8700	101.6640	100.8710	100.1750
Si	1.9177	1.8576	1.9308	1.9059	1.9136	1.8879	1.9459	1.9117
Ti	0.0174	0.0251	0.0126	0.0187	0.0198	0.0261	0.0098	0.0150
Al	0.1053	0.1732	0.0800	0.0995	0.1000	0.1213	0.0565	0.0970
Fe	0.2474	0.2523	0.2121	0.2803	0.2838	0.2667	0.2129	0.2308
Mn	0.0090	0.0039	0.0072	0.0105	0.0085	0.0088	0.0071	0.0073
Mg	0.8909	0.8740	0.9461	0.9260	0.9134	0.8784	0.9858	0.9606
Ca	0.8075	0.8305	0.8164	0.7651	0.7574	0.8186	0.7885	0.7896
K	0.0000	0.0000	0.0001	0.0000	0.0000	0.0000	0.0000	0.0000
Na	0.0343	0.0281	0.0230	0.0397	0.0404	0.0350	0.0189	0.0257
	SG2518-1C	SG2518-2M	SG2518-2C	SG2518-7C	SG2518-7M	SG2518-8M	SG2518-8C	SG2522-1M
SiO2	52.7850	50.6990	53.3190	51.8900	51.9420	55.0370	53.7450	50.7110
TiO2	0.2720	0.7710	0.3560	0.3240	0.4980	0.2880	0.3330	0.5680
Al2O3	1.8720	3.1270	1.9650	1.8810	2.0450	13.7600	2.0850	2.5800
FeO	5.7940	7.3700	5.5990	5.6790	6.8620	7.2290	11.8650	7.0010
MnO	0.1770	0.0990	0.1760	0.1450	0.1870	0.2690	0.3120	0.2350
MgO	17.1900	15.9250	17.0830	16.9290	17.1090	16.1440	29.2990	16.3900
CaO	21.0620	21.1570	21.4720	21.5250	20.7990	5.0970	1.8300	21.2880
K2O	0.0000	0.0020	0.0020	0.0010	0.0000	0.1710	0.0000	0.0130
Na2O	0.4380	0.4260	0.3550	0.4020	0.4150	2.6120	0.0000	0.3410
SUM	99.5900	99.5760	100.3270	98.7760	99.8570	100.6070	99.4690	99.1270
Si	1.9442	1.8876	1.9472	1.9320	1.9198	1.9057	1.9253	1.8961
Ti	0.0075	0.0216	0.0098	0.0091	0.0138	0.0075	0.0090	0.0160
Al	0.0813	0.1373	0.0846	0.0826	0.0891	0.5617	0.0881	0.1137
Fe	0.1785	0.2295	0.1710	0.1768	0.2121	0.2093	0.3555	0.2189
Mn	0.0055	0.0031	0.0054	0.0046	0.0059	0.0079	0.0095	0.0074
Mg	0.9436	0.8836	0.9298	0.9394	0.9424	0.8331	1.5642	0.9133
Ca	0.8313	0.8440	0.8402	0.8587	0.8237	0.1891	0.0702	0.8529
K	0.0000	0.0001	0.0001	0.0000	0.0000	0.0076	0.0000	0.0006
Na	0.0313	0.0308	0.0251	0.0290	0.0297	0.1754	0.0000	0.0247

TABLE 2 continued

	SG2522-1C	SG2522-2M	SG2522-2C	SG2522-4M	SG2522-4C	SG2522-5M	SG2522-5C	SG2525-1M
SiO2	52.6850	50.8680	52.4790	55.4420	55.0330	51.5420	51.3640	51.1230
TiO2	0.3030	0.6030	0.2940	0.1960	0.1690	0.4860	0.3870	0.6240
Al2O3	1.1020	2.4660	1.2400	1.0080	0.7840	1.8460	1.7820	2.9000
FeO	6.7850	6.5550	5.4240	11.1080	10.4500	6.1620	5.5180	7.8150
MnO	0.1910	0.1220	0.1140	0.2880	0.3240	0.2290	0.1900	0.2250
MgO	18.3770	16.9620	17.6090	30.6490	30.3970	17.1370	16.9150	16.6740
CaO	19.3320	20.6980	21.4100	1.5050	1.6810	21.5220	21.8350	19.7750
K2O	0.0010	0.0100	0.0000	0.0000	0.0000	0.0000	0.0000	0.0000
Na2O	0.1730	0.3930	0.3080	0.0700	0.0150	0.2800	0.3710	0.4150
SUM	98.9490	98.6770	98.8780	100.2660	98.8530	99.2040	98.3620	99.5510
Si	1.9527	1.9024	1.9472	1.9585	1.9674	1.9173	1.9237	1.8995
Ti	0.0084	0.0170	0.0082	0.0052	0.0045	0.0136	0.0109	0.0174
Al	0.0482	0.1087	0.0542	0.0420	0.0330	0.0810	0.0787	0.1270
Fe	0.2103	0.2050	0.1683	0.3282	0.3124	0.1917	0.1728	0.2428
Mn	0.0060	0.0039	0.0036	0.0086	0.0098	0.0072	0.0060	0.0071
Mg	1.0151	0.9454	0.9737	1.6135	1.6195	0.9500	0.9441	0.9233
Ca	0.7678	0.8294	0.8512	0.0570	0.0644	0.8578	0.8763	0.7873
K	0.0000	0.0005	0.0000	0.0000	0.0000	0.0000	0.0000	0.0000
Na	0.0124	0.0285	0.0222	0.0048	0.0010	0.0202	0.0269	0.0299

	SG2525-1M	SG2525-1C	SG2525-1C	SG2525-2M	SG2525-2C	SG2525-3M	SG2525-3C	SG2525-4M
SiO2	51.7260	52.9370	53.0690	55.7240	55.5900	55.9640	55.4290	56.5810
TiO2	0.6880	0.3520	0.3240	0.1990	0.1540	0.2190	0.2120	0.1400
Al2O3	2.9970	1.6610	1.8040	1.1110	1.2040	0.8760	1.0260	0.9080
FeO	7.6360	5.7370	5.5140	10.8080	10.6680	10.6100	10.7950	10.5500
MnO	0.2010	0.1570	0.1780	0.2390	0.2790	0.4530	0.3400	0.3830
MgO	16.6140	16.8600	16.7080	30.4500	30.5860	30.4820	30.7960	30.1160
CaO	20.0060	21.1640	21.4190	1.4430	1.5020	1.6730	1.3460	1.4100
K2O	0.0080	0.0000	0.0000	0.0000	0.0000	0.0000	0.0000	0.0000
Na2O	0.4530	0.3820	0.3990	0.0000	0.0000	0.0000	0.0000	0.0030
SUM	100.3290	99.2500	99.4150	99.9740	99.9830	100.2770	99.9440	100.0910
Si	1.9042	1.9552	1.9557	1.9681	1.9633	1.9719	1.9604	1.9909
Ti	0.0190	0.0098	0.0090	0.0053	0.0041	0.0058	0.0056	0.0037
Al	0.1301	0.0723	0.0784	0.0463	0.0501	0.0364	0.0428	0.0377
Fe	0.2351	0.1772	0.1699	0.3192	0.3151	0.3127	0.3193	0.3105
Mn	0.0063	0.0049	0.0056	0.0072	0.0083	0.0135	0.0102	0.0114
Mg	0.9115	0.9281	0.9176	1.6028	1.6098	1.6007	1.6232	1.5792
Ca	0.7892	0.8376	0.8458	0.0546	0.0568	0.0632	0.0510	0.0532
K	0.0004	0.0000	0.0000	0.0000	0.0000	0.0000	0.0000	0.0000
Na	0.0323	0.0274	0.0285	0.0000	0.0000	0.0000	0.0000	0.0002

TABLE 2 continued

	SG2525-4C	SG2525-5M	SG2525-5C	SG2525-6M	SG2525-6C	SG2525-7M	SG2525-7C	SG2525-8M
SiO2	55.6100	52.4510	53.4220	53.3100	53.0820	52.7390	53.0770	52.6350
TiO2	0.2050	0.4940	0.3850	0.3510	0.3200	0.3450	0.2830	0.4540
Al2O3	1.0000	2.1640	1.6270	1.1690	1.6910	1.4010	1.0680	1.8190
FeO	10.5700	6.8630	6.0590	6.2170	5.5490	6.8520	6.3210	6.6460
MnO	0.1830	0.2010	0.1090	0.1600	0.1220	0.1730	0.1310	0.1400
MgO	30.7360	17.0960	17.4350	17.8450	17.4450	18.0250	18.3400	16.9240
CaO	1.3760	20.7670	21.0270	20.4510	20.9600	19.8060	20.0760	20.8320
K2O	0.0000	0.0000	0.0000	0.0020	0.0000	0.0000	0.0000	0.0000
Na2O	0.0000	0.3650	0.4190	0.2500	0.3810	0.2770	0.2460	0.3340
SUM	99.6800	100.4010	100.4830	99.7550	99.5500	99.6180	99.5420	99.7840
Si	1.9677	1.9252	1.9499	1.9587	1.9515	1.9448	1.9544	1.9409
Ti	0.0055	0.0136	0.0106	0.0097	0.0088	0.0096	0.0078	0.0126
Al	0.0417	0.0936	0.0700	0.0506	0.0733	0.0609	0.0464	0.0791
Fe	0.3128	0.2107	0.1850	0.1910	0.1706	0.2113	0.1947	0.2050
Mn	0.0055	0.0062	0.0034	0.0050	0.0038	0.0054	0.0041	0.0044
Mg	1.6208	0.9352	0.9484	0.9771	0.9558	0.9906	1.0064	0.9301
Ca	0.0522	0.8168	0.8224	0.8051	0.8257	0.7826	0.7921	0.8231
K	0.0000	0.0000	0.0000	0.0001	0.0000	0.0000	0.0000	0.0000
Na	0.0000	0.0260	0.0297	0.0178	0.0272	0.0198	0.0176	0.0239

	SG2525-8C	SG2529-1M	SG2529-1C	SG2529-2M	SG2529-2C	SG2529-7M	SG2529-7M	SG2529-7C
SiO2	53.3100	55.2120	54.4350	56.3440	51.9390	55.3930	54.4580	51.6240
TiO2	0.3420	0.1600	0.1720	0.1730	0.2180	0.1890	0.2100	0.0500
Al2O3	1.1690	1.0850	1.5540	0.7370	3.4910	1.0770	1.1750	3.8730
FeO	6.5550	11.8780	11.9420	12.5430	17.3870	12.2640	12.0730	19.6840
MnO	0.1550	0.1750	0.2760	0.3820	0.3330	0.2190	0.2850	0.3090
MgO	18.1210	29.7250	29.3930	30.0230	25.5180	29.3920	29.0180	23.9380
CaO	19.6700	1.3250	1.2600	1.6420	1.2200	1.4410	1.4190	0.5570
K2O	0.0000	0.0000	0.0000	0.0000	0.0000	0.0000	0.0000	0.0000
Na2O	0.2300	0.0120	0.0420	0.0000	0.0840	0.0070	0.0090	0.0090
SUM	99.5520	99.5720	99.0740	101.8440	100.1900	99.9820	98.6470	100.0440
Si	1.9609	1.9672	1.9523	1.9704	1.8930	1.9693	1.9634	1.8982
Ti	0.0095	0.0043	0.0046	0.0046	0.0060	0.0051	0.0057	0.0014
Al	0.0507	0.0456	0.0657	0.0304	0.1500	0.0451	0.0499	0.1679
Fe	0.2016	0.3539	0.3582	0.3669	0.5300	0.3646	0.3640	0.6053
Mn	0.0048	0.0053	0.0084	0.0113	0.0103	0.0066	0.0087	0.0096
Mg	0.9934	1.5784	1.5711	1.5648	1.3861	1.5573	1.5591	1.3118
Ca	0.7752	0.0506	0.0484	0.0615	0.0476	0.0549	0.0548	0.0219
K	0.0000	0.0000	0.0000	0.0000	0.0000	0.0000	0.0000	0.0000
Na	0.0164	0.0008	0.0029	0.0000	0.0059	0.0005	0.0006	0.0006

TABLE 2 continued

	SG2529-7C	SG2529-8M	SG2529-8C	SG2529-9M	SG2529-9C	SG2532-1M	SG2532-1C	SG2532-2M
SiO2	50.5910	52.8170	52.1900	53.8580	50.5900	54.8460	50.5970	54.8060
TiO2	0.0520	0.3300	0.3980	0.2560	0.0260	0.2310	0.0760	0.2260
Al2O3	3.9870	1.6190	1.9180	1.8530	3.9590	0.7820	4.2930	1.3000
FeO	20.8980	5.7310	6.1900	12.8830	22.8640	13.6920	22.9450	12.3130
MnO	0.4350	0.1540	0.1610	0.3150	0.3700	0.5590	0.5020	0.2040
MgO	23.1860	16.8700	16.6970	28.6910	21.9210	28.6170	22.1800	29.5340
CaO	0.5200	21.4800	20.9610	1.6360	0.6660	1.5190	0.5060	1.4220
K2O	0.0000	0.0000	0.0000	0.0000	0.0000	0.0000	0.0000	0.0000
Na2O	0.0000	0.3100	0.4390	0.0530	0.0250	0.0050	0.0000	0.0340
SUM	99.6690	99.3110	98.9540	99.5450	100.4210	100.2510	101.0990	99.8390
Si	1.8822	1.9517	1.9395	1.9352	1.8846	1.9631	1.8727	1.9539
Ti	0.0015	0.0092	0.0111	0.0069	0.0007	0.0062	0.0021	0.0061
Al	0.1749	0.0705	0.0840	0.0785	0.1739	0.0330	0.1873	0.0546
Fe	0.6503	0.1771	0.1924	0.3871	0.7123	0.4099	0.7102	0.3671
Mn	0.0137	0.0048	0.0051	0.0096	0.0117	0.0169	0.0157	0.0062
Mg	1.2856	0.9290	0.9248	1.5364	1.2170	1.5265	1.2234	1.5692
Ca	0.0207	0.8505	0.8347	0.0630	0.0266	0.0583	0.0201	0.0543
K	0.0000	0.0000	0.0000	0.0000	0.0000	0.0000	0.0000	0.0000
Na	0.0000	0.0222	0.0316	0.0037	0.0018	0.0003	0.0000	0.0024

	SG2532-2C	SG2532-3M	SG2532-3C	SG2532-4M	SG2532-4C	SG2532-5M	SG2532-5C	SG2532-6M
SiO2	54.1080	52.7520	51.6030	52.2010	49.8540	55.3680	50.3980	54.9280
TiO2	0.1100	0.3840	0.2690	0.3530	0.4200	0.1640	0.0280	0.1260
Al2O3	2.4580	1.6920	2.0620	1.6110	5.4360	1.0590	3.4440	1.6190
FeO	11.8870	6.4180	6.0020	6.1130	10.2820	12.4920	23.6710	11.9030
MnO	0.2070	0.1550	0.1450	0.2030	0.1220	0.2100	0.4850	0.2290
MgO	29.5900	17.0010	16.7330	16.8820	11.7960	29.4170	21.8470	29.3510
CaO	1.3130	21.3160	21.3080	21.6920	20.7210	1.3950	0.4740	1.2430
K2O	0.0000	0.0000	0.0000	0.0000	0.0000	0.0000	0.0000	0.0000
Na2O	0.0590	0.3000	0.4240	0.2680	1.3950	0.0070	0.0000	0.0240
SUM	99.7320	100.0180	98.5460	99.3230	100.0260	100.1120	100.3470	99.4230
Si	1.9277	1.9413	1.9281	1.9366	1.8720	1.9678	1.8875	1.9599
Ti	0.0029	0.0106	0.0076	0.0098	0.0119	0.0044	0.0008	0.0034
Al	0.1032	0.0734	0.0908	0.0705	0.2406	0.0444	0.1521	0.0681
Fe	0.3542	0.1975	0.1876	0.1897	0.3229	0.3713	0.7414	0.3552
Mn	0.0062	0.0048	0.0046	0.0064	0.0039	0.0063	0.0154	0.0069
Mg	1.5711	0.9324	0.9318	0.9334	0.6601	1.5581	1.2194	1.5608
Ca	0.0501	0.8405	0.8531	0.8623	0.8337	0.0531	0.0190	0.0475
K	0.0000	0.0000	0.0000	0.0000	0.0000	0.0000	0.0000	0.0000
Na	0.0041	0.0214	0.0307	0.0193	0.1016	0.0005	0.0000	0.0017

TABLE 2 continued

	SG2532-6C	SG272-1M	SG272-1C	SG272-2M	SG272-2C	SG272-3M	SG272-3C	SG272-4M
SiO2	54.4590	51.1550	52.8040	51.0620	50.7170	50.8410	52.3760	50.7810
TiO2	0.1410	0.7080	0.4710	0.7470	0.6530	0.7600	0.4350	0.7410
Al2O3	1.8430	3.7320	2.1410	3.9670	3.4160	3.7530	2.1120	3.7560
FeO	11.4140	6.4530	6.1540	6.5650	6.1090	6.3630	6.1920	6.3770
MnO	0.2140	0.0000	0.1320	0.3980	0.0000	0.0690	0.1900	0.0320
MgO	29.9650	16.0190	17.4490	15.8530	16.0260	15.8530	17.2840	15.9880
CaO	1.2260	22.1900	21.1890	21.7340	22.0270	22.1180	21.4400	21.8030
K2O	0.0000	0.0000	0.0000	0.0000	0.0000	0.0000	0.0000	0.0000
Na2O	0.0500	0.3780	0.2650	0.4220	0.3200	0.3820	0.3410	0.3170
SUM	99.3120	100.6350	100.6050	100.7480	99.2680	100.1390	100.3700	99.7950
Si	1.9434	1.8785	1.9280	1.8748	1.8858	1.8768	1.9215	1.8787
Ti	0.0038	0.0196	0.0129	0.0206	0.0183	0.0211	0.0120	0.0206
Al	0.0775	0.1616	0.0922	0.1717	0.1497	0.1633	0.0913	0.1638
Fe	0.3406	0.1982	0.1879	0.2016	0.1900	0.1964	0.1900	0.1973
Mn	0.0065	0.0000	0.0041	0.0124	0.0000	0.0022	0.0059	0.0010
Mg	1.5936	0.8767	0.9495	0.8675	0.8881	0.8721	0.9450	0.8815
Ca	0.0469	0.8731	0.8290	0.8551	0.8776	0.8749	0.8428	0.8643
K	0.0000	0.0000	0.0000	0.0000	0.0000	0.0000	0.0000	0.0000
Na	0.0035	0.0269	0.0188	0.0300	0.0231	0.0273	0.0243	0.0227
	SG272-4C	SG272-5M	SG272-5C	SG272-9M	SG272-9C	SG272-10M	SG272-10C	SG2711-2C
SiO2	50.9960	50.8360	52.7910	47.8110	49.9720	46.8460	48.7460	47.6980
TiO2	0.5580	0.6910	0.4420	1.2140	0.7330	1.7400	1.0500	1.5330
Al2O3	3.2010	3.4960	1.9440	5.3150	3.2020	6.7850	5.1690	6.9440
FeO	5.9600	6.4530	6.1310	8.1280	7.6720	9.0860	8.0810	6.6550
MnO	0.1370	0.0660	0.0560	0.2630	0.1260	0.0680	0.2670	0.0000
MgO	16.1590	15.9780	17.5550	14.5290	16.2960	13.7160	14.6760	13.6070
CaO	22.1660	21.8480	21.0160	21.4080	20.4080	20.7680	21.2740	24.5440
K2O	0.0000	0.0000	0.0000	0.0000	0.0000	0.0010	0.0000	0.0000
Na2O	0.3400	0.4050	0.2770	0.3500	0.2510	0.3960	0.4190	0.3720
SUM	99.5170	99.7730	100.2120	99.0180	98.6600	99.4060	99.6820	101.3530
Si	1.8916	1.8833	1.9336	1.8065	1.8783	1.7673	1.8249	1.7613
Ti	0.0156	0.0193	0.0122	0.0345	0.0207	0.0494	0.0296	0.0426
Al	0.1400	0.1527	0.0839	0.2368	0.1419	0.3018	0.2281	0.3023
Fe	0.1849	0.1999	0.1878	0.2568	0.2412	0.2867	0.2530	0.2055
Mn	0.0043	0.0021	0.0017	0.0084	0.0040	0.0022	0.0085	0.0000
Mg	0.8933	0.8822	0.9583	0.8181	0.9129	0.7712	0.8188	0.7488
Ca	0.8810	0.8673	0.8248	0.8667	0.8219	0.8395	0.8534	0.9711
K	0.0000	0.0000	0.0000	0.0000	0.0000	0.0000	0.0000	0.0000
Na	0.0245	0.0291	0.0197	0.0256	0.0183	0.0290	0.0304	0.0266

TABLE 2 continued

	SG2711-2M	SG2711-3M	SG2711-3C	SG285-1M	SG285-1C	SG285-2M	SG285-2C	SG285-4M
SiO2	42.5030	46.1830	47.7540	50.7230	53.0570	53.1900	53.2010	52.6480
TiO2	3.1010	1.9580	1.5640	0.5680	0.2710	0.3640	0.2380	0.3470
Al2O3	10.0700	8.2450	6.8090	2.5780	0.9960	1.3040	1.2600	1.4600
FeO	8.6440	6.8730	6.4780	6.9540	7.2490	6.1010	5.5160	6.0570
MnO	0.0330	0.0000	0.0000	0.1550	0.2310	0.2520	0.1300	0.2790
MgO	11.1180	12.9460	13.3440	17.5250	20.1310	18.4500	18.2110	18.3970
CaO	24.2870	24.3720	24.1210	20.3490	17.7560	20.7680	21.1080	20.8840
K2O	0.0050	0.0000	0.0020	0.0080	0.0000	0.0040	0.0000	0.0060
Na2O	0.5510	0.3810	0.4280	0.4250	0.2110	0.2330	0.3240	0.4140
SUM	100.3120	100.9580	100.5000	99.2850	99.9020	100.6660	99.9880	100.4920
Si	1.6154	1.7167	1.7745	1.8886	1.9438	1.9397	1.9490	1.9273
Ti	0.0886	0.0547	0.0437	0.0159	0.0075	0.0100	0.0066	0.0096
Al	0.4512	0.3613	0.2983	0.1132	0.0430	0.0561	0.0544	0.0630
Fe	0.2748	0.2137	0.2013	0.2165	0.2221	0.1861	0.1690	0.1854
Mn	0.0011	0.0000	0.0000	0.0049	0.0072	0.0078	0.0040	0.0087
Mg	0.6298	0.7172	0.7390	0.9725	1.0991	1.0027	0.9943	1.0037
Ca	0.9891	0.9707	0.9604	0.8118	0.6970	0.8115	0.8286	0.8192
K	0.0002	0.0000	0.0001	0.0004	0.0000	0.0002	0.0000	0.0003
Na	0.0406	0.0275	0.0308	0.0307	0.0150	0.0165	0.0230	0.0294
	SG285-4C	SG285-6M	SG285-6C	SG285-8M	SG285-8C	SG285-11M	SG285-11C	SG285-12C
SiO2	51.5640	53.3520	52.8860	51.2460	52.5000	55.7690	55.6070	54.1710
TiO2	0.6130	0.4020	0.3460	0.5480	0.3050	0.1480	0.1630	0.1980
Al2O3	2.5490	1.3780	1.6690	2.8900	1.9460	0.5330	0.6330	1.3900
FeO	7.0560	7.0510	5.8480	7.1070	5.6560	10.2700	10.9510	10.9840
MnO	0.1530	0.1690	0.0480	0.1960	0.1680	0.2650	0.2450	0.2680
MgO	17.8240	19.3860	17.5270	16.6610	17.5590	31.4280	31.1510	30.8790
CaO	20.1930	18.4850	21.6860	21.4930	21.6150	1.6800	1.5820	1.6590
K2O	0.0000	0.0000	0.0000	0.0000	0.0030	0.0000	0.0000	0.0000
Na2O	0.3330	0.3230	0.4250	0.3710	0.3970	0.0430	0.0330	0.0050
SUM	100.2850	100.5460	100.4350	100.5120	100.1490	100.1360	100.3650	99.5540
Si	1.8968	1.9425	1.9355	1.8892	1.9267	1.9660	1.9615	1.9311
Ti	0.0170	0.0110	0.0095	0.0152	0.0084	0.0039	0.0043	0.0053
Al	0.1105	0.0591	0.0720	0.1256	0.0842	0.0222	0.0263	0.0584
Fe	0.2171	0.2147	0.1790	0.2191	0.1736	0.3028	0.3231	0.3275
Mn	0.0048	0.0052	0.0015	0.0061	0.0052	0.0079	0.0073	0.0081
Mg	0.9771	1.0519	0.9560	0.9154	0.9604	1.6512	1.6376	1.6405
Ca	0.7959	0.7211	0.8504	0.8490	0.8500	0.0635	0.0598	0.0634
K	0.0000	0.0000	0.0000	0.0000	0.0001	0.0000	0.0000	0.0000
Na	0.0238	0.0228	0.0302	0.0265	0.0283	0.0029	0.0023	0.0003

TABLE 2 continued

	SG285-12M	SG288-1M	SG288-1C	SG288-2M	SG288-2C	SG2813-1M	SG2813-1C	SG2813-2M
SiO2	54.9780	45.5970	49.2230	43.9980	45.0110	44.7720	46.5650	48.0460
TiO2	0.2270	2.3790	1.2340	2.8930	2.4060	2.7890	1.9280	1.5600
Al2O3	1.1720	8.5140	4.8990	9.5970	9.4760	9.2170	9.3470	7.1280
FeO	10.8210	7.1120	6.5140	8.5570	8.1720	8.3890	8.1310	6.7110
MnO	0.2330	0.0940	0.1170	0.0690	0.1010	0.0950	0.1490	0.0900
MgO	30.7360	12.3890	14.2590	11.0990	11.5730	11.8860	12.4690	13.6730
CaO	1.7350	23.9110	24.1100	24.1040	24.0120	22.6490	21.9930	22.8270
K2O	0.0000	0.0040	0.0030	0.0070	0.0090	0.0030	0.0000	0.0000
Na2O	0.0540	0.3900	0.3540	0.4520	0.3670	0.5220	0.6150	0.3960
SUM	99.9560	100.3900	100.7130	100.7760	101.1270	100.3220	101.1970	100.4310
Si	1.9480	1.7065	1.8237	1.6567	1.6810	1.6829	1.7222	1.7800
Ti	0.0060	0.0670	0.0344	0.0819	0.0676	0.0788	0.0536	0.0435
Al	0.0490	0.3756	0.2140	0.4260	0.4172	0.4084	0.4075	0.3113
Fe	0.3207	0.2226	0.2018	0.2695	0.2552	0.2637	0.2515	0.2079
Mn	0.0070	0.0030	0.0037	0.0022	0.0032	0.0030	0.0047	0.0028
Mg	1.6231	0.6910	0.7873	0.6228	0.6441	0.6658	0.6873	0.7549
Ca	0.0659	0.9589	0.9572	0.9725	0.9609	0.9122	0.8716	0.9062
K	0.0000	0.0002	0.0001	0.0003	0.0004	0.0001	0.0000	0.0000
Na	0.0037	0.0283	0.0254	0.0330	0.0266	0.0380	0.0441	0.0284

	SG2813-2C	SG2813-5M	SG2813-5C	SG2813-7M	SG2813-7C
SiO2	49.3000	44.0070	44.3350	45.4080	43.7800
TiO2	1.3010	3.1490	3.0210	2.5860	3.1200
Al2O3	5.8460	10.0320	9.8820	8.9000	9.3450
FeO	7.1160	8.6580	8.1320	8.1550	8.5500
MnO	0.0310	0.1460	0.1220	0.1090	0.0590
MgO	14.3600	11.4930	11.8420	12.2250	11.6980
CaO	22.0070	22.7230	22.6720	22.6640	22.8830
K2O	0.0000	0.0050	0.0000	0.0200	0.0110
Na2O	0.4300	0.5540	0.4350	0.5470	0.3910
SUM	100.3910	100.7670	100.4410	100.6140	99.8370
Si	1.8229	1.6516	1.6630	1.6985	1.6592
Ti	0.0362	0.0889	0.0852	0.0727	0.0889
Al	0.2548	0.4439	0.4370	0.3925	0.4175
Fe	0.2201	0.2718	0.2551	0.2551	0.2710
Mn	0.0010	0.0046	0.0039	0.0035	0.0019
Mg	0.7913	0.6428	0.6620	0.6815	0.6607
Ca	0.8719	0.9138	0.9112	0.9084	0.9292
K	0.0000	0.0002	0.0000	0.0010	0.0005
Na	0.0308	0.0403	0.0316	0.0397	0.0287

TABLE 3 Plagioclase Composition

	SG2191-M	SG2191-C	SG2192-M	SG2192-C	SG2193-M	SG2193-C	SG2194-M	SG2194-C
SiO2	56.6860	56.3130	54.9690	54.6030	55.5260	55.4710	56.2470	55.0240
TiO2	0.1020	0.0570	0.0970	0.0780	0.0890	0.1330	0.1130	0.0720
Al2O3	26.6250	27.6570	26.7040	28.3120	27.1810	27.6240	25.8920	26.8140
FeO	1.0680	1.2290	1.1880	1.0130	1.2350	1.1200	1.2690	1.1930
MnO	0.0000	0.0440	0.0210	0.0270	0.0000	0.0000	0.0000	0.0000
MgO	0.1660	0.1880	0.1550	0.1750	0.1790	0.1980	0.1520	0.1570
CaO	8.2550	9.0320	8.7930	9.9760	8.7300	9.2130	8.0700	8.7550
K2O	0.6960	0.5670	0.6220	0.4610	0.6470	0.5680	0.7330	0.6120
Na2O	6.1990	5.8170	5.9570	5.4160	6.0120	5.9030	6.3940	5.8120
SUM	99.7970	100.9040	98.5060	100.0610	99.5990	100.2300	98.8700	98.4390
Si	10.2455	10.0872	10.1009	9.8854	10.0872	10.0184	10.2821	10.1070
Ti	0.0139	0.0077	0.0134	0.0106	0.0122	0.0181	0.0155	0.0099
Al	5.6733	5.8405	5.7851	6.0428	5.8214	5.8818	5.5800	5.8066
Fe	0.1614	0.1841	0.1826	0.1534	0.1876	0.1692	0.1940	0.1833
Mn	0.0000	0.0067	0.0033	0.0041	0.0000	0.0000	0.0000	0.0000
Mg	0.0447	0.0502	0.0424	0.0472	0.0485	0.0533	0.0414	0.0430
Ca	1.5987	1.7336	1.7313	1.9352	1.6993	1.7829	1.5807	1.7231
K	0.1605	0.1296	0.1458	0.1065	0.1500	0.1309	0.1709	0.1434
Na	2.1725	2.0204	2.1225	1.9012	2.1177	2.0672	2.2664	2.0700
	SG219-M	SG219-C	SG2195-M	SG2195-C	SG2221-M	SG2221-C	SG2223-M	SG2223-C
SiO2	55.5700	60.4820	55.7020	54.8080	55.2750	52.0800	54.0820	58.3580
TiO2	0.0000	0.0950	0.0890	0.0720	0.0900	0.1120	0.0730	0.1330
Al2O3	27.1870	22.1410	27.7840	27.4920	26.9520	30.5320	28.2570	25.5200
FeO	0.4930	1.4360	1.3410	1.1890	1.4040	1.0560	1.5040	0.9880
MnO	0.0480	0.0480	0.0480	0.0000	0.0710	0.0000	0.0000	0.0060
MgO	0.1430	0.5200	0.1900	0.1820	0.1600	0.1560	0.1830	0.1190
CaO	8.3130	5.9350	9.3450	9.6070	9.5710	12.3670	10.7350	6.8010
K2O	0.6800	1.3640	0.5850	0.4870	0.4280	0.2620	0.3900	0.9110
Na2O	6.0780	6.0220	5.8440	5.6090	5.6870	4.0770	5.0620	6.9730
SUM	98.5120	98.0430	100.9280	99.4460	99.6380	100.6420	100.2860	99.8090
Si	10.1546	11.0378	10.0044	9.9850	10.0579	9.4258	9.8090	10.5100
Ti	0.0000	0.0130	0.0120	0.0099	0.0123	0.0152	0.0100	0.0180
Al	5.8569	4.7637	5.8830	5.9047	5.7817	6.5147	6.0420	5.4184
Fe	0.0753	0.2192	0.2014	0.1812	0.2137	0.1598	0.2281	0.1488
Mn	0.0074	0.0074	0.0073	0.0000	0.0109	0.0000	0.0000	0.0009
Mg	0.0389	0.1414	0.0509	0.0494	0.0434	0.0421	0.0495	0.0319
Ca	1.6277	1.1606	1.7984	1.8754	1.8661	2.3983	2.0863	1.3124
K	0.1585	0.3176	0.1340	0.1132	0.0994	0.0605	0.0902	0.2093
Na	2.1536	2.1310	2.0352	1.9814	2.0065	1.4308	1.7802	2.4350

TABLE 3 continued

	SG2224-M	SG2224-C	SG2225-M	SG2225-C	SG2226-M	SG2226-C	SG2241-M	SG2241-C
SiO2	54.2510	51.6670	52.0950	52.0330	54.1130	63.2780	55.4350	51.9410
TiO2	0.0800	0.0470	0.0590	0.0570	0.0840	0.1870	0.0740	0.0430
Al2O3	28.3810	31.6480	30.3990	30.6950	27.3180	21.1010	27.1150	30.4550
FeO	1.4380	0.8670	1.0570	0.8720	1.5710	0.6790	1.2980	0.8470
MnO	0.0000	0.0000	0.0430	0.0020	0.0680	0.0290	0.0390	0.0680
MgO	0.1830	0.1760	0.1570	0.2130	0.1770	0.0890	0.1660	0.2110
CaO	10.8000	12.9860	12.2590	12.3170	9.7120	2.1540	8.8040	12.1310
K2O	0.3640	0.2350	0.2860	0.2550	0.4350	4.4180	0.5190	0.2590
Na2O	4.9220	3.8650	4.3970	4.2240	5.4050	7.0460	6.0390	4.2230
SUM	100.4190	101.4910	100.7520	100.6680	98.8830	98.9810	99.4890	100.1780
Si	9.8157	9.2796	9.4305	9.4105	9.9392	11.4508	10.0839	9.4362
Ti	0.0109	0.0063	0.0080	0.0078	0.0116	0.0254	0.0101	0.0059
Al	6.0538	6.7012	6.4876	6.5447	5.9154	4.5017	5.8149	6.5228
Fe	0.2176	0.1302	0.1600	0.1319	0.2413	0.1028	0.1975	0.1287
Mn	0.0000	0.0000	0.0066	0.0003	0.0106	0.0044	0.0060	0.0105
Mg	0.0493	0.0471	0.0424	0.0574	0.0485	0.0240	0.0450	0.0571
Ca	2.0938	2.4991	2.3779	2.3869	1.9114	0.4177	1.7160	2.3615
K	0.0840	0.0538	0.0661	0.0588	0.1019	1.0200	0.1204	0.0600
Na	1.7268	1.3460	1.5434	1.4813	1.9250	2.4723	2.1300	1.4876
	SG2242-M	SG2242-C	SG2243-M	SG2243-C	SG2244-C	SG2244-M	SG224G2-M	SG224G2-C
SiO2	53.9330	52.1890	55.9710	52.3140	51.2120	54.6410	54.0340	52.8790
TiO2	0.0820	0.0690	0.0800	0.0680	0.0480	0.0770	0.0790	0.0340
Al2O3	29.2230	29.5540	27.4860	30.0000	32.0400	27.9160	28.1480	30.5980
FeO	0.9060	0.9650	1.3510	0.8810	0.7330	1.2930	1.1370	0.8410
MnO	0.0550	0.0000	0.0270	0.0830	0.0730	0.0000	0.0240	0.0000
MgO	0.2160	0.2310	0.1620	0.2240	0.2250	0.1750	0.1830	0.2040
CaO	10.9650	11.4250	9.6170	11.8470	13.6260	9.9400	10.4490	11.5470
K2O	0.3640	0.2680	0.4890	0.2670	0.1540	0.4750	0.4560	0.2970
Na2O	4.8890	4.4770	5.6840	4.4700	3.5000	5.3680	5.1050	4.5690
SUM	100.6330	99.1780	100.8670	100.1540	101.6110	99.8850	99.6150	100.9690
Si	9.7223	9.5623	10.0515	9.5051	9.1934	9.9198	9.8443	9.5107
Ti	0.0111	0.0095	0.0108	0.0093	0.0065	0.0105	0.0108	0.0046
Al	6.2105	6.3839	5.8192	6.4261	6.7808	5.9748	6.0458	6.4880
Fe	0.1366	0.1479	0.2029	0.1339	0.1100	0.1963	0.1732	0.1265
Mn	0.0084	0.0000	0.0041	0.0128	0.0111	0.0000	0.0037	0.0000
Mg	0.0580	0.0631	0.0434	0.0607	0.0602	0.0473	0.0497	0.0547
Ca	2.1180	2.2430	1.8506	2.3064	2.6210	1.9336	2.0398	2.2253
K	0.0837	0.0626	0.1120	0.0619	0.0353	0.1100	0.1060	0.0682
Na	1.7089	1.5906	1.9793	1.5748	1.2183	1.8896	1.8034	1.5934

TABLE 3 continued

	SG233-M	SG233-C	SG2331-C	SG2331-M	SG2332-C	SG2332-M	SG2333-M	SG2333-C
SiO2	56.0280	57.8600	53.5110	59.3910	54.5490	56.4350	57.0130	55.1040
TiO2	0.0720	0.0160	0.0450	0.1130	0.0440	0.0730	0.1100	0.0920
Al2O3	27.5880	26.8050	29.7750	25.3450	28.9220	27.7930	27.1140	27.7660
FeO	0.9160	0.3170	1.0480	0.9050	1.0400	1.2910	1.1570	1.3560
MnO	0.0220	0.0000	0.0410	0.0090	0.0000	0.0150	0.0130	0.0000
MgO	0.1300	0.1000	0.1990	0.1130	0.1960	0.2110	0.1320	0.1950
CaO	9.1060	7.7490	11.4340	6.6020	10.8590	9.2550	8.2460	9.9450
K2O	0.4500	0.6460	0.3510	0.9860	0.3820	0.4820	0.5860	0.4350
Na2O	6.1810	6.6160	4.9410	7.0300	4.9580	5.6110	6.6310	5.4940
SUM	100.4930	100.1090	101.3450	100.4940	100.9500	101.1660	101.0020	100.3870
Si	10.0744	10.3617	9.6082	10.6041	9.7979	10.0777	10.1949	9.9549
Ti	0.0097	0.0022	0.0061	0.0152	0.0059	0.0098	0.0148	0.0125
Al	5.8482	5.6592	6.3029	5.3350	6.1244	5.8511	5.7160	5.9136
Fe	0.1377	0.0475	0.1574	0.1351	0.1562	0.1928	0.1730	0.2049
Mn	0.0034	0.0000	0.0062	0.0014	0.0000	0.0023	0.0020	0.0000
Mg	0.0348	0.0267	0.0533	0.0301	0.0525	0.0562	0.0352	0.0525
Ca	1.7544	1.4869	2.1998	1.2631	2.0899	1.7709	1.5800	1.9251
K	0.1032	0.1476	0.0804	0.2246	0.0875	0.1098	0.1337	0.1003
Na	2.1550	2.2974	1.7203	2.4338	1.7268	1.9428	2.2992	1.9245
	SG2334-M	SG2334-C	SG2361-M	SG2361-C	SG2362-M	SG2362-C	SG2363-M	SG2363-C
SiO2	55.5420	53.5590	54.3010	53.6750	54.3970	53.9470	55.7430	54.4520
TiO2	0.0890	0.0630	0.0590	0.0650	0.0650	0.0280	0.0820	0.0350
Al2O3	28.6350	30.3220	28.1910	30.0490	29.0630	29.7900	28.1200	28.7600
FeO	1.1670	1.0330	1.1580	0.9540	0.9630	0.8950	1.2220	1.0800
MnO	0.0000	0.0090	0.0160	0.0000	0.0460	0.0000	0.0000	0.0000
MgO	0.1940	0.1890	0.1480	0.1250	0.1810	0.2020	0.1580	0.1550
CaO	10.2550	11.6370	9.8790	11.2330	11.0000	11.0420	9.9160	10.4650
K2O	0.3950	0.3030	0.4530	0.3460	0.3690	0.3540	0.4610	0.4040
Na2O	5.4230	4.6470	5.6320	4.8520	5.0940	4.7130	5.5230	5.3110
SUM	101.7000	101.7620	99.8370	101.2990	101.1780	100.9710	101.2250	100.6620
Si	9.8951	9.5665	9.8684	9.6207	9.7594	9.6824	9.9726	9.8128
Ti	0.0119	0.0085	0.0081	0.0088	0.0088	0.0038	0.0110	0.0047
Al	6.0143	6.3851	6.0400	6.3497	6.1472	6.3034	5.9309	6.1102
Fe	0.1739	0.1543	0.1760	0.1430	0.1445	0.1343	0.1828	0.1628
Mn	0.0000	0.0014	0.0025	0.0000	0.0070	0.0000	0.0000	0.0000
Mg	0.0515	0.0503	0.0401	0.0334	0.0484	0.0540	0.0421	0.0416
Ca	1.9576	2.2272	1.9237	2.1574	2.1146	2.1235	1.9009	2.0208
K	0.0898	0.0690	0.1050	0.0791	0.0845	0.0811	0.1052	0.0929
Na	1.8733	1.6094	1.9846	1.6863	1.7721	1.6402	1.9159	1.8558

TABLE 3 continued

	SG24A21-M	SG24A21-C	SG24A22-M	SG24A22-C	SG24A23-M	SG24A23-C	SG24A2-C	SG24A2-M
SiO2	55.5940	53.2520	55.4430	53.0110	58.0000	55.7030	52.0290	52.9590
TiO2	0.0850	0.0680	0.1190	0.0150	0.1220	0.1050	0.0790	0.0180
Al2O3	27.5990	29.9550	27.7400	29.0010	25.8150	28.0670	29.3970	29.2180
FeO	1.2520	0.9090	1.4340	0.9780	1.2730	1.2500	0.9990	0.5620
MnO	0.0160	0.0000	0.0000	0.0000	0.0340	0.0060	0.1010	0.0560
MgO	0.1610	0.1430	0.1650	0.1500	0.1370	0.1450	0.1450	0.1220
CaO	9.0870	11.3800	9.3790	10.9220	7.4400	9.4400	11.1510	10.5970
K2O	0.4990	0.3560	0.4650	0.3530	0.8570	0.5010	0.3420	0.3600
Na2O	6.0670	4.7740	6.0720	4.8700	6.6050	5.7630	4.5900	5.0230
SUM	100.3600	100.8370	100.8170	99.3000	100.2830	100.9800	98.8330	98.9150
Si	10.0305	9.5949	9.9786	9.6923	10.4238	9.9868	9.5732	9.6968
Ti	0.0115	0.0092	0.0161	0.0021	0.0165	0.0142	0.0109	0.0025
Al	5.8705	6.3630	5.8859	6.2512	5.4696	5.9324	6.3768	6.3071
Fe	0.1889	0.1370	0.2158	0.1495	0.1913	0.1874	0.1537	0.0861
Mn	0.0024	0.0000	0.0000	0.0000	0.0052	0.0009	0.0157	0.0087
Mg	0.0433	0.0384	0.0443	0.0409	0.0367	0.0387	0.0398	0.0333
Ca	1.7568	2.1971	1.8087	2.1397	1.4327	1.8135	2.1985	2.0791
K	0.1149	0.0818	0.1068	0.0823	0.1965	0.1146	0.0803	0.0841
Na	2.1225	1.6679	2.1190	1.7265	2.3017	2.0034	1.6376	1.7833
	SG2521-C	SG2521-M	SG2522-M	SG2522-C	SG2581-M	SG2581-C	SG2510A-M	SG2510A-C
SiO2	53.1700	54.5420	55.0030	53.6300	52.8880	64.9620	55.4630	57.2550
TiO2	0.0300	0.0890	0.0680	0.0560	0.0570	0.4780	0.0860	0.1160
Al2O3	29.5080	26.6800	27.4140	28.9770	30.5520	19.8700	26.7020	25.5230
FeO	0.8350	1.1440	0.9750	1.0340	0.9030	1.0750	1.0830	1.0070
MnO	0.0460	0.0180	0.0060	0.0000	0.0570	0.0000	0.0000	0.0000
MgO	0.1610	0.5030	0.1550	0.1340	0.1430	0.2000	0.1670	0.1400
CaO	11.4790	9.5170	9.6590	10.8160	12.2410	3.9220	8.4840	7.0910
K2O	0.2930	0.4000	0.3860	0.3080	0.2490	2.1150	0.5370	0.7150
Na2O	4.6360	5.6390	5.3340	5.0290	4.4250	6.4540	5.9790	6.4030
SUM	100.1580	98.5320	99.0000	99.9840	101.5150	99.0760	98.5010	98.2500
Si	9.6385	10.0284	10.0344	9.7336	9.4828	11.6272	10.1616	10.4616
Ti	0.0041	0.0123	0.0093	0.0076	0.0077	0.0643	0.0118	0.0159
Al	6.3062	5.7833	5.8961	6.2002	6.4582	4.1928	5.7675	5.4980
Fe	0.1266	0.1759	0.1488	0.1570	0.1354	0.1609	0.1659	0.1539
Mn	0.0071	0.0028	0.0009	0.0000	0.0087	0.0000	0.0000	0.0000
Mg	0.0435	0.1378	0.0421	0.0362	0.0382	0.0533	0.0456	0.0381
Ca	2.2297	1.8750	1.8881	2.1034	2.3518	0.7522	1.6655	1.3883
K	0.0678	0.0938	0.0898	0.0713	0.0570	0.4830	0.1255	0.1667
Na	1.6295	2.0104	1.8869	1.7698	1.5384	2.2399	2.1241	2.2686

TABLE 3 continued

	SG2510A-M	SG25101-C	SG25101-M	SG25102-M	SG25102-C	SG2510-C	SG2510-M	SG25103-C
SiO2	54.6250	55.1680	55.4600	58.9330	57.4740	62.1360	59.3680	55.1810
TiO2	0.0840	0.0710	0.0950	0.0790	0.0980	0.1010	0.0040	0.0910
Al2O3	27.3110	28.9680	28.5730	25.5130	26.1590	23.2140	24.8430	27.9430
FeO	1.0170	1.0090	0.9080	1.2450	1.1910	0.7900	0.5020	1.1930
MnO	0.0000	0.0000	0.0740	0.0410	0.0000	0.0000	0.0180	0.0000
MgO	0.1570	0.1550	0.1650	0.1360	0.1390	0.1070	0.1220	0.1630
CaO	8.9190	10.3040	10.1450	7.3340	7.8150	4.9860	5.9110	9.5720
K2O	0.4740	0.4460	0.4540	0.7150	0.6800	1.9450	1.0310	0.4970
Na2O	5.6260	5.1410	5.5770	6.8170	6.4240	6.4020	7.0750	5.6480
SUM	98.2130	101.2620	101.4510	100.8130	99.9800	99.6810	98.8740	100.2880
Si	10.0419	9.8595	9.9021	10.5176	10.3560	11.1028	10.7246	9.9648
Ti	0.0116	0.0095	0.0128	0.0106	0.0133	0.0136	0.0005	0.0124
Al	5.9190	6.1034	6.0144	5.3680	5.5569	4.8902	5.2908	5.9489
Fe	0.1564	0.1508	0.1356	0.1858	0.1795	0.1181	0.0758	0.1802
Mn	0.0000	0.0000	0.0112	0.0062	0.0000	0.0000	0.0028	0.0000
Mg	0.0430	0.0413	0.0439	0.0362	0.0373	0.0285	0.0328	0.0439
Ca	1.7568	1.9732	1.9409	1.4025	1.5088	0.9546	1.1442	1.8521
K	0.1112	0.1017	0.1034	0.1628	0.1563	0.4434	0.2376	0.1145
Na	2.0054	1.7815	1.9308	2.3590	2.2444	2.2181	2.4782	1.9777
	SG25103-M	SG25131-M	SG25131-C	SG25131-M	SG25131-C	SG25132-M	SG25132-C	SG25132-M
SiO2	64.3450	56.7690	55.3940	56.6510	57.3560	55.9450	55.3950	57.1290
TiO2	0.1470	0.0920	0.0840	0.1250	0.1310	0.0570	0.0760	0.0880
Al2O3	21.9460	27.0420	28.1460	27.1650	25.9600	27.3490	28.1980	26.6470
FeO	0.9800	1.1640	1.1360	1.1500	1.1340	1.0430	0.9120	1.1030
MnO	0.0000	0.0060	0.0000	0.0000	0.1140	0.0000	0.0000	0.0000
MgO	0.0670	0.1280	0.1610	0.1640	0.1610	0.1650	0.1830	0.1640
CaO	2.7670	8.5170	9.4490	8.2270	7.5850	9.2000	9.8690	8.5560
K2O	2.3190	0.5680	0.4300	0.6410	0.7470	0.5250	0.4820	0.5830
Na2O	7.7740	6.1120	5.6530	6.3710	6.5160	5.6080	5.3380	6.0560
SUM	100.3450	100.3980	100.4530	100.4940	99.7040	99.8920	100.4530	100.3260
Si	11.3998	10.2010	9.9721	10.1767	10.3681	10.1094	9.9664	10.2652
Ti	0.0196	0.0124	0.0114	0.0169	0.0178	0.0077	0.0103	0.0119
Al	4.5838	5.7287	5.9735	5.7530	5.5324	5.8263	5.9810	5.6448
Fe	0.1452	0.1749	0.1710	0.1728	0.1714	0.1576	0.1372	0.1658
Mn	0.0000	0.0009	0.0000	0.0000	0.0175	0.0000	0.0000	0.0000
Mg	0.0177	0.0343	0.0432	0.0439	0.0434	0.0444	0.0491	0.0439
Ca	0.5253	1.6399	1.8226	1.5836	1.4692	1.7813	1.9025	1.6473
K	0.5242	0.1302	0.0988	0.1469	0.1723	0.1210	0.1106	0.1336
Na	2.6706	2.1296	1.9733	2.2192	2.2839	1.9649	1.8622	2.1100

TABLE 3 continued

	SG25132-C	SG25132-M	SG25132-C	SG25171-M	SG25171-C	SG25172-C	SG25172-M	SG25181-M
SiO2	56.9880	57.9420	54.6890	64.6510	54.6370	53.1160	54.4670	53.9140
TiO2	0.0130	0.0480	0.0480	0.1040	0.0710	0.0540	0.0290	0.0790
Al2O3	26.5430	26.3950	28.4680	21.5240	28.8230	29.9850	29.4940	29.0260
FeO	1.1590	1.2210	1.0050	0.8480	0.8870	1.0490	0.8930	1.0190
MnO	0.0000	0.0000	0.0580	0.0060	0.0000	0.0000	0.0000	0.0970
MgO	0.1420	0.1610	0.1650	0.1300	0.1680	0.1500	0.1620	0.1540
CaO	8.6880	8.0880	10.3580	2.5880	10.7190	11.7770	11.0310	10.4000
K2O	0.5910	0.6110	0.4420	4.3070	0.3630	0.3200	0.3760	0.4220
Na2O	6.0470	6.2740	5.1200	6.8640	5.2800	4.8230	4.9900	4.8830
SUM	100.1710	100.7400	100.3530	101.0220	100.9480	101.2740	101.4420	99.9940
Si	10.2644	10.3564	9.8721	11.4550	9.8125	9.5522	9.7360	9.7700
Ti	0.0018	0.0065	0.0065	0.0139	0.0096	0.0073	0.0039	0.0108
Al	5.6362	5.5619	6.0583	4.4961	6.1027	6.3573	6.2154	6.2011
Fe	0.1746	0.1825	0.1517	0.1257	0.1332	0.1578	0.1335	0.1544
Mn	0.0000	0.0000	0.0089	0.0009	0.0000	0.0000	0.0000	0.0149
Mg	0.0381	0.0429	0.0444	0.0343	0.0450	0.0402	0.0432	0.0416
Ca	1.6767	1.5490	2.0034	0.4913	2.0627	2.2694	2.1128	2.0194
K	0.1358	0.1393	0.1018	0.9736	0.0832	0.0734	0.0857	0.0976
Na	2.1119	2.1744	1.7921	2.3582	1.8387	1.6818	1.7295	1.7158
	SG25181-C	SG25182-M	SG25182-C	SG25183-M	SG25183-C	SG25221-C	SG25221-M	SG25222-M
SiO2	52.9270	59.2710	54.5550	56.5910	53.8200	57.6510	58.3230	58.5280
TiO2	0.0440	0.2900	0.0780	0.2150	0.0810	0.1120	0.1010	0.4190
Al2O3	29.7520	24.3190	29.2020	21.2130	29.9200	25.9260	26.1530	24.4230
FeO	0.9410	1.0710	0.9440	3.2680	0.9750	1.3900	1.3140	1.6460
MnO	0.0000	0.0000	0.0000	0.0560	0.0000	0.0000	0.0000	0.0000
MgO	0.1600	0.0920	0.1870	5.8130	0.1720	0.1100	0.1340	0.3900
CaO	11.2590	7.5010	10.6870	6.1300	11.1510	8.2390	7.2600	7.3620
K2O	0.3140	1.7470	0.3820	0.5420	0.3450	0.5460	0.7850	1.2480
Na2O	4.7960	5.2260	5.1140	5.5740	4.7580	5.6830	6.7820	5.9210
SUM	100.1930	99.5170	101.1490	99.4020	101.2220	99.6570	100.8520	99.9370
Si	9.5973	10.7015	9.7753	10.3611	9.6470	10.4034	10.4148	10.5659
Ti	0.0060	0.0394	0.0105	0.0296	0.0109	0.0152	0.0136	0.0569
Al	6.3603	5.1765	6.1687	4.5788	6.3227	5.5156	5.5058	5.1979
Fe	0.1427	0.1617	0.1415	0.5004	0.1462	0.2098	0.1962	0.2485
Mn	0.0000	0.0000	0.0000	0.0087	0.0000	0.0000	0.0000	0.0000
Mg	0.0432	0.0248	0.0499	1.5861	0.0459	0.0296	0.0357	0.1049
Ca	2.1876	1.4512	2.0518	1.2026	2.1417	1.5931	1.3891	1.4241
K	0.0726	0.4024	0.0873	0.1266	0.0789	0.1257	0.1788	0.2874
Na	1.6863	1.8296	1.7768	1.9788	1.6537	1.9885	2.3483	2.0726

TABLE 3 continued

	SG25222-C	SG25223-M	SG25223-C	SG25251-C	SG25251-M	SG25252-M	SG25252-C	SG25253-M
SiO2	55.5730	56.3930	54.8530	56.3000	56.9630	56.1930	55.4540	56.0630
TiO2	0.0700	0.0850	0.0730	0.0890	0.0690	0.0600	0.0930	0.0710
Al2O3	27.7840	27.6400	28.5910	27.2920	26.9080	27.9160	27.5630	27.8570
FeO	1.1840	1.1560	1.1340	1.1870	1.1550	1.0130	1.0690	1.1550
MnO	0.0190	0.0000	0.0250	0.0000	0.0000	0.0000	0.0090	0.0000
MgO	0.1370	0.1470	0.1370	0.2320	0.1660	0.1610	0.1720	0.2040
CaO	8.7390	8.6460	10.0350	9.2160	8.6100	9.2030	9.3390	9.4990
K2O	0.5030	0.5880	0.4530	0.4490	0.8760	0.3690	0.3860	0.3820
Na2O	6.0550	6.1090	5.3640	6.0350	5.9880	6.0080	5.9050	5.8520
SUM	100.0640	100.7640	100.6650	100.8000	100.7350	100.9230	99.9900	101.0830
Si	10.0386	10.1074	9.8728	10.1016	10.2166	10.0540	10.0298	10.0303
Ti	0.0095	0.0115	0.0099	0.0120	0.0093	0.0081	0.0127	0.0096
Al	5.9169	5.8404	6.0667	5.7731	5.6896	5.8884	5.8772	5.8757
Fe	0.1789	0.1733	0.1707	0.1781	0.1732	0.1516	0.1617	0.1728
Mn	0.0029	0.0000	0.0038	0.0000	0.0000	0.0000	0.0014	0.0000
Mg	0.0369	0.0393	0.0367	0.0620	0.0444	0.0429	0.0464	0.0544
Ca	1.6915	1.6604	1.9353	1.7718	1.6547	1.7643	1.8099	1.8210
K	0.1159	0.1345	0.1040	0.1028	0.2004	0.0842	0.0891	0.0872
Na	2.1208	2.1231	1.8720	2.0996	2.0825	2.0843	2.0709	2.0301
	SG25253-C	SG25254-M	SG25254-C	SG25254-M	SG25254-C	SG25255-M	SG25255-C	SG25255-M
SiO2	56.2100	56.3490	53.9840	57.0560	56.2100	57.5840	54.5830	55.6000
TiO2	0.0710	0.0860	0.0810	0.1100	0.0550	0.1380	0.0470	0.0780
Al2O3	28.4310	27.5180	29.0150	27.0860	26.5400	26.0220	27.7870	27.4220
FeO	0.7850	1.1430	1.0550	1.2250	1.0090	1.1980	1.0660	1.1450
MnO	0.0000	0.0130	0.0050	0.0040	0.0270	0.0000	0.0000	0.0000
MgO	0.1710	0.1830	0.1450	0.1520	0.1200	0.1800	0.1580	0.1650
CaO	9.5610	9.4350	10.3860	8.3500	9.2420	8.1860	9.4930	9.3220
K2O	0.4340	0.4690	0.4120	0.4780	0.4930	0.4320	0.4050	0.4720
Na2O	5.5730	5.8450	5.2000	6.2720	5.6100	6.4570	5.6600	6.0340
SUM	101.2360	101.0410	100.2830	100.7330	99.3060	100.1970	99.1990	100.2380
Si	10.0129	10.0845	9.7634	10.2135	10.2120	10.3539	9.9570	10.0433
Ti	0.0095	0.0116	0.0110	0.0148	0.0075	0.0187	0.0064	0.0106
Al	5.9707	5.8060	6.1865	5.7162	5.6844	5.5161	5.9759	5.8397
Fe	0.1169	0.1711	0.1596	0.1834	0.1533	0.1802	0.1626	0.1730
Mn	0.0000	0.0020	0.0008	0.0006	0.0042	0.0000	0.0000	0.0000
Mg	0.0454	0.0488	0.0391	0.0406	0.0325	0.0482	0.0430	0.0444
Ca	1.8249	1.8093	2.0127	1.6016	1.7991	1.5771	1.8555	1.8043
K	0.0986	0.1071	0.0951	0.1092	0.1143	0.0991	0.0943	0.1088
Na	1.9249	2.0283	1.8236	2.1770	1.9762	2.2512	2.0020	2.1134

TABLE 3 continued

	SG25255-M	SG2525-M	SG2525-C	SG25293-C	SG25293-M	SG25294-M	SG25294-C	SG25295-M
SiO2	57.9980	55.1140	54.2570	53.8790	54.4170	55.4190	54.4860	57.0250
TiO2	0.1030	0.0550	0.0590	0.0650	0.0580	0.0280	0.0550	0.0690
Al2O3	26.8300	28.3110	29.0010	29.1780	28.7980	28.4740	29.2420	26.3090
FeO	1.1900	1.0730	1.0190	1.0570	1.1690	0.8930	0.9130	1.1780
MnO	0.0000	0.0000	0.0000	0.0000	0.0100	0.0000	0.0000	0.0180
MgO	0.1450	0.1970	0.1450	0.1550	0.1420	0.1250	0.1490	0.1510
CaO	7.8430	9.8750	10.9170	10.9780	10.5920	10.4380	11.0260	8.2090
K2O	0.5570	0.3780	0.2100	0.3320	0.3260	0.3890	0.3040	0.5470
Na2O	6.5550	5.5140	5.0660	4.8860	5.0900	5.3650	4.9350	6.3910
SUM	101.2210	100.5170	100.6740	100.5300	100.6020	101.1310	101.1100	99.8970
Si	10.3152	9.9229	9.7706	9.7254	9.8083	9.9184	9.7654	10.2954
Ti	0.0138	0.0074	0.0080	0.0088	0.0079	0.0038	0.0074	0.0094
Al	5.6257	6.0093	6.1569	6.2091	6.1194	6.0078	6.1787	5.5997
Fe	0.1770	0.1616	0.1535	0.1596	0.1762	0.1337	0.1369	0.1779
Mn	0.0000	0.0000	0.0000	0.0000	0.0015	0.0000	0.0000	0.0028
Mg	0.0384	0.0529	0.0389	0.0417	0.0381	0.0333	0.0398	0.0406
Ca	1.4947	1.9051	2.1065	2.1233	2.0457	2.0017	2.1175	1.5880
K	0.1264	0.0868	0.0482	0.0765	0.0750	0.0888	0.0695	0.1260
Na	2.2606	1.9250	1.7689	1.7101	1.7789	1.8618	1.7150	2.2373

	SG25295-M	SG25295-C	SG25295-C	SG25296-M	SG25296-C	SG25322-C	SG25322-M	SG25324-C
SiO2	57.6560	55.9260	55.9470	54.4560	52.6040	52.3320	52.4320	63.7600
TiO2	0.1080	0.0620	0.0800	0.0660	0.0330	0.0650	0.1790	0.3520
Al2O3	26.0320	28.1660	26.9810	28.0720	29.8080	30.6340	29.7720	21.1040
FeO	1.2070	1.0320	1.1590	1.2050	0.8870	0.8630	0.9590	0.8760
MnO	0.0070	0.0090	0.0000	0.0000	0.0030	0.0000	0.0440	0.0160
MgO	0.1250	0.1560	0.1690	0.2620	0.1670	0.1210	0.1390	0.0930
CaO	7.8220	9.7420	8.9730	10.3290	11.2540	12.3650	11.8950	3.0410
K2O	0.5220	0.4160	0.4700	0.3050	0.2490	0.2370	0.2740	2.7460
Na2O	6.6690	5.5910	5.8040	5.3340	4.7790	4.3810	6.2690	6.9410
SUM	100.1480	101.1000	99.5830	100.0290	99.7840	100.9980	101.9630	98.9290
Si	10.3715	9.9990	10.1439	9.8739	9.5745	9.4353	9.4352	11.4629
Ti	0.0146	0.0083	0.0109	0.0090	0.0045	0.0088	0.0242	0.0476
Al	5.5207	5.9368	5.7673	6.0007	6.3961	6.5115	6.3161	4.4730
Fe	0.1816	0.1543	0.1757	0.1827	0.1350	0.1301	0.1443	0.1317
Mn	0.0011	0.0014	0.0000	0.0000	0.0005	0.0000	0.0067	0.0024
Mg	0.0335	0.0416	0.0457	0.0708	0.0453	0.0325	0.0373	0.0249
Ca	1.5077	1.8663	1.7433	2.0068	2.1948	2.3888	2.2936	0.5858
K	0.1198	0.0949	0.1087	0.0706	0.0578	0.0545	0.0629	0.6298
Na	2.3261	1.9383	2.0405	1.8753	1.6866	1.5316	2.1874	2.4196

TABLE 3 continued

	SG25324-C	SG25324-M	SG25324-M	SG25325-M	SG25325-C	SG2722-M	SG2722-C	SG2724-M
SiO2	67.4210	54.9640	54.8710	55.2500	52.4890	54.1260	51.9510	52.6930
TiO2	0.1210	0.0430	0.0490	0.0490	0.0010	0.0840	0.0860	0.1110
Al2O3	18.7320	28.0200	28.8300	28.7340	30.8080	28.7750	30.4760	29.6870
FeO	0.8350	1.1500	1.0210	0.6140	0.7510	1.2180	0.9960	1.1270
MnO	0.2410	0.0320	0.0000	0.0030	0.0220	0.0000	0.1320	0.0000
MgO	0.1200	0.1140	0.1370	0.1320	0.1420	0.2950	0.2760	0.2910
CaO	2.6340	9.6040	10.2000	9.7640	12.0810	11.1640	12.5000	12.4180
K2O	1.6490	0.4330	0.3560	0.4040	0.2530	0.3140	0.2420	0.2370
Na2O	6.6690	5.9010	5.4760	5.7140	4.5380	4.8120	4.1250	4.1690
SUM	98.4220	100.2610	100.9400	100.6640	101.0850	100.7880	100.7840	100.7330
Si	12.0146	9.9376	9.8466	9.9126	9.4455	9.7552	9.4014	9.5304
Ti	0.0162	0.0058	0.0066	0.0066	0.0001	0.0114	0.0117	0.0151
Al	3.9354	5.9725	6.0993	6.0777	6.5360	6.1141	6.5019	6.3301
Fe	0.1244	0.1739	0.1532	0.0921	0.1130	0.1836	0.1507	0.1705
Mn	0.0364	0.0049	0.0000	0.0005	0.0034	0.0000	0.0202	0.0000
Mg	0.0319	0.0307	0.0366	0.0353	0.0381	0.0792	0.0744	0.0784
Ca	0.5029	1.8606	1.9613	1.8771	2.3295	2.1560	2.4238	2.4066
K	0.3749	0.0999	0.0815	0.0925	0.0581	0.0722	0.0559	0.0547
Na	2.3044	2.0687	1.9054	1.9878	1.5834	1.6816	1.4474	1.4621

	SG2724-C	SG2851-C	SG2851-M	SG2852-M	SG2852-C	SG2853-M	SG2853-C	SG28131-C
SiO2	51.6620	55.4030	55.9050	57.3570	57.8000	56.0780	55.7720	50.8600
TiO2	0.0470	0.0680	0.0840	0.0930	0.0990	0.0650	0.0400	0.1100
Al2O3	30.8760	29.0270	27.9540	26.9960	26.6260	28.4870	28.3100	31.9630
FeO	0.8590	0.9860	1.1490	1.1780	1.2620	1.0140	1.0220	1.1350
MnO	0.0290	0.0000	0.0030	0.0450	0.0260	0.0360	0.0300	0.0000
MgO	0.2410	0.1970	0.2010	0.1620	0.1930	0.1830	0.1660	0.1450
CaO	12.5880	10.4740	9.4250	8.1820	8.0260	9.7540	9.5550	14.0340
K2O	0.1790	0.4180	0.5320	0.6970	0.6830	0.5130	0.4860	0.1890
Na2O	4.2260	5.0390	5.7290	6.2970	6.4800	5.4800	5.5310	3.4640
SUM	100.7070	101.6120	100.9820	101.0070	101.1950	101.6100	100.9120	101.9000
Si	9.3507	9.8641	10.0151	10.2438	10.3032	9.9765	9.9868	9.1387
Ti	0.0064	0.0091	0.0113	0.0125	0.0133	0.0087	0.0054	0.0149
Al	6.5885	6.0927	5.9039	5.6841	5.5955	5.9747	5.9764	6.7709
Fe	0.1300	0.1468	0.1721	0.1760	0.1881	0.1509	0.1531	0.1706
Mn	0.0044	0.0000	0.0005	0.0068	0.0039	0.0054	0.0046	0.0000
Mg	0.0650	0.0523	0.0537	0.0431	0.0513	0.0485	0.0443	0.0388
Ca	2.4413	1.9982	1.8092	1.5658	1.5330	1.8594	1.8333	2.7020
K	0.0413	0.0949	0.1216	0.1588	0.1553	0.1164	0.1110	0.0433
Na	1.4831	1.7396	1.9901	2.1807	2.2397	1.8904	1.9204	1.2069

TABLE 3 continued

	SG28132-C
SiO2	55.2710
TiO2	0.2520
Al2O3	29.1470
FeO	1.0810
MnO	0.0000
MgO	0.1750
CaO	9.9450
K2O	0.7060
Na2O	5.3370
SUM	101.9140
Si	9.8309
Ti	0.0337
Al	6.1119
Fe	0.1608
Mn	0.0000
Mg	0.0464
Ca	1.8954
K	0.1602
Na	1.8407

APPENDIX H GEOLOGIC AND TOPOGRAPHIC MAPS

Topographic Map of northern half of Sierra Grande

compiled from USGS 7.5 minute quadrangles:
Folsom, Des Moines, Capulin and Little Grande

Folsom	AMS 5257 IV SW Series V881
Des Moines	AMS 5257 IV SE Series V881
Capulin	AMS 5257 III NW Series V881
Little Grande	AMS 5257 III NE Series V881

Map Area

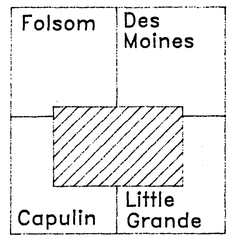

Sample Location ● 25

Scale 1 : 24000

0 miles 1

0 kilometers 1

TN MN

Contour Interval 20 feet
National Geodetic Vertical Datum 1929

Geologic Map of the northern half of Sierra Grande

Matthew G. Trainum

1992

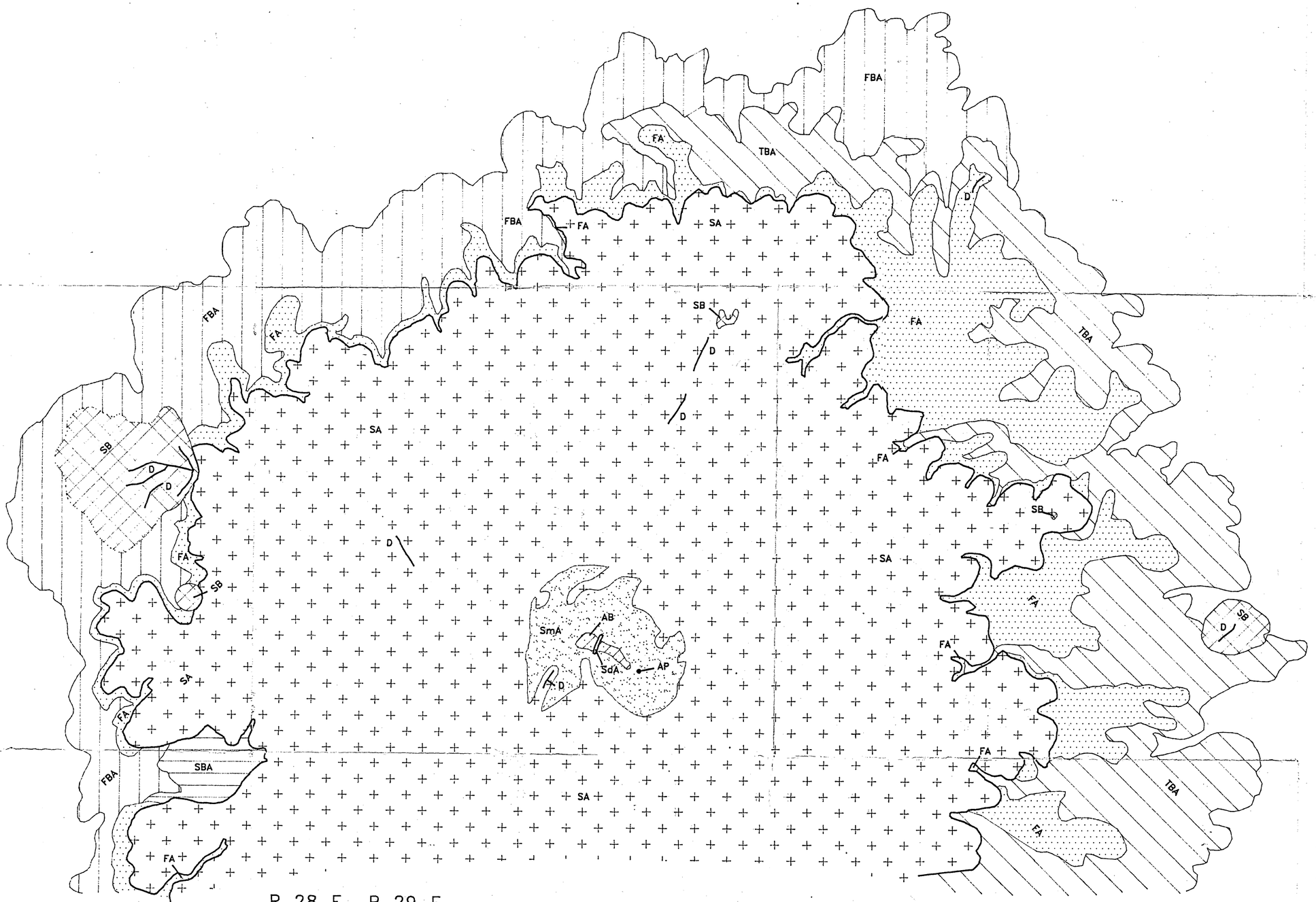

FBA First Basaltic Andesite

SBA Second Basaltic Andesite

TBA Third Basaltic Andesite

FA First Andesite

SA Second Andesite

SmA Summit Andesite

AB Andesitic Breccia

SdA Saddle Andesite

AP Andesitic Plug

SB Scoria and Basalt

D Basaltic & Andesitic Dikes

Contact
known
inferred
concealed

TN MN

Scale 1 : 24000

0 miles 1

0 kilometers 1